ISTANBUL TECHNICAL UNIVERSITY ★ GRADUATE SCHOOL OF SCIENCE ENGINEERING AND TECHNOLOGY

EVOLUTIONARY ENGINEERING AND MOLECULAR CHARACTERIZATION OF FREEZE-THAW RESISTANT
Saccharomyces cerevisiae

Ph.D. THESIS

Ülkü YILMAZ

Department of Advanced Technologies

Molecular Biology-Genetics and Biotechnology Programme

APRIL 2013

ISTANBUL TECHNICAL UNIVERSITY ★ GRADUATE SCHOOL OF SCIENCE
ENGINEERING AND TECHNOLOGY

EVOLUTIONARY ENGINEERING AND MOLECULAR
CHARACTERIZATION OF FREEZE-THAW RESISTANT
Saccharomyces cerevisiae

Ph.D. THESIS

Ülkü YILMAZ
(521072037)

Department of Advanced Technologies

Molecular Biology-Genetics and Biotechnology Programme

Thesis Advisor: Prof. Dr. Zeynep Petek ÇAKAR

APRIL 2013

İSTANBUL TEKNİK ÜNİVERSİTESİ ★ FEN BİLİMLERİ ENSTİTÜSÜ

DONMA-ERİME STRESİNE DİRENÇLİ *Saccharomyces cerevisiae*' **nin EVRİMSEL MÜHENDİSLİĞİ ve MOLEKÜLER KARAKTERİZASYONU**

DOKTORA TEZİ

Ülkü YILMAZ
(521072037)

İleri Teknolojiler Anabilim Dalı

Moleküler Biyoloji-Genetik ve Biyoteknoloji Programı

Tez Danışmanı: Prof. Dr. Zeynep Petek ÇAKAR

NİSAN 2013

Ülkü YILMAZ, a **Ph.D.** student of ITU **Graduate School of Science Engineering and Technology**, student ID **521072037**, successfully defended the **thesis** entitled "**EVOLUTIONARY ENGİNEERING AND MOLECULAR CHARACTERİZATION OF FREEZE-THAW RESİSTANT** *Saccharomyces cerevisiae*", which she prepared after fulfilling the requirements specified in the associated legislations, before the jury whose signatures are below.

Thesis Advisor :   **Prof. Dr. Zeynep Petek ÇAKAR**   ....
İstanbul Technical University

Jury Members :   **Assoc. Prof. Dr. Ayten YAZGAN KARATAŞ** ....
Istanbul Technical University

Assoc. Prof. Dr. Mustafa TÜRKER   ....
Pakmaya

Assoc. Prof. Dr. Fatma Neşe KÖK   ....
Istanbul Technical University

Assoc. Prof. Dr. Melek ÖZKAN   ....
Gebze Institute of Technology

Date of Submission : 28 December 2012
Date of Defense :   12 April 2013

To my family,

FOREWORD

I would like to sincerely thank to my supervisor Prof. Dr. Zeynep Petek Çakar for her invaluable help and guidance. Without her I could not find energy to reachout this point. Thank you my teacher.

I am thankful to my lovely friends Burcu Turanlı Yıldız, Ceren Alkım, Berrak Gülçin Balaban and Tuğba Aloğlu for their helps and patience. We all started together and finally succeed. I owe them a lot as a friend and scientist.

I specially thank to Assoc. Prof. Dr. Servet Özcan, Assoc. Prof. Dr. Ayten Yazgan Karataş and Prof. Dr. Süleyman Yazar for their guidance and belief to me.

I would also thank to my beloved family for their belief, love and support.

I would like to thank to my lab friends and graduate students in ITU YEAST Laboratory.

December 2012   Ülkü Yılmaz
                                                                          (M.Sc.)

x

TABLE OF CONTENTS

ABBREVIATIONS

CDW   : Cell dry weight
EMS   : Ethyl methane sulphonate
ESR   : Environmental stress response
GSH   : Glutathione
HPLC   : High performance liquid chromatography
MPN   : Most probable number
PCR   : Polimerase Chain Reaction
Q-PCR   : Quantitative Real-Time Polimerase Chain Reaction
ROS   : Reactive oxygen species
YMM   : Yeast minimal medium
YPD   : Yeast complex medium

LIST OF TABLES

LIST OF FIGURES

EVOLUTIONARY ENGINEERING AND MOLECULAR CHARACTERIZATION OF FREEZE-THAW RESISTANT *SACCHAROMYCES CEREVISIAE*

SUMMARY

The aim of this study was first to obtain freeze-thaw stress resistant *Saccharomyces cerevisiae* mutant strains from a laboratory strain and an industrial strain, and second to characterize the freeze-thaw stress resistant mutants at a molecular level. To obtain resistant strains, a reverse metabolic engineering strategy; evolutionary engineering was used.

Evolutionary engineering is a "natural" process to obtain mutant strains with specific and desired phenotypes just as freeze-thaw resistant mutants. Predominantly, evolutionary engineering involves four main steps that are obtaining the chemically/physically mutagenized genetically variant cell population, repetitive cycles of selection pressure to obtain improved strain, analysis of the strains' performance and design of the next target.

Here, *Saccharomyces cerevisiae* CEN.PK113-7D (mat a) haploid strain and *Saccharomyces cerevisiae* R625 polyploid strain selected to improve desired freeze-thaw resistance phenotype. In order to obtain genetically variant mutant population, a chemically mutagenic agent ethyl methane sulphonate (EMS) was used on haploid and polyploid *Saccharomyces cerevisiae* yeast strains. The EMS-mutagenized genetically variant mutant populations; haploid *906* and polyploid *R625_M* were used as the starting point to obtain generations by the application of iterative cycles of stress for selection of the desired phenotypes. Freeze-thaw stress was used as the selective pressure. Pulse increasing freeze-thaw stress selection application was performed to haploid *906* and polyploid *R625_M* genetically variant mutant cell populations. Ten mutant generations were obtained by pulse increasing freeze-thaw stress selection strategy. The stress cycles were gradually increased at each continued generation. The final mutant generations haploid *FG10* and polyploid *R625_10FG* were obtained after ten consecutive freeze-thaw stress cycles. As a result of iterative cycles of selective pressure, the last generations were consisted of heterogeneous freeze-thaw resistant mutant individuals. Then, mutant individuals were selected randomly from the haploid *FG10* and polyploid *R625_10FG* final mutant generations to isolate freeze-thaw resistant mutant individuals. Thereafter, the phenotypic characterizations of the mutant individuals; *F1, F2, F3, F4, F5, F6, F7, F8, F9, F10* selected from the haploid *FG10* and *P1, P2, P3, P4, P5, P6, P7, P8, P9, P10* selected from the polyploid *R625_10FG* final mutant generations were performed via spotting assay and five-tube most probable number method (MPN). First the freeze-thaw resistances were determined then, the characterization of the mutant individuals with respect to their potential cross resistances to metal and other non-metal industrial stresses were investigated. The most resistant mutant individuals; haploid *F1* and polyploid *P8* were detected. It was found out that

haploid mutant individual *F1* was resistant against; boron, chromium, cobalt, zinc, nickel and oxidative (hydrogen peroxide) stresses and sensitive to iron, copper and osmotic (NaCl) stresses. On the other hand, polyploid mutant individual *P8* gained cross-resistance to boron, iron, cobalt, zinc and oxidative stresses (H_2O_2).

At the same time, the cross-resistance results of haploid wild-type, mutant individual *F1*, polyploid wild-type and mutant individual *P8* were also analyzed by Principle Component Analysis (PCA). By adapting the multiple cross-resistance data on two dimensional plane, the variance between variables were observed and this data were given qualitative conclusions. The response is completely related with the distance between the component scores. The similar behaviour between observation and individuals indicated difference in response and there was a high variance between haploid wild-type and mutant individual *F1* in response to different types of stress. Likewise, the similar behaviour between observation and individuals indicated difference in response and there was a high variance between polyploidy wild-type and mutant individual *P8* in response to different types of stress.

Physiological analysis were also performed at normal growth conditions in a batch culture without stress treatment to closely determine the behavior of haploid and polyploid freeze-thaw resistant mutant individuals with respect to their wild-types. Growth curve analysis were examined via spectrophotometric measurements and metabolite analysis via high performance liquid chromatography (HPLC) and glucose oxidase/peroxidase assay.

In order to understand the development and genetic background of high levels of freeze-thaw resistance in *S. cerevisiae* along with the multiple-stress resistance characteristics, transcriptomic analysis were performed by using quantitative real time-PCR methods (QPCR). The expression levels were determined in haploid mutant individual *F1*, compared to wild-type. The relative transcriptional changes of freeze-thaw stress related genes *AQY1*, *AQY2*, *CTT1*, *GSH1* and *FPS1* were studied at control and freeze-thaw stress conditions.

To enlighten the genetic basis underlying the freeze-thaw resistance mechanism, whole genome transcriptomic analysis was performed by using high throughput DNA microarray technology. The microarray data was analyzed by GeneSpring GX 9.0 software. The mean expression profile of *F1* was normalized to wild-type by this software and then the molecular and functional categorization of up and down regulated genes were done according to FunSpec and Funcat databases. It is remarkable that 1287 genes were upregulated and 891 genes were downregulated at freeze-thaw stress resistant mutant individual *F1*. Those of the high numbered, differentially regulated genes resulted in multiple-stress tolerance.

To summarize, highly freeze-thaw resistant haploid and diploid mutant individuals, were selected successfully using evolutionary engineering methodology. Microarray data gave more important knowledge about freeze-thaw resistant haploid mutant individual *F1*. Further transcriptomic investigations under freeze-thaw stress conditions and the deletion and/or overexpression studies might help to understand resistance mechanisms of the mutant individuals.

In conclusion, in industrial applications, it is more safe and acceptable to use improved baker's yeast with high freeze-thaw resistance without including any foreign genes that do not belong to the yeast natural genome. Thus, it is a safer way to use baker's yeast in industry that have a highly re-regulated genome and improved freeze-thaw resistance.

DONMA-ERİME STRESİNE DİRENÇLİ
Saccharomyces cerevisiae' nin EVRİMSEL MÜHENDİSLİĞİ
ve MOLEKÜLER KARAKTERİZASYONU

ÖZET

Bu çalışmanın amacı donma-erime stresine dirençli *Saccharomyces cerevisiae* mutant suşlarının laboratuvar ve endüstriyel suşlar kullanılarak elde edilmesidir.Bu amaç ile bir tersine metabolizma mühendisliği yöntemi olan; evrimsel mühendislik kullanılmıştır.

Evrimsel mühendislik, donma-erime stresine direnç gibi, özel ve istenilen fenotiplerdeki mutant suşların elde edilmesinde kullanılan "doğal" bir prosestir.Genel olarak, evrimsel mühendislik dört ana basamaktan oluşmaktadır.Bu aşamalar; genetik olarak karışık hücre populasyonunun kimyasal/fiziksel mutasyon ile elde edilmesi, istenilen özellikteki geliştirilmiş suşun elde edilmesi için tekrarlayan döngülerde seleksiyon baskısının uygulanması, elde edilen suşun performansının analizi ve bir sonraki hedefin dizaynı.

Bu çalışmada haploid *Saccharomyces cerevisiae* CEN.PK113-7D (mat a) ve poliploid *Saccharomyces cerevisiae R625* suşları, istenilen donma-erime stresine dirençli fenotipi geliştirmek amacı ile kullanılmışlardır. Genetik çeşitliliği arttırılmış mutant populasyonu elde etmek amacı ile, kimyasal bir mutajenik ajan olan etilmetansülfonat (ethyl methane sulphonate, EMS) haploid ve poliploid *Saccharomyces cerevisiae* maya suşları üzerinde kullanılmıştır. EMS ile mutajenize edilmiş olan genetik olarak çeşitliliği arttırılmış mutant populasyonlar; haploid *906* ve poliploid *R625_M* istenilen fenotipin seçilmesi için stresin tekrarlayan döngüler ile uygulanması ile nesil eldesi amacı ile başlangıç populasyonu olarak kullanılmışlardır. Seçici baskı olarak donma-erime stresi kullanılmıştır.Şok artan donma-erime stres seleksiyon uygulaması genetik çeşitliliği arttırılmış olan, haploid *906* ve poliploid *R625_M'* de gerçekleştirilmiştir. On mutant nesil, şok artan donma-erime stres seleksiyon stratejisi kullanılarak elde edilmiştir. Stres döngüleri herbir devam eden nesilde dereceli olarak arttırılmıştır. Ard arda on döngü donma-erime stresi sonrasında, son mutant nesiller; haploid *FG10* ve poliploid *R625_10FG* elde edilmişlerdir. Tekrarlayan döngülerde uygulanan selektif baskı uygulaması sonucunda, son nesiller heterojen bir yapıda donma-erime stresine dirençli mutant bireylerden oluşmaktadırlar.Daha sonra, mutant bireyler haploid *FG10* ve poliploid *R625_10FG* son mutant jenerasyonlardan rastgele bir şekilde donma-erime stresine dirençli mutant bireyleri izole etmek amacı ile seçilmişlerdir. Bundan sonra, haploid *FG10'* dan izole edilmiş olan *F1, F2, F3, F4, F5, F6, F7, F8, F9, F10* ve poliploid *R625_10FG'* den izole edilmiş olan *P1, P2, P3, P4, P5, P6, P7, P8, P9, P10* mutant bireylerinin fenotipik karakterizasyonları damlatma yöntemi (spotting assay) ve 5-tüp en muhtemel sayı yöntemi (five-tube most probable number method, MPN) kullanılarak gerçekleştirilmiştir.

İlk olarak, mutant bireylerin donma-erime stress dirençleri belirlenmiştir, daha sonra da metal ve diğer metal olmayan endüstriyel streslere karşı olası çapraz-dirençlerinin araştırılması amacı ile mutant bireylerin karakterizasyonları gerçekleştirilmiştir. En dirençli mutant bireyler; haploid *F1* ve poliploid *P8* olarak belirlenmişlerdir. Haploid mutant birey *F1*; bor, krom, kobalt, nikel, çinko ve oksidatif (hidrojen peroksit) streslerine karşı direnç göstermiştir ve demir, bakır ve ozmotik (NaCl) strese karşı hassasiyet göstermiştir. Diğer taraftan, poliploid mutant birey *P8*; bor, demir, kobalt, krom, çinko ve oksidatif (H_2O_2) streslere çapraz-direnç kazanmıştır.

Aynı zamanda, haploid yaban-tip, mutant birey *F1*, poliploid yaban-tip ve mutant birey *P8*' in çapraz-direnç sonuçları, Principle Component Analysis (PCA) ile de analiz edilmiştir. Multiple çapraz-direnç datası iki boyutlu bir düzleme adapte edilerek, değişkenler arasındaki varyans gözlemlenmiş ve bu data kalitatif sonuçlar vermiştir. Cevap, component skorlar arasındaki mesafe ile ilişkilidir. Gözlemler ve bireyler arasındaki benzer davranışlar, cevap olarak farklılık göstermiştir ve farklı türdeki streslere karşı, haploid yaban-tip ve mutant birey *F1* arasında büyük bir varyans vardır. Aynı şekilde, farklı türdeki streslere karşı, haploid yaban-tip ve mutant birey *P8* arasında büyük bir varyans vardır ve gözlemler ve bireyler arasındaki benzer davranışlar, cevap olarak farklılık göstermiştir.

Fizyolojik analizler, normal üreme koşullarında, stres uygulaması yapılmadan kapalı kültürde (batch culture), donma-erime stresine dirençli, haploid ve poliploid mutant bireylerin kendi yaban-tiplerine oranla davranışlarını yakından belirlemek amacı ile gerçekleştirilmiştir.Büyüme eğrisi analizleri, spektrofotometrik ölçümler ile ve metabolit analizleri, yüksek performanslı sıvı kromatografisi (high performance liquid chromatography, HPLC) ve glikoz oksidaz/peroksidaz (glucose oxidase/peroxidase assay) yöntemi ile çalışılmıştır.

S. cerevisiae' deki yüksek seviyelerdeki donma-erime stress direncinin ve beraberinde multiple-stress direncinin gelişimi ve genetik altyapısının anlaşılması amacı ile transkriptomik analizler kantitatif gerçek zamanlı-PCR (quantitative real time-PCR, QPCR) metodu kullanılarak gerçekleştirilmiştir. Haploid mutant birey *F1*' in anlatım düzeyleri yaban-tipe kıyasla belirlenmiştir. Donma-erime stres direnci ile ilişkili olan *AQY1*, *AQY2*, *CTT1*, *GSH1* ve *FPS1* genlerinin, relatif transkripsiyonel değişimleri kontrol ve donma-erime stress koşullarında çalışılmıştır.

Donma-erime stress direnç mekanizmasının altında yatan genetik temellerin aydınlatılması amacı ile tüm genom transkriptomik analizleri için DNA microarray teknolojisi kullanılmıştır. Mikroarray datası, GeneSpring GX 9.0 yazılım program kullanılarak analiz edilmiştir. *F1*' in anlamlı ekspresyon profili, bu yazılım program ile yaban-tipe normalize edilmiştir ve sonra da regülasyonları artan ve azalan genlerin (up and down regulated genes) moleküler ve fonksiyonel kategorizasyonları FunSpec ve Funcat veritabanları kullanılarak gerçekleştirilmiştir. Anlamlı ölçüde, donma-erime stresine dirençli mutant birey *F1*' in 1287 geninin regülasyonu artmış ve 891 genin regülasyonu azalmıştır. Çoklu-stres direnci, bu kadar yüksek sayıda farklı olarak regülasyon gösteren genlerin sonucunda ortaya çıkmıştır.

Özetle, yüksek seviyelerde donma-erime stresine dirençli haploid ve poliploid mutant bireyler, evrimsel mühendislik yöntemi ile başarılı bir şekilde seçilmişlerdir. Mikroarray sonucunda elde edilen veriler, donma-erime stresine dirençli haploid mutant birey *F1* ile ilgili çok önemli bilgiler vermiştir. Donma-erime stres koşulları altında, daha ileri transkriptomik araştırmalar, gen silme (gene deletion) ve/veya

yüksek derecede anlatım (overexpression) çalışmaları, mutant bireylerin direnç mekanizmalarının anlaşılmasında yardımcı olabilirler.

Sonuç olarak, endüstriyel uygulamalarda, yüksek derecede donma-erime stresine dirençli, mayanın kendi genomu dışında yabancı herhangi bir gen içermeyen, geliştirilmiş ekmek maya hücrelerinin kullanımı, daha güvenli ve kabul edilebilirdir. Böylece, bu yöntem, donma-erime stres direnci ile sonuçlanan yüksek derecede regüle edilmiş genomu ile ekmek mayasının endüstride kullanımının güvenli bir yoludur.

1. INTRODUCTION

1.1 Literature Review

1.1.1 The model eukaryotic organism *Saccharomyces cerevisiae*

Saccharomyces cerevisiae is a small, unicellular, cell walled eukaryotic organism. It has a small genome consisting of sixteen chromosomes and more than 6000 genes (Feldmann, 2005). *S. cerevisiae* cells can undergo mitotic cell division in every 100 min and bud almost 20 times in a life period (Herskowitz, 1988; Burke et al., 2000). In general, yeast cells has three mating types; MAT a (haploid cells), MAT α (haploid cells) and MAT a/α (diploid cells). The reproduction of the yeast cells occurs via vegetatively and sexually. In vegetative proliferation, the reproduction realizes via mitotic cell division. MAT a, MAT α and MAT a/α cells can have mitotic cell proliferation. In sexual proliferation, haploid MAT a and MAT α cells are coming together and then fuse to generate diploid MAT a/α cells. MAT a/α cells have not the ability of mating, however they can undergo meiotic division to form haploid cells (Feldmann, 2005; Zetic et al., 2001).

It is also important that, yeast cells have the ability of mating-type interconversion, so that they have homothallic and heterothallic life cycle (Herskowitz, 1988). Homothallic life cycle is the reason of mating-type switching, where a single haploid cell forms diploid ones. On the other hand, heterothallic life cycle is the reason of meeting two different mating type cells, where haploid MAT a and MAT α cells forms diploid ones (Herskowitz, 1988).

Generally, natural and domesticated industrial yeast strains show homothallic life cycle, however heterothallic life cycle preferred in laboratory haploid strains (Zeyl, 2009; Perez-Torrado et al., 2010). The life cycle of the yeast *S. cerevisiae* is seen in Figure 1.1.
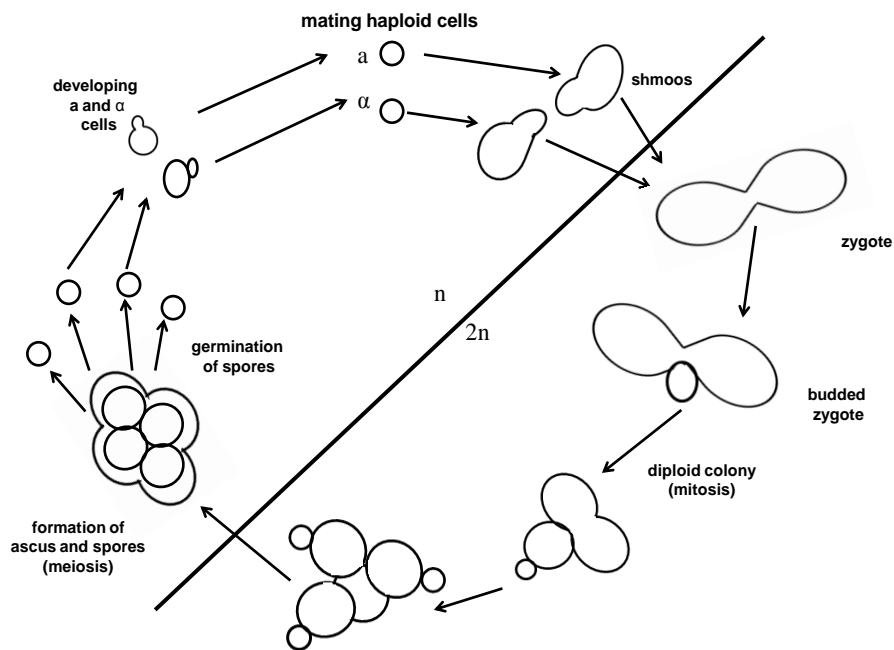
Figure 1.1: The life cycle of *Saccharomyces cerevisiae* (Feldman, 2005).

1.1.2 Industrial importance of *Saccharomyces cerevisiae*

S. cerevisiae is an appropriate and commonly used industrial organism that has been used safely for centuries in wine production for alcoholic fermentation and in baking industries for the leavening of the dough. In addition to those applications, nowadays this organism is used in another applications such as fuel ethanol and biodiesel production.

The biochemical and genetic characterizations of *S. cerevisiae* are the reasons of its importance in both basic and biotechnological research areas. Especially, the bread-making and wine industries are dominantly related to the yeast *S. cerevisiae* (Park et al., 1997; Branduardi et al., 2008; Tanghe et al., 2002).

The chronological milestones of *S. cerevisiae* in the life of mankind is seen in Figure 1.2.

Chronology	Milestones
6000-2000 BC	Brewing (Sumeria, Babylonia)
1680	Yeast under the microscope (van Leeuwenhoek)
1835	Alcoholic fermentation associated with yeast
1837	Name (S.cerevisiae) created for yeast observed in malt
1839	Sugar as a food source for yeast growth
1857	Fermentation correlated with metabolism (Pasteur)
1876	'Etudes sur la levure de bière' (Pasteur)
1877	Term "enzyme" (in yeast) introduced (Kühne)
1880	Single yeast cells and pure strains for brewing (Hansen)
1883	Alcohol and CO2 by cell-free extracts (Buchner)
1915	Production of glycerol
1920	Yeast physiology reviewed
1949	First genetic map (Lindegren); mating type system
1930-1960	Yeasts' taxonomy by Kluyver
1966	First tRNA structures from yeast
1978	First transformation of yeast (Hinnen, Hicks & Fink)
1990-1994	First commercial pharmaceutical products from recombinant yeast (Hepatitis B vaccine)
1990-1996	Completion of the yeast genome project

Figure 1.2: The chronological milestones of *Saccharomyces cerevisiae* (Hernández-López et al., 2007).

In baking industry, besides *S. cerevisiae*, *Issatchenkia orientalis*, *Pichia membranaefaciens* and *Torulaspora delbrueckii* have also dough-leavening ability. Especially, an isolated strain of *T. delbrueckii*, *T. delbrueckii PYCC5321* involves osmotolerance and freeze tolerance characteristics, which are suitable for frozen dough industry. However, it has a small size that is improper for filtration before packaging the frozen dough and leads to challenges in the industrial processes. To solve this drawback, Sasaki and Ohshima in 1987 did diploidization of *T. delbrueckii* that might result in loss of stress related properties (Hernández-López et al., 2007). Nearly, 2 million tons/ year of baker's yeast are consumed in bakery. In bread making process baker's yeast, increases dough volume, develops dough texture and gives flavour to the dough (Shima and Takagi, 2009). However, during those processes baker's yeast encounters various stresses that are summarized in Figure 1.3.
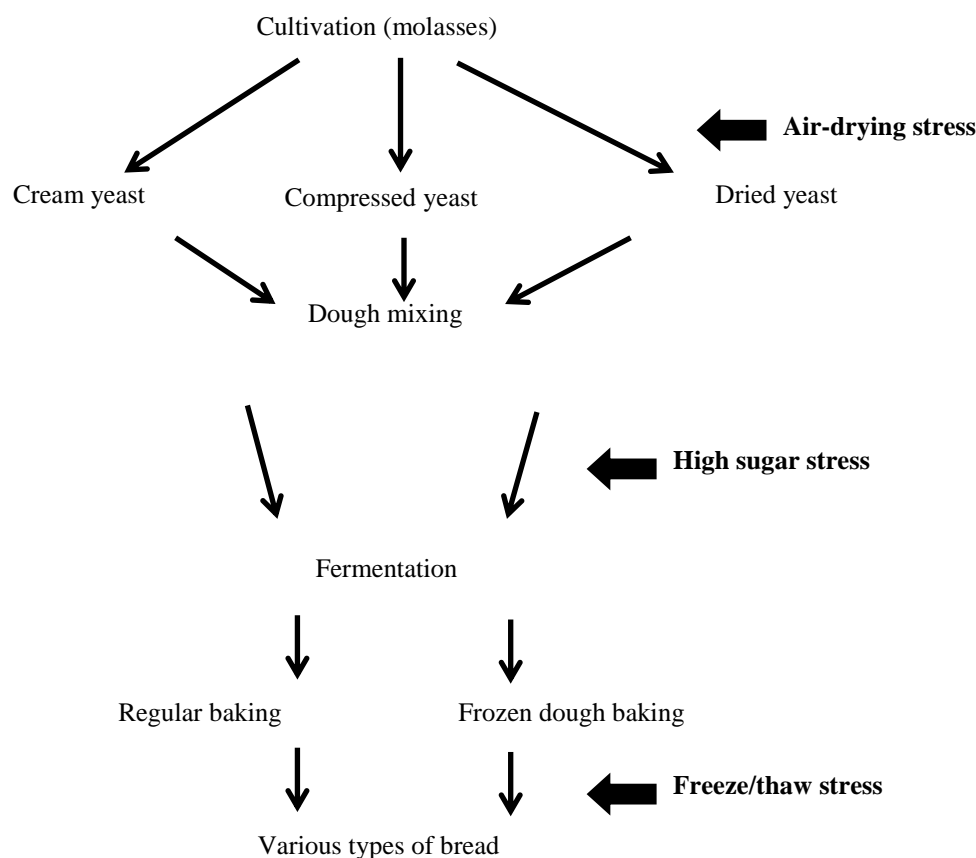
Figure 1.3: The life cycle of *Saccharomyces cerevisiae* in baking industry (Shima and Takagi, 2009).

1.1.3 General stress response of *Saccharomyces cerevisiae*

Bauer and Pretorius stated that " the molecular and physiological response of an organism to changes in the environment is referred to as "stress response", while the ability to withstand unfavourable or changing external conditions is defined as 'stress resistance' or stress tolerance" (Bauer and Pretorius, 2000).

S. cerevisiae cells can exposed different environmental stress conditions such as heat or cold shock, metal toxicity, essential nutrient limitations, hyper-osmotic or hypo-osmotic pressure and ethanol toxicity during the growth. To cope with those stress conditions S. cerevisiae cells were evolved to detect stress signals and responses to that signals via "general or specific stress response and protection programmes" (Bauer and Pretorius, 2000; Gasch et al., 2000). General stress response protection programme involves environmental stress response (ESR) mechanism. Environmental stress response genes were regulated via three different evolutionary-tuned signaling pathways and transcriptional factors, according to the stress types. Those are cAMP-PKA (cyclic adenosine monophosphate protein kinaseA), HOG

(high osmolarity glycerol) and TOR (target of rapamycin) signal transduction pathways. Signal transduction cascade composed of three elements; sensing via stress signal sensors (receptors), transduction via intermediate signalling modules (kinases) or second messengers (cAMP, calcium ions) and implementation via induction or repression of specific target proteins (such as transcription factors, metabolic enzymes) for cellular adaptation to survive. (Aguilera et al., 2007; Bauer and Pretorius, 2000; Rubio-Texeira et al., 1998). For example, G protein-coupled receptors (GPCRs) sense the glucose and transfer the answer to carbon signaling Ras/cAMP/PKA pathway that is responsible nutrient control, growth and glucose stress response of the cell (Rubio-Texeira et al., 1998).

S. cerevisiae has two oxidative stress defense systems, that are enzymatic and non-enzymatic mechanisms, to cope with the oxidative stress and detoxifying reactive oxygen species (ROS) to maintain the steady state redox balance (Jamieson, 1998).

Enzymatic oxidative stress defense mechanism includes catalases, superoxide dismutases, thioredoxins (*TRX1*, *TRX2*) and glutaredoxins (*GRX1* and *GRX2*). *S. cerevisiae* encodes two superoxide dismutase SOD1 and SOD2 that have a role in superoxide anion (O_2^-) generated after aerobic respiration via mitochondria. *S. cerevisiae* has two catalases; *CTT1* encodes catalase A and *CTA1* encodes catalase T enzymes. Both enzymes have a role to protect cells against oxidative stress damage by hydrogen peroxide. Catalase enzymes break down the hydrogen peroxide molecule into oxygen and water. Glutaredoxin encoding genes *GRX1* is effected on superoxide anion and *GRX2* is effected on hydrogen peroxide. The thioredoxin encoding genes *TRX1* and *TRX2* deoxidize the GSH for redox balance (Odani et al., 2003; Herrero et al., 2008; Luikenhuis et al., 1998).

Non-enzymatic oxidative stress defense mechanism includes glutathione (*GSH1* and *GSH2*) and metallothioneins (*CUP1* and *CRS5*) (Luikenhuis et al., 1998). Glutathione is an antioxidant molecule to protect cells against oxidative stress damage by hydrogen peroxide (Izawa et al., 1995h). Metallothioneins are metal binding proteins to protect cells against metal toxicity. In addition, metallothioneins are the scavenger of hydroxyl radicals against oxidative stress in yeast cells (Liu and Thiele, 1997).

Metal toxicity causes carcinogenic effects and direct/ indirect oxidative damages, impaired DNA repair, altered gene expression, inhibition/disruption of proteins and enzymes function on cellular metabolic processes. To overcome those hazardous effects of metals, yeast cells developed different detoxification mechanisms such as metal efflux pumps, transport and sequestration of metals in vacuoles and chelation of metals via metallothioneins and glutathione (Ruotolo et al., 2008; Wysocki and Tamas, 2010).

Another important stress defense mechanism against heat and cold shock stress is the induction of heat shock proteins to prevent protein aggregation (Wei, 2007). In addition, yeast cells accumulates reserve carbohydrates; trehalose and glycogen under starvation, heat shock, freeze-thaw and osmotic stress conditions (Kanwal 2011).

1.1.4 Freeze-thaw stress in industrial processes

Freeze-thaw stress resistance is important in cryopreservation, which is a long term storage method of a variety of living cells and used in many industrial, medical, agricultural, and food technologies. However, this method involves freezing and thawing processes that leads to lethal damage to cells. Cells subjected to multi-stress types under freeze-thaw stress conditions just as cold, dehydration, osmotic, ice crystal formation in freezing and oxidative stress in thawing process. For that reason, it is very desirable to obtain freeze-thaw tolerant organisms and explain the whole freeze-thaw tolerance mechanisms (Odani et al., 2003; Park et al., 1997).

Yeasts have high survival ratios when frozen quickly at -80 °C. However, this temperature is not used in preservation of commercial products. Generally -20 °C is applied in commercial products and causes high damage to cells and it is dominantly lethal for cells. At -20 °C application, membrane integrity of cells is disrupted due to ice crystal formation and high osmotic pressure (Codoni et al., 2003). In addition, freeze-thaw stress results in denaturation and aggregation of proteins and enzymes in cells (Santagapita et al., 2007). On the other hand, yeast viability in freeze-thaw stress is influenced by many chemical, temporal and physiological factors, including nutritional status, freeze-thaw rate, freeze-thaw temperature, duration of frozen storage, growth phase and growth rate (Lewis et al., 1993; Alves-Araujo et al., 2004). According to the growth phase, lag phase and stationary phase cells are relatively tolerant to freeze-thaw stress with their robust cellular membranes

comparing to logharitmic phase cells (Carlquist et al., 2012).

In industrial processes, the main target is to obtain desired phenotypes for production technology and quality improvement (Branduardi et al., 2008). There is a great economic interest to obtain such strains. In industrial applications, beginning from upstream to downstream processes *S. cerevisiae* cells are exposed to different environmental stress conditions. Therefore it is crucial for cells to overcome these stresses and continue to survive to produce high-quality products (Hernández-López et al., 2007; Kronberg et al., 2008).

Frozen dough is important in baking industry by saving time, space and equipment costs (Santagapita et al., 2007). Specifically, in baking industry, during the frozen dough application yeast cells are exposed to freeze-thaw stress conditions which causes reduced viability and dough leavening capacity. The freeze-thaw stress on yeast cells has significant commercial importance and economical impact in frozen dough technology. The reduced viability of cells causes high decrease in gassing rate and damaged cells secretes various reducing agents that disrupt the quality (Codoni et al., 2003,Vargas et al., 2002). To solve this problem, additional safe cryoprotecting agents such as glycerol, trehalose and prolin can be used and they have no negative effect on frozen dough quality, flavour, colour and texture (Myers et al., 1998). On the other hand, *S. cerevisiae* cells have low permeability to most of the cryoprotectant agents and especially for trehalose. Trehalose import inside the cell is an active transport process, so temperature shift to sub-zero results in inhibition of the process. Since then, those cryoprotectant agents have low benefit to cells under those stress circumstances (Todorova et al., 2012). Most of the researchers are interested in freeze-thaw stress and studied to prevent its damage to cells.

1.1.5 Freeze-thaw stress response of the yeast *Saccharomyces cerevisiae*

In industrial applications freeze-thaw stress has another importance because of its stimulating effect on multiple stress tolerances besides freeze thaw tolerance. Freeze thaw resistant strains are known to have multiple-stress tolerances to acetic acid, ethanol, H_2O_2, osmotic and heat-shock stresses. In *S. cerevisiae*, freeze-thaw stress applications induce these cross-resistances to overcome the stress effects of freeze-thaw applications (Izawa et al., 2004a). In order to obtain multiple and freeze-thaw stress tolerances, additional mechanism(s) at gene expression levels are thought to be

triggered and maintained during the freeze-thaw exposure (Vargas et al., 2002). However, tolerance responsive genes are not fully understood and well characterized. There are extensive studies about freeze-thaw stress in *S. cerevisiae*, however the molecular mechanisms behind the freeze-thaw stress tolerance remains unclear (Wei et al., 2007).

In freeze-thaw stress, the primary cell target of freeze stress was the plasma membrane. Here, two main damage mechanisms are known, which are related to cooling rate. Low cooling rates causes slow freeze and concentrated solute around the extracellular fluid of the cells that results in dehydration of cells and leads to osmotic stress. In contrast, high cooling rates lead to intracellular ice formation (nucleation) during freezing that results in cell mortality. The cellular viability can be optimized by adjusting the cooling rate, however, it is not well controlled (Odani et al., 2003; Dumont et al., 2006).

Besides freezing stage, thawing process is an another stress causing condition to cells. In thawing process, intracellular osmolarity and pH causes aggregation of macromolecules and denaturation of proteins (Vargas et al., 2002). In addition, cells exposed oxidative stress in thawing process via the formation of reactive oxygen species (Park et al., 1997).

The freeze-thaw stress has not been characterized in detail, however, according to the previous studies freeze-thaw tolerance correlates with cellular factors and cellular components including growth phase, respiratory metabolism, lipid composition of the membrane, heat shock protein levels, charged amino acids and accumulation of trehalose and glycerol. The respiratory ability and functional mitochondria are also necessary to confer resistance to freeze-thaw stress (Tanghe et al., 2002; Park et al., 1997).

Several attempts have been performed by different research groups to understand the freeze-thaw stress resistance mechanisms and to increase the freeze-thaw stress tolerance. In *S. cerevisiae*, three cold shock induced genes have been identified, *TIP1* (temperature-inducible protein) and its homologues *TIR1* and *TIR2*. The significance of the upregulation of those three genes in response to freeze stress is uncertain, however, deletion mutants of these three genes (Δtip1, Δtir1, Δtir2) lead to freeze-thaw sensitive phenotypes (Vargas et al., 2002). Moreover, it was demonstrated that

there is a high correlation between trehalose and freeze thaw stress. However, in industrial applications, trehalose accumulating abilities of the cells are decreased during the pre-fermentation period before freezing in frozen dough technology (Codoni et al., 2003).

Pre-fermentation period affects the cellular physiology of the yeast cells and leads to fermentation-induced loss of stress resistance of cells during the dough preparation process (Park et al., 1997). This action may be caused by the activation of the Ras-cyclic AMP (cAMP) protein kinase pathway and resulted in the loss of stress resistance (Tanghe et al., 2002; Verstrepen et al., 2004). Decrease in freeze-thaw tolerance due to the activation of Ras-cyclic AMP (cAMP) protein kinase pathway is related to degradation of intracellular trehalose by activation of trehalase, repression of heat shock proteins, and disappearance of other, unknown stress related protection factors (Park et al., 1997; Van Dijck et al., 2000; Tanghe et al., 2002).

Another important study includes the strong correlation between the overexpression of aquaporin genes and freeze thaw stress tolerance of *S. cerevisiae*. There are two identified aquaporin-encoding genes which are *AQY1* and *AQY2* in yeast cells. The aquaporin channels; Aqy1 and Aqy2 have function on water and glycerol transport activity across the cell membranes and determine freeze tolerance in *S. cerevisiae* (Tanghe et al., 2002; Tanghe et al., 2005).

Another reported freeze resistance mechanism comprises the glycerol dehydrogenase (*GDH*) gene. It was shown that quadruple deletion mutations of glycerol dehydrogenase genes (ara1Δgcy1Δ-gre3Δypr1Δ) caused intracellular glycerol enriched cells and conferred tolerance to freeze-thaw stress (Izawa et al., 2004a).

Frozen dough industry offers a great convenience, automation and economy in industrial scale (Park et al., 1997; Tanghe et al., 2002). Normally, 4-5 % (based on the dry weight (w/w) of the yeast) yeast is used in frozen dough, because of the reduction of leavening capacity during freeze storage. On the other hand, in the standard dough industry, this ratio is 3 %.

There is a significant increase in cost among with the standard and frozen dough. In order to minimize the costs, specialized equipment is needed for cold and rapid mixing of the dough to prevent the reduction of viability. However, the optimization of the production conditions are not enough to save increased costs and activity drop

during long-term storage. Since then, it is very important to obtain strains which have intrinsic freeze-thaw tolerance. There is much effort to produce such strains that can survive during operations comprising pre-fermentation, freezing, frozen storage and thawing (Tanghe et al., 2002; Lewis et al., 1993; Salas-Mellado et al., 2003).

Freeze-thaw stress tolerance has complex interplay in the yeast cells and genetic modification of the specific target genes does not allow freeze tolerance (Tanghe et al., 2002). There is no single factor that affects the stress tolerance and the exact mechanisms of freeze–thaw stress damages and responses of the cells are not fully identified yet (Kronberg et al., 2008).

1.1.6 Metabolic engineering

Bailey stated that metabolic engineering is "the improvement of cellular activities by manipulation of enzymatic, transport, and regulatory functions of the cell with the use of recombinant DNA technology" (Bailey et al., 1991).

The methodology of metabolic engineering has two approachs; forward and inverse metabolic engineering strategies that are thoroughly different in the manner of application. Forward metabolic engineering needs to a knowledge-based (literature, database information about the relevant phenotype) desing to improve the strain, however inverse metabolic engineering does not need any information about the relevant phenotype (Oud et al., 2012).

Forward and inverse metabolic engineering strategies are clearly summarized in Figure 1.4.

Here, to obtain the ideal phenotype two approachs which are forward and inverse metabolic engineering can be applied in turn (Oud et al., 2012).
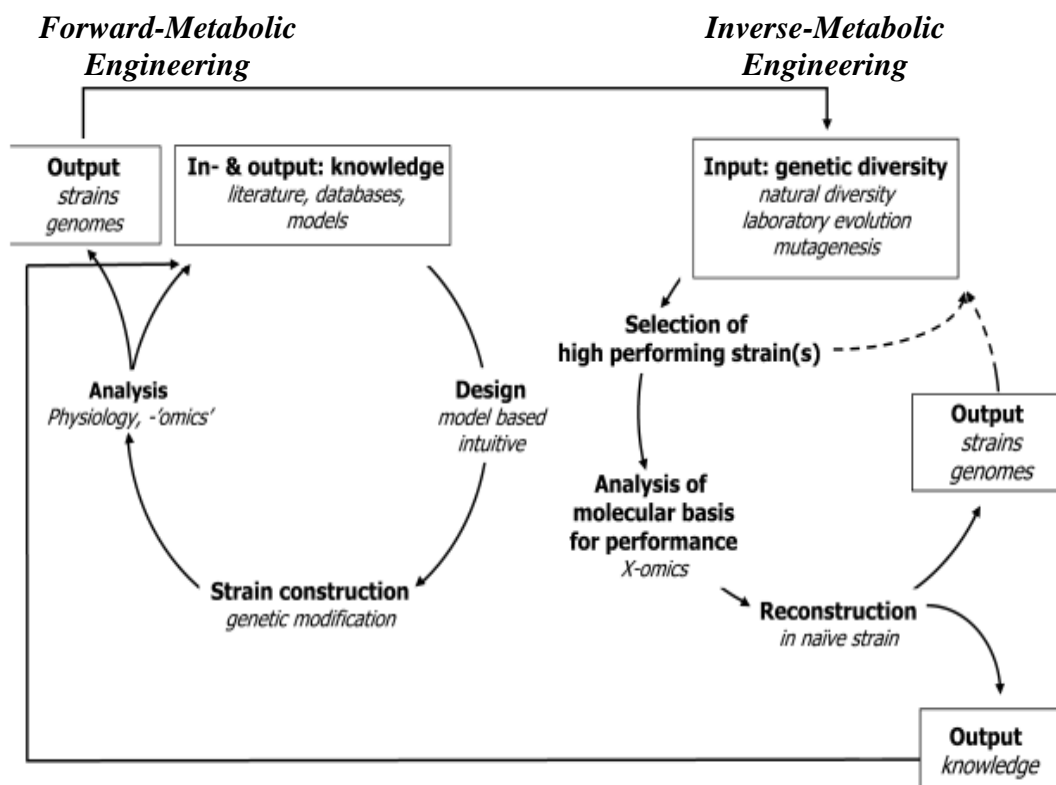
Figure 1.4: Forward and reverse metabolic engineering (Oud et al., 2012).

1.1.6.1 Evolutionary engineering to improve desired freeze-thaw resistant *Saccharomyces cerevisiae* strains

Strain improvement on the basis of inverse metabolic engineering techniques such as mutagenesis with mutagenic agents to cells and mutagenesis with recombination, error prone PCR and genome shuffling methods to genomes are useful approaches to obtain desired phenotypes. Inverse metabolic engineering techniques emphasises the "natural design principles" (Nevoigt, 2008). One of the important tools of the inverse metabolic engineering strategy is "evolutionary engineering". To improve phenotypically desired *S. cerevisiae* mutant strains, evolutionary engineering is the right choice and the perfect tool. Here, the random, non-targeted and combinatorial approach of evolutionary engineering ensures to obtain desired phenotypes and then detailed investigations of the resistance mechanism on those phenotypes would be possible (Bailey et al., 1996, Çakar et al., 2005).

Previous studies attempt to use different strategies to improve multiple stress tolerance in yeast. However, these rational approaches have met serious drawbacks because of not having clearly identified and characterized genetic basis of the

11

detailed molecular mechanism underlying freeze-thaw stress tolerance. Having the desired phenotype, ensures the presence of all of the responsible components of tolerance to stress and gives an opportunity to characterize the mechanism. Furthermore, detailed characterization of the phenotype would have a potential for various industrial applications (Çakar et al., 2005, Çakar et al., 2012).

Inverse metabolic engineering strategy involves identifying a desired phenotype, determining the genetic or the important environmental factors of that desired phenotype and improving or constructing that desired phenotype on another strain or organism by using directed genetic or environmental manipulations (Gill et al., 2003; Çakar et al., 2012). Briefly, on the basis of evolutionary engineering strategy, repetitive cycles of variation and selection is presented. Three specific steps, that are synthesis of an improved strain, analysis of the strains' performance and design of the next target for further optimization, are necessary (Petri et al., 2004).

Previous studies have shown that evolutionary engineering best fits to improve freeze-thaw resistant mutant yeast strains under extreme (-196 ºC) and industrially important frozen storage (-20 ºC) conditions (Çakar et al., 2005; Merico et al., 2011). Merico and colleagues (2001), had improved a glycerol assimilating mutant yeast strain, beside that was tolerant to freeze-thaw stress (Merico et al., 2011). However, the freeze-thaw stress assay had been performed after growing on a cryoprotectant molecule glycerol as the sole carbon source.

In this study, haploid and polyploid freeze-thaw resistant *S. cerevisiae* cells were obtained by using evolutionary engineering strategy and the molecular characterization of those resistant mutants were performed. Determination of stress resistance characteristics in *S. cerevisiae* would have a potential for various industrial applications.

1.2 Purpose of the Thesis

The aim of the present study was to obtain freeze-thaw resistant yeast strains via evolutionary engineering strategy. For this purpose haploid laboratory strain *Saccharomyces cerevisiae* CEN.PK113-7D and polyploid industrial strain *Saccharomyces cerevisiae R625* were used. It is important to obtain a laboratory

resistant strain to analyze the detailed mechanism of a complex resistance phenotype however, it is better to obtain the same phenotype on an industrial strain to contribute biotechnological area.

2. MATERIALS AND METHODS

2.1 Materials

2.1.1 Yeast strain

Saccharomyces cerevisiae haploid CEN.PK113-7D (MAT a) and its opposite mating type CEN.PK113-1A (MATα) were kindly provided by Dr. Laurent Benbadis from Toulause University, INSA-Toulouse Research Center.

Saccharomyces cerevisiae R625 polyploid strain was kindly provided by Assoc. Prof. Dr. Mustafa Türker from Pakmaya Industries.

Genetically variant *906* and *R625_M* mutant populations were obtained by EMS mutagenesis in our laboratory.

2.1.2 The compositions of yeast culture media

2.1.2.1 Yeast minimal medium (YMM)

Yeast Nitrogen Base without amino acids	6.7 g
Dextrose	20 g
Agar (for solid media)	20 g

per 1 liter of distilled water.

2.1.2.2 Yeast complex medium (YPD)

Bacto Yeast Extract	10 g
Dextrose	20 g
Bacto Peptone	20 g
Agar (for solid media)	20 g

per 1 liter of distilled water.

2.1.2.3 Yeast sporulation medium

Bacto Yeast Extract	1 g
Dextrose	0.5 g
Potassium acetate (KAc)	10 g
Bacto Agar	20 g

per 1 liter of distilled water.

2.1.3 Yeast cultivation conditions

Yeast cells were cultivated at 30˚C. The agitation rates were 150 rpm for each cultivation.

2.1.4 Chemicals

Table 2.1 : The list of chemicals.

Absolute Ethanol (99 %)	J.T.Baker
Acetic acid	Merck (Germany)
Ammonium iron (II) sulfate hexahydrate	Merck (Germany)
Agar agar	AppliChem (Germany)
Agarose	Applichem (Germany)
Bacto Peptone	BD DifcoTM (USA)
Boric Acid	Fluka
Chromium (III)- chloride - hexahydrate	Acros Organics (USA)
Cobalt (II)- chloride–hexahydrate	Merck (Germany)
Copper (III)- chloride	Sigma Aldrich (USA)
DEPC (Diethylene Pyrocarbonate)	Ambion (USA)
D-Glucose	VWR BDH PROLABO (UK)
DNA markers	Fermentas (Lithuania)
Ethylenediaminetetraacetic acid disodium salt dihydrate, EDTA	Merck (Germany)
EMS	Alpha-Aeasar
Ethanol	J.T.Baker (The Netherlands)

Table 2.1 (continued): The list of chemicals.

Glycerol	Sigma Aldrich (USA)
HPLC grade water	Merck (Germany)
Hydrogen peroxide (% 35, v/v)	Merck (Germany)
Iso-propanol	Merck (Germany)
Magnesium chloride hexahydrate	Merck (Germany)
Methanol	Merck (Germany)
Mycological Agar	AppliChem (Germany)
NaCl	Carlo Erba (Italy)
Nickel (II)- chloride - hexahydrate	Sigma Aldrich (USA)
Nitric acid 65%	Merck (Germany)
Sodium thiosulphate pentahydrate	J.T.Baker (Holland)
Sulphuric acid 95-98%	Merck (Germany)
Trehalase (from porcine kidney)	Sigma Aldrich (USA)
Tris	Merck (Germany)
Tyrptone	Merck (Germany)
Yeast Extract	Merck (Germany)
Yeast Nitrogen Base (YNB)	BD DifcoTM (USA)
$ZnCl_2$	Riedel- de Haën (The Netherlands)
Zymolyase	Zymo Research
Glycose oxidase/peroxidase reagent	Sigma Aldrich (USA)
Lithium acetate	Sigma Aldrich (USA)

2.1.5 The compositions of buffers and solutions

2.1.5.1 Composition of phosphate buffer saline (PBS) 50 mM, pH 7.4

NaCl (Sodium Chloride)	8 g
KCl (Potassium Chloride)	0.2 g
Na_2HPO_4 (Disodium Hydrogen Phosphate)	1.44 g
KH_2PO_4 (Potassium Dihydrogen Phosphate)	0.24 g

per 1 liter of DEPC treated distilled water.

2.1.6 Kits and markers

Table 2.2 : The list of kits, DNA and protein markers.

MassRuler™ Express Reverse DNA Ladder Mix (SM 1293)	(Fermentas, Lithuania)
High Pure PCR Template Preparation Kit (Cat: 11796828001)	Roche (Switzerland)
High Pure RNA Isolation Kit (Cat No: 11 828 665 001)	Roche (Switzerland)
Transcriptor First Strand cDNA Synthesis Kit (Cat No: 04 379 012 001)	Roche (Switzerland)
LightCycler® 480 SYBR Green I Master Kit (Cat No: 05 091 284 001)	Roche (Switzerland)
RNA SuperScript® III First-Strand cDNA Synthesis Kit	Invitrogen (USA)
Low Input Quick Amp Labeling Kit	Agilent (USA)
One-color RNA Spike-In Kit	Agilent (USA)
Absolutely RNA Nanoprep Kit	Agilent (USA)
RNA 6000 Nano LabChip Kit	Agilent (USA)
Qubit RNA Kit	Invitrogen(USA)
Yeast DNA Purification Kit (Master Pure TM)	Epicentre, MPY2-70921 (USA)

2.1.7 Laboratory equipment

Table 2.3 : The list of laboratory equipments.

Autoclaves	Tomy SX 700E (China) Tuttnauer Systec Autoclave 2540ml - 2870ELVC(Switzerland)
Balances	Precisa BJ 610C (Switzerland) Precisa 620C SCS (Switzerland)
Deep Freezers and Refrigerators	-80 ˚C Sanyo Ultralow (Japan), -20 ˚C, +4˚C Arçelik (Turkey)
Ultrapure Water System	USF-Elga UHQ (USA)
Thermal Cycler	T-100 Thermal Cycler (Bio-Rad, USA)
Transilluminator	Vilber Lourmat (Germany)

Table 2.3 (continued): The list of laboratory equipments.

Elecrophoresis Tanks	Minicell PrimoTM EC 320
Power supply for Electrophoresis	EC Apparatus Corporation EC 250-90
HPLC (High Performance Liquid Chromatography) System	
- Refractive Index Detector	Shimadzu RID10A (Japan)
- System Controller	Shimadzu SCL10A) (Japan)
- Liquid Chromatography	Shimadzu LC-10AD (Japan)
- Degasser	Shimadzu ss DGU-14A (Japan)
- Column Oven	Shimadzu CT0-10AC (Japan)
Laminar Flow	Faster BH-EN (Italy)
Real Time-PCR	LightCycler 480 II Roche (Switzerland)
Light Microscope	Olympus CH30 (Japan)
Microfuge	Eppendorf Santrifüj 5424 (Germany)
Micropipettes	Eppendorf (Germany)
Microplate Reader	Biorad Model 3550 UV (USA)
Orbital Shaker Incubators	Certomat S II Sartorius (Germany)
pH Meter	Mettler Toledo MP220 (Switzerland)
Qubit Quantification Platform	İnvitrogen (USA)
Rotor	Beckman Coulter JA-30.50i (USA)
Thermal cycler	Bio-Rad My cyclerTM (USA)
Thermomixer	Eppendorf (Germany)
Ultrapure Water System	USF-Elga UHQ (USA)
UV-Visible Spectrophotometer	Shimadzu UV-1700 (Japan)
Nano Drop	Nano Drop 2000-Thermo SCIENTIFIC (USA)
Centrifuge	Beckman Coulter Allegra 25R Benchtop Centrifuge (USA)
Bioanalyser 2100	Agilent Technologies (USA)
Bioreactor	B. Braun, Biostat Q with Digital Measurement and Control System DCU 3 (Germany)
Vortex mixer	Heidolph (Germany)
Hybridization Chamber	Discovery from Ventana Medical System (USA)
Digital Color Camera	Leica, DFC 300FX (Germany)
Glass slides	Agilent (USA)
Incubators	Nüve EN400 - EN500 (Turkey)
Magnetic Stirrer	Labworld (Germany)

2.1.8 Softwares and websites

Table 2.4: The list of software, websites and database.

Primer3Plus	http://www.bioinformatics.nl/cgibin/primer3plus/primer3plus.cgi)
Amlify3 3.1.4 version MacOS X	http://engels.genetics.wisc.edu/amplify/
Fast PCR 6.0	http://primerdigital.com/fastpcr.html
S. cerevisiae Genome Database	http://www.yeastgenome.org
SGD Yeast CYC Biochemical Pathways	http://pathway.yeastgenome.org/
Funcat	http://mips.helmholtz-muenchen.de/proj/funcatDB/
FunSpec	http://funspec.med.utoronto.ca/
GO Princeton	http://go.princeton.edu/
GeneSpring GX	Agilent Technologies (USA)
PCA	Matlab Principal Component Analysis Code
The Princeton growth rate/gene expression relationship database	http://growthrate.princeton.edu/transcriptome/analyze.shtml

2.2 Methods

To obtain freeze-thaw resistant *Saccharomyces cerevisiae* mutant individuals, evolutionary engineering strategy was performed. The studies were maintained in two parallel ways with two different *S. cerevisiae* strains, which were laboratory strain *Saccharomyces cerevisiae* CEN.PK113-7D and industrial strain *Saccharomyces cerevisiae R625*.

2.2.1 Studies with haploid *Saccharomyces cerevisiae* CEN.PK113-7D

2.2.1.1 Evolutionary engineering strategy to obtain freeze-thaw resistant mutants

- **EMS mutagenesis**

Ethyl methane sulphonate (EMS) mutagenized *Saccharomyces cerevisiae* CEN.PK 113-7D (also named as *905* throughout this study) cells were obtained by applying the EMS mutagenesis method (Lawrence et al., 1991). *Saccharomyces cerevisiae*

CEN.PK 113-7D stock culture was taken from the frozen stock (-80 ˚C) and inoculated into 50 mL test tube which contained 10ml YMM. After overnight incubation at 30 ˚C and 150 rpm, 500µl of this preculture was inoculated into 25 mL YPD. This culture was incubated overnight at 30 ˚C and 150 rpm. The 2.5 mL of this culture was washed twice by using 50 mM potassium phosphate buffer (pH 7). Then the culture cell pellets were resuspended in 10 mL of the same solution and the final cell number was set of $5*10^7$ cells/ml. The resuspended cells were transferred into a screw-cap glass tube and 300 µl EMS was added onto it and this tube was incubated at 30 ˚C for 30 min. There after, freshly prepared and filter-sterilized sodium thiosulphate solution (10 %, w/v) was equally added to the solution to stop the mutagenesis. The solution was then entirely mixed and centrifuged at 10000 rpm for 10 min. The supernatant was discarded and the cell pellet was washed twice by using YMM without dextrose. The mutagenized cells were inoculated into YPD and named as *906*.

- **Selection of mutant populations by using pulse stress selection strategy**

In pulse stress selection strategy, gradually increasing type of stress selections were applied to the mutant generations. At the beginning of the selection strategy, EMS mutagenized *906* cell cultures were exposed to freeze-thaw stress only for 120 min (freezing time) plus 10 min (thawing time) for obtaining the first generation. Frozen stock aliquot of *906* culture was inoculated into 10 mL YMM and overnight incubated at 30 ˚C, 150 rpm. After overnight incubation, spectrophotometric measurements were done and cells were inoculated into 10 mL YMM by adjusting optical density (600 nm) to 0.2. When the culture OD_{600} values reached 4.5 to 5.5, two set of one mL cells from the culture was transferred into a 2 mL microfuge tubes. One of them was used as control, the other one for gradually increasing freeze-thaw-stress application. Cells were centrifuged at 12000 rpm for 5 min, supernatants were discarded and the cell pellets were washed twice by using YMM without dextrose. Then cells were resuspended in YMM without dextrose. The control one was inoculated into YMM containing 96 well plates for five tube-MPN (Most Probable Method) analysis and the other one exposed to -20 ˚C freeze stress for 120 min. After one cycle freeze stress, cells were thawed 10 min at 30 ˚C. Then cells were both inoculated into YMM containing 96 well plates for 5 tube-MPN (Most Probable Method) analysis and 10 mL YMM containing 50 mL test tubes for

obtaining the first generation. Next generations were obtained by the same procedure, except the freeze-thaw cycles were gradually increased. Frozen stock cultures were prepared after each mutant generation was obtained. The steps of the experimental procedure are shown in the Figure 2.1. Here, we started freeze-thaw stress application with the cells optical density between 4.5 – 5.5. It is because; the cells were more fragile to freeze-thaw stress at this late exponential phase.
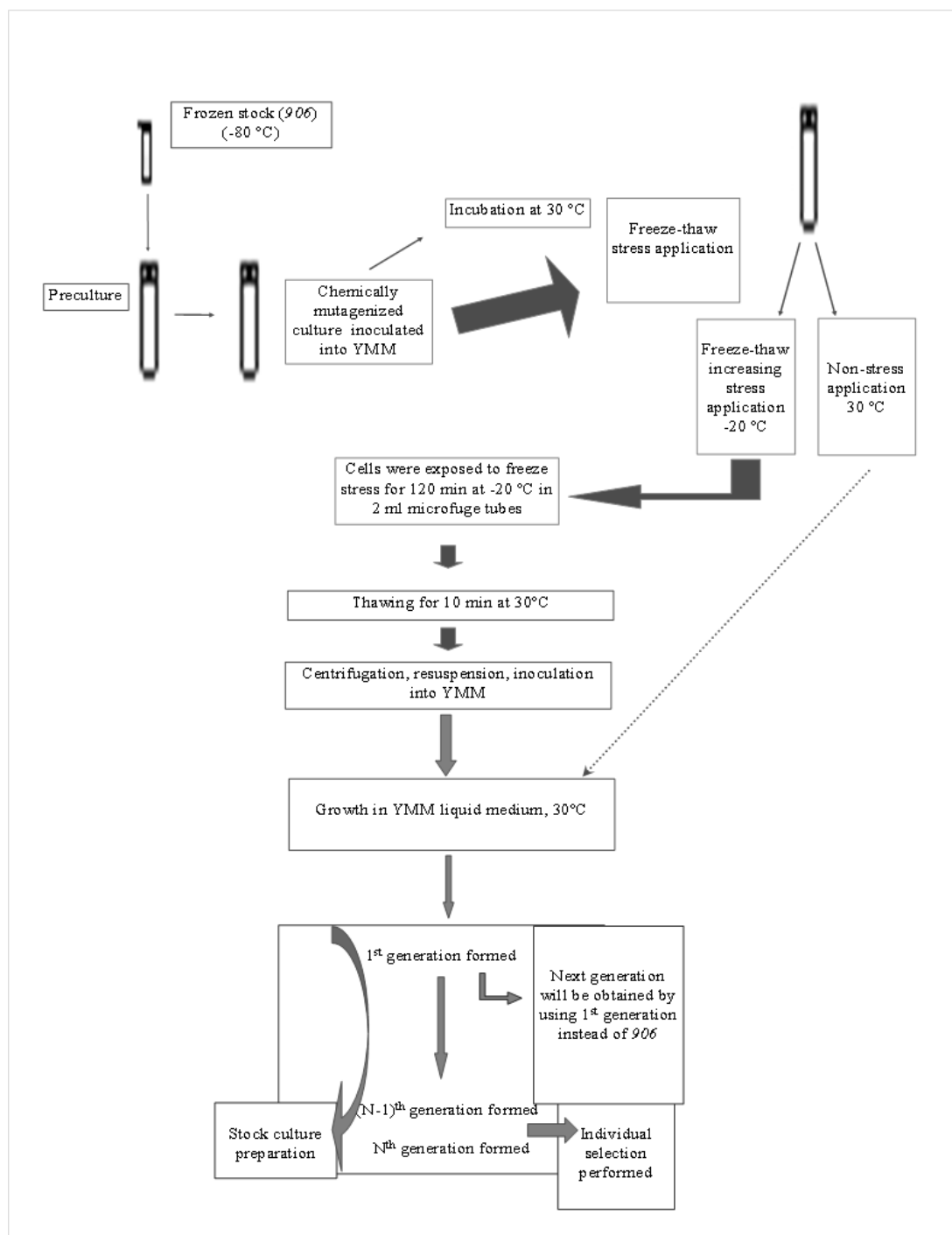
Figure 2.1: The schematic representation of the process of evolutionary selection strategy.

The survival ratios of each mutant generation were determined according to MPN results by dividing the cell/ml numbers of stress applied ones to the cell/ml numbers of its control one.

- **Selection of individual mutants from final mutant generation**

After obtaining the increasing stress final generation, selection of the individual mutants were performed. The last mutant generation was inoculated onto solid agar plates by spreading method, after serial dilution (the last dilution was 10^{-6}). The cultures were incubated at 30 ˚C for 48 h. The yeast colonies were then chosen randomly by using sterile toothpicks then transferred into 10 mL YMM. The individual stock cultures were prepared after overnight incubation.

2.2.1.2 Phenotypic analysis of thewild-type and mutant individual *F1*

- **Screening of the mutant individuals**

Screening of freeze-thaw resistance of individual mutants was performed by two cycles of freeze-thaw stress application.

Individual mutants were exposed to freeze-thaw stress only for 120 min (freezing time) plus 10 min (thawing time) for obtaining the first cycle. Individual mutant cultures were inoculated into 10 mL YMM and incubated at 30 ˚C, 150 rpm. When the culture OD_{600} values reached at 4.5 to 5.5, three set of one mL cells from each culture was transferred into a 2 mL microfuge tubes. One of them was used as control and the other two were used for gradually increasing freeze-thaw stress application. Cells were centrifuged at 12000 rpm for 5 min and supernatants were discarded and the cell pellets were washed twice by using YMM without dextrose. Then cells were resuspended in YMM without dextrose. The control one was inoculated into YMM containing 96 well plates for five tube-MPN (Most Probable Method) analysis and the others exposed to -20 ˚C freeze stress for 120 min. After one cycle freeze stress, two set of microfuge tube cells were thawed 10 min at 30 ˚C. Then one of the microfuge tubes that were containing each individual mutant cells were inoculated into YMM containing 96 well plates for 5 tube-MPN (Most Probable Method) analysis. The other microfuge tubes were exposed to second freeze-thaw application. After the second cycle each individual mutant cells were inoculated into YMM containing 96 well plates for 5 tube-MPN analysis.

The survival ratios of each individual mutant was determined according to MPN results after 72 h incubation by dividing the cell/ml numbers of stress applied ones to the cell/ml numbers of its control one. The most freeze-thaw resistant mutant individual *F1* was selected among the other resistant ones.

- **Cross-resistance analysis of the freeze-thaw resistant mutant individual *F1***

905 and all the individuals which were obtained from pulse freeze-thaw stress strategies were screened by applying different type of stress conditions in order to determine their potential cross-resistances to corresponding stresses.

By using continuous stress strategies, different stress factors (nickel, cobalt, chromium, iron, magnesium, zinc, boron and ethanol) were applied to the mutant individuals by using spotting assay and 5-tube MPN method.

- **Cross-resistance analysis via spotting assay**

The optical densities (OD_{600}) of the overnight incubated *905* and *F1* cell cultures were measured and transferred into a microfuge tubes at corresponding 8 optical density units. The cell cultures were then centrifuged at 14000 rpm, 5 min. Supernatant were discarded and then 100 µl sterile dH_2O were added onto pellets in microfuge tubes. After then, the cell cultures were diluted from 10^{-1} to 10^{-4} in 96-well plates and dropped on to YMM w/wo stress factor containing plates. The cultures were incubated at 30 $^{\circ}$C. After 72 h time period, the growth images were taken.

- **Cross-resistance analysis via MPN (Most Probable Number) method**

S. cerevisiae cells and freeze-thaw resistant mutant individual *F1* were screened at different stress conditions via 5-tube MPN methodology. Overnight incubated *905* and *F1* cells were precultured and incubated at 30 $^{\circ}$C until the cells were reached at exponantially growth phase. Then the MPN analysis were performed at control and stress conditions. The cross-resistance of mutant individual *F1* was determined under various metal, oxidative, osmotic and heat stress conditions.

- **Principle component analysis (PCA)**

Principal Component Analysis (PCA) is a mathematical technique to reveal internal variance of the multi-dimensional data. It is a true eigenvector-based multivariate analyses. Briefly in PCA, the axes are the principal components (PCs) that were

ordered by variance. The eigenvector of the covariance matrix are the principal components. First Principal component (the eigenvector) indicates the largest variance (the eigenvalue) of the data. The second component, indicates the largest variance (the eigenvalue) orthogonal to the first principle component (Novembre and Stephens, 2008).

Here, this computational analysis method was used to reveal phenotypic variance between wild-type and mutant individuals by means of responses to stresses. Experimentally measured cross-resistance data was used for the pca analysis.

- **Diploidization of wild-type and freeze-thaw resistant mutant individual *F1***

Mat a type *S. cerevisiae 905* and *F1* coded cells and mat α type *S. cerevisiae 934* coded cells were overnight incubated on YPD containing solid medium. Then, those two different mating type cells were mixed on YPD containing solid medium by the help of a sterile tip. After overnight incubation at 30 $^{\circ}$C, *905 / 934* and *F1/ 934* coded cells were inoculated on solid medium by streaking to obtain single colonies from the cells. Cultures were 48 h incubated at 30 $^{\circ}$C. Then 10 single colonies were picked from each culture and transferred to the sporulation (2 % potassium acetate, pH 7.0) medium. Only the diploidized cells can form tetrads so, the tetrad formations were checked under the microscope after 6 h incubation.

- **Cross resistance analysis of haploid and diploid wild-type and mutant individual *F1***

After diploidization of wild-type and mutant cells, cross resistance analyses were performed. Different types of stresses were investigated by using spotting assay. This method enables us to compare haploid and diploid cells at those stress conditions. Overnight incubated cell cultures were diluted from 10^{-1} to 10^{-4} and dropped on to YMM w/wo stress factor containing plates. Then the cultures were incubated at 30 ^{0}C for 72 hours.

2.2.1.3 Physiological analysis of the wild-type and mutant individual *F1*

Physiological analysis were performed via batch culture and bioreactor.

- **Growth curve analysis of wild-type and mutant individual *F1***

Growth curve analysis was done for both freeze-thaw resistant mutant individual *F1* and wild-type strains. Exponentially growth wild-type and freeze-thaw resistant mutant individual *F1* cells were inoculated in 10 mL liquid yeast minimal medium (YMM) for growth curve analysis. After overnight incubation, cells were inoculated into 400 mL YMM. The initial OD_{600} value was adjusted to 0.1. Then, cells were incubated at 30 °C, 150 rpm for 30 hours. Appropriate volume of triplicate samples were taken from each culture for spectrophotometric measurements and HPLC analysis at different time intervals. Growth curve of two strains were constructed as lnOD / time.

In bioreactor analysis, both freeze-thaw resistant mutant *F1* and wild-type strains were analyzed. After overnight incubation, cells were inoculated into 400 mL YMM containing bioreactor vessels (1 L volume). The initial OD_{600} value was adjusted to 0.2, the aeration rate was adjusted to 0.1 L/ min air, the pH was adjusted to 4.5± 0.1 with 3 M HCl. Then, cells were incubated at 30 °C, 150 rpm for 30 hours. Before starting the inoculation, all of the parameters; pH, aeration, stirring and temperature were calibrated and controlled. In addition, the pH was maintained constant with 3 M KOH solution and aeration rate was maintained constant with an air compressor during the experiments. To prevent foaming, 500 µl PEG2000 was added on each bioreactor vessels.

- **High performance liquid chromatography (HPLC) analysis of wild-type and mutant individual *F1***

HPLC analysis was used for determination of metabolites in samples which were taken from mutant and wild-type strains at certain times while the growth curve analysis in batch and bioreactor experiments. Samples were centrifuged at 14000 rpm for 5 minutes. The supernatants were collected by an injector and then filtered (0.22 pore sized filter) for HPLC analysis.

Aminex® HPLCcolon was used for the separation of the metabolites. The isocratic method was used according to the manufacturer's protocol for the analysis. 5 mM sulfuric acid was used as mobile phase. The analytical procedure was adjusted to 0.6 mL/min flow rate, 60 ºC temperature and 20 µl sample volume. Measurements were performed by using refractive index (RI) detector.

Standard curve method was used for the quantitative analysis of the metabolites. Standart solutions were prepared for each metabolite at specific consentrations.

A and B stock solutions were prepared as in the Table 2.1 in order to prepare standard solutions to construct standard curves.

Table 2.5: The composition of stock A and B solutions.

Stock Solution A		Stock Solution B	
Content	**Amount**	**Content**	**Amount**
Glucose	120 g	Succinate	1 g
adjust final volume to 1 L with ddH$_2$O		Acetate	4 g
		Glycerol	2 g
		Ethanol	30 g
		adjust final volume to 1 L with ddH$_2$O	

The standard solutions for the standard curves are prepared as in Table 2.2. Sulfuric acid (5 mM) was used as the eluent for preparation of the standards.

Table 2.6: The preparation of standard solutions.

Standard Solutions	Mixing Volumes	Volume of Eluent (ml)	Final Volume (ml)
Std 1	1 mL Solution A 3 mL Solution B	2.000	6
Std 2	0.750 mL Std 1	0.250	1
Std 3	0.500 mL Std 1	0.500	1
Std 4	0.250 mL Std 1	0.750	1
Std 5	0.125 mL Std 1	0.875	1
Std 6	0.063 mL Std 1	0.937	1

The concentrations of succinate, acetate, glycerol, glucose and ethanol at the standard solutions are indicated in Table 2.3.

Table 2.7: The metabolite concentrations of HPLC standards.

Metabolite	Std 1	Std 2	Std 3	Std 4	Std 5	Std 6	Retention Time
			(g/L)				(min)
Glucose	20	15	10	5	2.5	1.25	8.84
Succinate	0.5	0.375	0.250	0.125	0.0625	0.03125	11.53
Glycerol	1	0.750	0.500	0.250	0.1250	0.06250	13.53
Acetate	2	1.500	1.000	0.500	0.2500	0.12500	15.13
Ethanol	15	11.25	7.500	3.750	1.8750	0.93750	22.65

After preparation of the standard solutions, 1 mL of each standard and the samples were transferred into the HPLC tubes. HPLC measurements were performed by using refractive index detector.

- **Reserve carbohydrate analysis of wild-type and mutant individual *F1***

The reserve carbohydrates, glycogen and trehalose were analyzed by using glucose oxidase/peroxidase assay (Parrou and François, 1997).

Overnight incubated *F1* and wild-type cells were inoculated into 500 mL flask containing 100 mL YMM and incubated at 30 °C, 150 rpm. Then the cultures were scaled up to 2 l flask containing 400 mL YMM, when they were reached at exponantial growth phase. 25 OD_{600} unit cells were collected at certain times while the wild-type and *F1* cells were growing. For cell dry weight analysis 1 mL extra samples were collected at each specific sampling points. The samples were centrifuged at 14000 rpm for 5 minutes. The supernatants were dropped and the pellets were transferred into -20 °C refrigerator. After collecting the all samples at specific growth points, the stored samples were thawed and the analysis were started. 250 μl 0.25 M Na_2CO_3 were added onto each pellets and vortexed. Samples were incubated at 95 °C for 2-4 h. Then 150 μl 1 M acetic acid and 600 μl 0.2 M sodium acetate (pH 5.2) were added onto samples and vortexed. Thereafter, each sample were divided into 2 microfuge tubes, one for trehalose and the other for glycogen determination. For trehalose analysis, 10 μl trehalase enzyme was added onto first set samples and overnight incubated at 37 °C. For glycogen analysis, 20 μl alpha-glycosidase enzyme was added onto second set samples and overnight incubated at 57°C. After overnight incubation measurements were performed by multiwell plate reader. To measure the glucose contents of each samples; first, the glucose standards were prepared and then the standart curve was constructed to determine the

concentration of the unknown samples. For this reason, 200 μl glucose oxidase/peroxidase reagent (Sigma) was added into 96 well plates, then 20 μl standards and the samples were added into wells. After 30 min incubation at 37°C, the absorbance measurements were performed at 490 nm.

2.2.1.4 Genetic analysis of the wild-type and mutant individual *F1*

- **Transcriptomic analysis via real time-PCR (Q-PCR)**
- ❶ **Primer design**

The specific primer design of the interested genes were analyzed by "Primer3 Plus Software" and "Amplify3 - 3.1.4 version - MacOS X" softwares. The specific primers are listed in Table 2.4.

AQY1, AQY2, CTT1, GSH1 and FPS1 genes were studied for transcriptomic analysis.

Table 2.8: The list of primer sequences.

Gene Name	Primer Sequence		Amplicon (bp)
	Forward	**Reverse**	
ACT1	CTTTCAACGTTCCAGCCTTC	TCACCGGAATCCAAAACAAT	94
AQY1	TCGGCATCTCCCTGTTTATC	TGAGCTTTTTCCTTGGTGCT	244
AQY2	ACCATGATGTGGCTTTGAC	ATCCCAGCAATGATCTGAGG	212
CTT1	TGCAAGACTTCCATCTGCTG	ACGGTGGAAAAACGAACAAG	193
FPS1	CGTGGTGATGGGCTATTTCT	AACATTCCCGCAACACTTTC	240
GSH1	CCCCAGCGTAATTTTCTCAC	GTGCAGACCGACAACCTTTT	202

❷ **Total RNA isolation from yeast cells (wild-type and mutant individual *F1*)**

Wild type and *F1* cultures were inoculated into 10 mL YMM and incubated at 30 ˚C, 150 rpm. When the culture OD_{600} values reached at 4.5 to 5.5, two set of one mL cells from each culture was transferred into a 2 mL microfuge tubes. One of them was used as a control group to isolate total RNA and the other one was used as a stress group to isolate total RNA. Cells were centrifuged at 12000 rpm for 5 min and supernatants were discarded and the cell pellets were washed twice by using YMM without dextrose. Then cells were resuspended in YMM without dextrose. The control one was isolated and the other one exposed to -20 ˚C freeze stress for 120

min. After one cycle freeze stress, cells were thawed 10 min at 30 ˚C. Then cells were exposed to second freeze-thaw stress application. After the second cycle stress application, the total RNA isolation was performed. Roche - High Pure RNA Isolation Kit (Cat. No. 11 828 665 001) was used to isolate total RNA from yeast cells.

❸ Measurement of total RNA concentration

Quant-iT™ RNA Assay Kit (Cat. No. Q32855) and Qubit® Florometer were used to measure total RNA concentrations and also the results were confirmed by nano drop.

❹ cDNA synthesis

Transcriptor High Fidelity cDNA Synthesis Kit (Cat. No. 05 081 955 001) was used for cDNA synthesis from total RNA samples.

❺ Real time-PCR applications

Roche-LightCycler® 480 DNA SYBR Green I Master Kit (Cat. No. 04 707 516 001) was used for real time-PCR applications. The ingredients of the reaction mix are indicated in Table 2.5. Standard curves were constructed for each gene and the internal control housekeeping gene beta-actin (ACT1). The relative expression levels of each target genes were examined by using $2^{-\Delta\Delta Ct}$ method (Livak and Schmittgen, 2001). The efficiency, error and slope values of each standard curve and the melting curves of each Q-PCR was analyzed in detail (Dorak, 2006).

Table 2.9: The Q-PCR protocol.

PCR Components	Volume
Water	3 µl
PCR Primers (F+R)	2 µl
Syber Mix	10 µl
Template	5 µl
Total Volume	20 µl

The optimized program for Q-PCR analysis is indicated in Table 2.6.

Table 2.10: The optimized program used in Q-PCR analysis.

	Temperature (C°)		Time	Cycle
Pre-incubation	95		10dk	1
Amplification	Denaturation	95	10 sec	
	Annealing	56	18 sec	45
	Elongation	72	20 sec	
Melting	95		5 sec	
	65		1 min	1
	97			
Cooling	40		10 sec	1

- **Whole genome transcriptomic analysis via DNA microarray technology**

The whole genome transcriptomic analysis was performed by using high throughput DNA microarray technology.

❶ **Isolation of total RNA**

Frozen stock cultures of wild-type and freeze-thaw resistant mutant individual *F1* were inoculated into 10 mL YMM and overnight incubated at 30 °C, 150 rpm. Exponentially growth wild-type and *F1* cultures were re-inoculated into 100 mL YMM and the OD_{600} values were adjusted to 0.1. The inoculations were prepared as triplicate for each sample. Cultures were incubated at 30 °C, 150 rpm until their OD_{600} values reached ~1 (5 x 10^7 cells/ml). The specific growth rates of wild-type and mutant were different from each other so, cells were cought at the same optical density value to minimize the error. Then the total RNA isolations of each triplicate were performed by using "Qiagen RNeasy Mini Kit" (Cat: 74104, Qiagen, USA). The total RNA isolates were stored at -80 °C.

❷ **Determination of RNA Integrity Numbers (RIN)**

"RNA 6000 Nano Assay Kit" (Cat: 5067-1511, Agilent, USA) was used to check the concentrations and quality of isolated RNA. The samples were analyzed with Agilent BioAnalyzer 2100 and the RNA integrity numbers (RIN) were calculated.

❸ **DNA Microarray Analysis**

Before starting, "Agilent one-color RNA spike-in kit" (Cat: 5188-5282, Agilent, ABD) was used to obtain internal controls with known concentrations. Then the total RNA samples were mixed with diluted RNA spike-in controls and labelled with Cy3 by using "Agilent low input quick amp labeling Kit" (Cat: 5190-2305, Agilent, USA). The Cy3-labelled samples were purified with "Absolutely RNA Nanoprep

Kit" (Cat: 400753, Agilent, USA). The concentrations of the samples were measured by nanodrop and then same volume of each triplicate samples were placed on microarray slides (RNA 6000 NanoLabChip® Kit, Cat: 5065-4476, Agilent, USA). The microarray slides were transferred into Agilent Microarray Hybridization Chamber. After 17 h hybridization process, the slides were washed and then transferred into Agilent C scanner device. The microarray data was analyzed by GeneSpring GX 9.0 software. The mean expression profile of *F1* was normalized to wild-type by this software and then the functional categorization of up and down regulated genes were done according to FunSpec and FunCat databases. The gene expression and growth relation analysis were done by using Princeton growth rate/gene expression relationship database.

2.2.2 Studies with polyploid baker's yeast *Saccharomyces cerevisiae R625*

2.2.2.1 Evolutionary engineering strategy to obtain freeze-thaw resistant mutants

- **EMS mutagenesis**

Polyploid Baker's Yeast *Saccharomyces cerevisiae R625* cells were mutagenized by applying the ethyl methane sulphonate (EMS) mutagenesis method (Lawrence et al., 1991). *S. cerevisiae R625* stock culture was taken from the frozen stock (-80 ˚C) and inoculated into 50 mL test tube which contained 10 mL YPD. After overnight incubation at 30 ˚C and 150 rpm, 500µl of this pre-culture was inoculated into 25 mL YPD. This culture was incubated overnight at 30 ˚C and 150 rpm. The 2.0 mL of this culture was washed twice by using 50 mM potassium phosphate buffer (pH7). Then the culture cell pellets were resuspended in 10 mL of the same solution and the final cell number was set of $5x10^7$cells/ml. The resuspended cells were transferred into a screw-cap glass tubes and 300 µl, 600 µl, 900 µl EMS was added and they were incubated at 30 ˚C for 30 min. Thereafter, freshly made filter-sterilized sodium thiosulphate solution (10 %, w/v) was equally added to the EMS containing tubes to stop the mutagenesis. The solution was then entirely mixed and centrifuged at 10000 rpm for 10 min. The supernatant was discarded and the cell pellet was washed twice by using YMM without dextrose. The mutagenized cells were inoculated into YMM. After 48 h incubation at 30˚C, the mutagenized cell cultures were labeled and preserved in 30 % glycerol (v/v) solution at -80 ˚C.

- **Screening of polyploid baker's yeast *Saccharomyces cerevisiae* and Mutant population under freeze-thaw stress conditions**

S. cerevisiae R625 cells and genetically variant *Saccharomyces cerevisiae R625_M* mutant population were screened by applying 1-4 cycle freeze-thaw stress.

R625 and *R625_M* mutant population was inoculated into 10 mL YMM and overnight incubated at 30°C, 150 rpm. After overnight incubation, spectrophotometric measurements were done and cells were inoculated into 10 mL YMM by adjusting optical density (600 nm), 0.2. When the cultures OD_{600} values reached 4.5 to 5.5, five set of one mL cells from each culture was transferred into 2 mL microfuge tubes. One set of each culture was used as control, the other ones for freeze-thaw stress application. Cells were centrifuged at 12000 rpm for 5 min and supernatants were discarded and the cell pellets were washed twice by using YMM without dextrose. Then cells were resuspended in YMM without dextrose. The control one was inoculated into YMM containing 96 well plates for five tube-MPN (Most Probable Method) analysis and the other ones exposed to -20 °C freeze stress for 120 min. After one cycle freeze stress, cells were thawed 10 min at 30 °C. One of them was inoculated into YMM containing 96 well plates for 5 tube-MPN (Most Probable Method) analyses. The other samples were transferred -20 °C freeze storage for the next freeze-thaw stress cycles. Here, we started freeze-thaw stress application with the cells optical density between 4.5-5.5. It is because; the cells were more fragile to freeze-thaw stress at this late exponential phase.

- **Selection of mutant generations by using pulse stress selection strategy**

The process of pulse, increasing stress selection strategy was applied by the same as the Section 2.2.1.1.2 and the schematic representation is indicated in Figure 2.1.

The first generation was from one cycle freeze-thaw stress application and the last that called *R625_10FG* final generation was obtained by repetetive ten cycles of stress application.

- **Selection of mutant individuals from final mutant generation**

After obtaining the pulse increasing stress final generation, selection of the mutant individuals were performed randomly on solid YMM.

2.2.2.2 Phenotypic analysis of the wild-type and the mutant individual*s*

- **Screening of the mutant individuals**

Screening of *R625* and the mutant individuals were performed at freeze-thaw stress condition with two different methods which were 5- tube MPN and spotting assay.

- **Cross-resistance analysis of the freeze-thaw resistant mutant individual*s***

Wild-type *R625* and the individuals were screened by applying different type of stress conditions in order to determine their potential cross-resistances to corresponding stresses. By using continuous stress strategies, different stress factors (nickel, cobalt, chromium, iron, magnesium, zinc, boron, NaCl and ethanol) were applied to the mutant individuals by using spotting assay and 5-tube MPN method.

- **Cross-resistance analysis via spotting assay**

R625 and the mutant individuals were screened at different stress conditions via spotting assay and after 72 h period, the growth images were taken.

- **Cross-resistance analysis via MPN (Most Probable Number) method**

R625 and the mutant individuals were screened at different stress conditions via 5-tube MPN method and after 72 h time period, the cell number / mL values were noted and the survival ratios were determined.

2.2.2.3 Physiological analysis of wild-type and mutant individual *R625_P8*

The physiological analyses were performed via batch culture and bioreactor.

- **Growth curve analysis of wild-type and mutant individual *R625_P8***

Growth curve analysis was done for both freeze-thaw resistant polyploid mutant *R625_P8* and wild-type strains. Exponentially growth cells were inoculated in 100 mL liquid yeast minimal medium (YMM) for growth curve analysis. After overnight incubation, cells were inoculated into 400 mL YMM. The OD_{600} value was adjusted to 0.1. Then, cells were incubated at 30 °C, 150 rpm for 30 hours. Appropriate volume of sample was taken from each culture for spectrophotometric measurements

and HPLC analysis at different time intervals. Growth curve of two strains were constructed as lnOD / time.

In bioreactor analysis, overnight incubated cells were inoculated into 400 mL YMM containing bioreactor vessels (1 L volume). The initial OD_{600} value was adjusted to 0.1, the aeration rate was adjusted to 0.1 L/ min air, the pH was adjusted to 4.5± 0.1 with 3 M HCl. Then, cells were incubated at 30 °C, 150 rpm for 30 hours. Before starting the inoculation all of the parameters; pH, aeration, stirring and temperature were controlled. In addition, the pH was maintained constant with 3 M KOH solution and aeration rate was maintained constant with an air compressor during the experiments.

- **High performance liquid chromatography (HPLC) analysis of wild-type and mutant individual *R625_P8***

HPLC analysis was performed by using the samples which were collected from mutant and wild-type cells during the growth curve analysis in batch culture and bioreactor. Samples were centrifuged at 14000 rpm for 5 minutes. The supernatants were collected by an injector and then filtered (0.22 pore sized filter) for HPLC analysis.

Aminex® HPLC column was used for the separation of the metabolites. The isocratic method was used according to the manufacturer's protocol. 5 mM sulfuric acid was used as mobile phase. The analytical procedure was adjusted to 0.6 mL/min flow rate, 60 ºC temperature and 20 µl sample volume. Measurements were performed by using refractive index (RI) detector.

Standard curve method was used for the quantitative analysis of the metabolites. Standard solutions were prepared for each metabolite at specific concentrations same as in the Table 2.1.

The concentrations of metabolites as the standard solutions are indicated in Table 2.3. After preparation of the standard solutions, 1 mL of each standard and the samples were transferred into the HPLC tubes and the measurements were performed.

- **Reserve carbohydrate analysis of wild-type and mutant individual R625_P8**

The reserve carbohydrates, glycogen and trehalose were analyzed by using glucose oxidase/peroxidase assay (Parrou and François, 1997).Overnight incubated *P8* and wild-type cells were inoculated into 500 mL flask containing 100 mL YMM and incubated at 30 °C, 150 rpm. Then the cultures were scaled up to 2 liter flask containing 400 mL YMM, when they were reached at exponantial growth phase. 25 OD_{600} unit cells were collected at certain times while the wild-type and *P8* cells were growing. For cell dry weight analysis 1 mL extra samples were collected at each specific sampling points. The samples were centrifuged at 14000 rpm for 5 minutes. The supernatants were dropped and the pellets were transferred into -20 °C refrigerator. After collecting the all samples at specific growth points, the stored samples were thawed and the analysis were started according to the procedure of Parrou and François, 1997 (see Section 2.2.1.3.3).

3. RESULTS

3.1 Studies with the Yeast *Saccharomyces cerevisiae* CEN.PK113-7D

3.1.1 Obtaining freeze-thaw resistant generations by evolutionary engineering

Gradually increasing pulse stress selection strategy, which is an evolutionary engineering approach, was used to obtain the freeze-thaw stress resistant generations. The gradually increasing stress selection applications were performed according to the survival ratios of mutant generations. When the lowest survival ratio was obtained, selection of the mutant generations was stopped. 10 mutant generations were obtained from freeze-thaw stress application after exposure to ten repetitive cycles of freeze-thaw stress.

In order to determine the responses of the cells towards the freeze-thaw stress, survival ratios of each generation was obtained from the five tube-MPN data. The MPN results of the pulse increasing stress mutant generations and their corresponding stress cycles are indicated in Table 3.1.

Table 3.1: MPN results (cell/ml) of pulse increasing stress generations.

Freeze-thaw cycle number	Increasing stress generations	Incubation time (h)	Control (cell/ml)	Generation (cell/ml)	Survival Ratio	% Survival Ratio
1	*FG1*	24	$0.54*10^7$	$5.4*10^4$	$1*10^{-2}$	1.00
2	*FG2*	24	$5.4*10^7$	$0.54*10^4$	$1*10^{-4}$	0.01
3	*FG3*	24	$2.2*10^7$	$1.1*10^4$	$5*10^{-4}$	0.05
4	*FG4*	24	$3.5*10^7$	$0.35*10^4$	$1*10^{-4}$	0.01
5	*FG5*	24	$2.4*10^7$	$24*10^4$	$1*10^{-2}$	1.00
6	*FG6*	24	$1.7*10^7$	$920*10^4$	$5.4*10^{-1}$	54.1
7	*FG7*	24	$24*10^7$	$30*10^4$	$0.01*10^{-1}$	0.10
8	*FG8*	24	$0.35*10^7$	$35*10^4$	$1.0*10^{-1}$	10.00
9	*FG9*	24	$0.92*10^7$	$24*10^4$	$2.6*10^{-2}$	2.60
10	*FG10*	24	$0.7*10^7$	$2.2*10^4$	**$3.1*10^{-3}$**	0.31

Survival ratio values of the pulse increasing stress generations / freeze-thaw stress cycles are indicated in Figure 3.1.
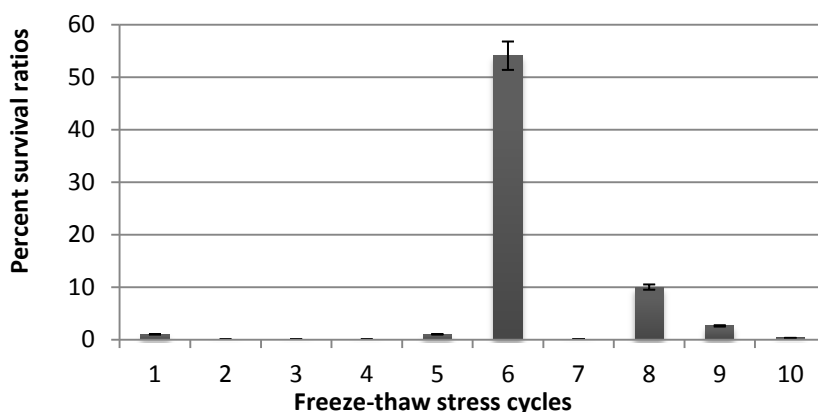
Figure 3.1: Percent survival ratio values of the increasing stress generations.

In order to find out the responses of the cells towards the freeze-thaw stress, survival ratios of each generation after freezing and thawing exposure were obtained by using MPN method.

3.1.1.1 Selection of the mutant individuals from the final mutant generation

Individual selection was performed from the final freeze-thaw stress resistant generation *F10G*. Ten mutant individuals were selected from *F10G* final heterogeneous mutant population. The nomenclature, for the pulse increasing stress individuals that obtained from the final freeze-thaw stress generation are indicated in Table 3.2.

Table 3.2: Nomenclature of mutant individuals, selected from pulse increasing freeze-thaw stress final population (*F10G*).

Freeze-thaw Resistant Mutant Individuals	Code of individuals
1ˢᵗ mutant individual	*F1*
2ⁿᵈ mutant individual	*F2*
3ʳᵈ mutant individual	*F3*
4ᵗʰ mutant individual	*F4*
5ᵗʰ mutant individual	*F5*
6ᵗʰ mutant individual	*F6*
7ᵗʰ mutant individual	*F7*
8ᵗʰ mutant individual	*F8*
9ᵗʰ mutant individual	*F9*
10ᵗʰ mutant individual	*F10*

The selected individuals were labeled and coded as freeze-thaw resistant mutant individuals.

3.1.1.2 Screening of freeze-thaw resistant mutant individuals

After obtaining pulse increasing stress final generation, selection of individual mutants were performed. Then, screening of freeze-thaw resistance of individual mutants was performed after two cycles of freeze-thaw stress application.

In order to determine the freeze-thaw stress responses of the mutant individuals, survival ratios of one and two cycle freeze-thaw stress application was obtained from the five tube-MPN data. The MPN results of one and two cycle freeze-thaw stress application are indicated in Table 3.3.

Table 3.3: MPN results (cell/ml) of one and two cycle freeze-thaw stress application.

Wildtype and mutant individuals	Incubation time (h)	Control (cell/ml)	1_cycle freeze-thaw stress application (cell/ml)	Survival Ratio	2_cycle freeze-thaw stress application (cell/ml)	Survival Ratio
Wild type	24	$22*10^6$	$24*10^6$	1.09	$1.6*10^6$	**0.07**
F1	24	$3.1*10^6$	$24*10^6$	**7.74**	$22*10^6$	**7.10**
F2	24	$17*10^6$	$18*10^6$	1.06	$17*10^6$	**1.00**
F3	24	$11*10^6$	$24*10^6$	**2.18**	$35*10^6$	3.18
F4	24	$28*10^6$	$14*10^6$	0.50	$24*10^6$	**0.86**
F5	24	$11*10^6$	$7*10^6$	0.64	$9.2*10^6$	**0.84**
F6	24	$7*10^6$	$5.4*10^6$	0.77	$6.3*10^6$	**0.90**
F7	24	$11*10^6$	$9.2*10^6$	0.84	$7*10^6$	**0.64**
F8	24	$3.5*10^6$	$35*10^6$	**10.00**	$16*10^6$	4.57
F9	24	$1.1*10^6$	$5.4*10^6$	**4.91**	$7*10^6$	**6.36**
F10	**24**	$17*10^6$	$16*10^6$	0.94	$54*10^6$	3.18

Survival ratios as fold of wild-type values of the mutant individuals / freeze-thaw stress cycles are indicated in Figure 3.2.
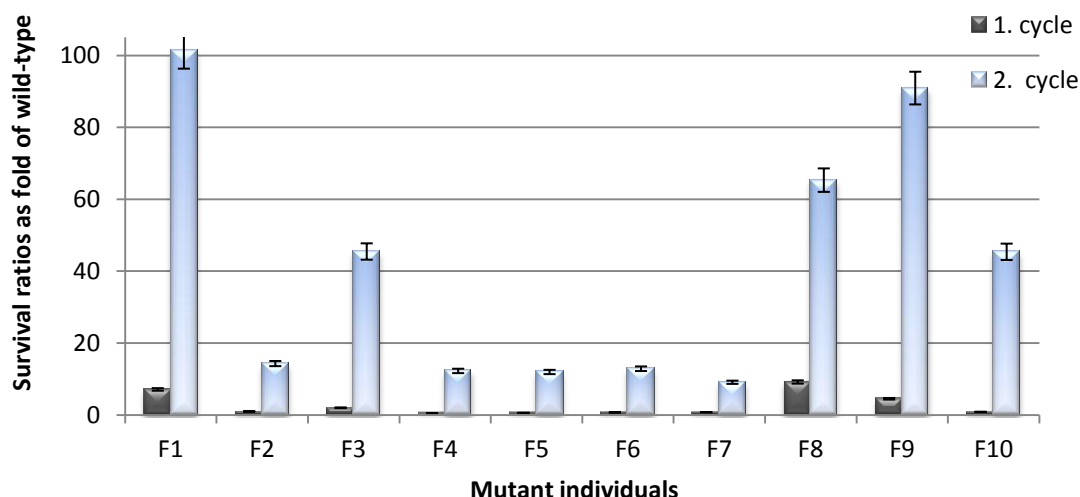
Figure 3.2: Relative survival ratios of the mutant individuals.

3.1.1.3 Cross-resistance analysis

Cross-resistance analysis were performed by using spotting assay and MPN (Most Probable Number) methods.

Cross-resistance analysis via spotting assay

Saccharomyces cerevisiae cells and freeze-thaw resistant mutant individuals were screened at different stress conditions via spotting assay. The cross-resistance analysis were performed by using continuous stress screening strategy. Before MPN analysis spotting assay was performed to see the responses of cells to those concentration of stress levels.

Wild-type and freeze-thaw resistant mutant individuals; *F1*, *F2*, *F3*, *F4*, *F5*, *F6*, *F7*, *F8*, *F9*, *F10* were exposed to toxic levels of boron, chromium, nickel, iron, magnesium, cobalt, zinc metal stresses and ethanol stress. The stress levels are indicated in Table 3.4.

Table 3.4: Stress factors and concentrations for cross resistance analysis.

Stress factors	$NiCl_2$	$CoCl_2$	$CrCl_3$	$FeCl_3$	$ZnCl_2$	$MgCl_2$	$B(OH)_3$	Ethanol
Stress levels	0.5 mM	1 mM	1 mm	15 mM	3 mM	3 mM	50 mM	5 %

The spotting assay images and the cell growth at different dilutions of control group (without stress factor) are indicated in Figure 3.3.
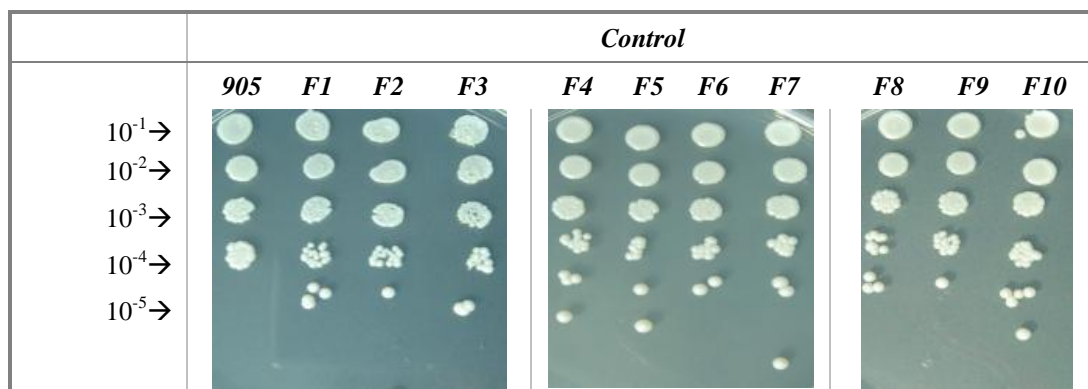
Figure 3.3: Control group images of wild-type and individuals after 72 hour incubation.

The spotting assay images and the cell growth at different dilutions of magnesium stress containing plates are indicated in Figure 3.4.
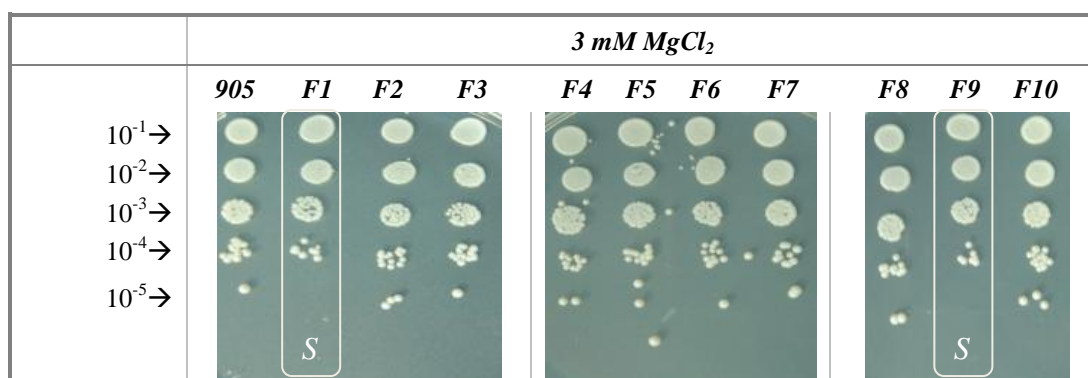
Figure 3.4: 3 mM MgCl$_2$ stress condition images of wild type and individuals after 72 hour incubation.

According to the results indicated in Figure 3.4, *F1* and *F9* were *sensitive* against MgCl$_2$ stress.

The spotting assay images and the cell growth at different dilutions of cobalt stress containing plates are indicated in Figure 3.5.
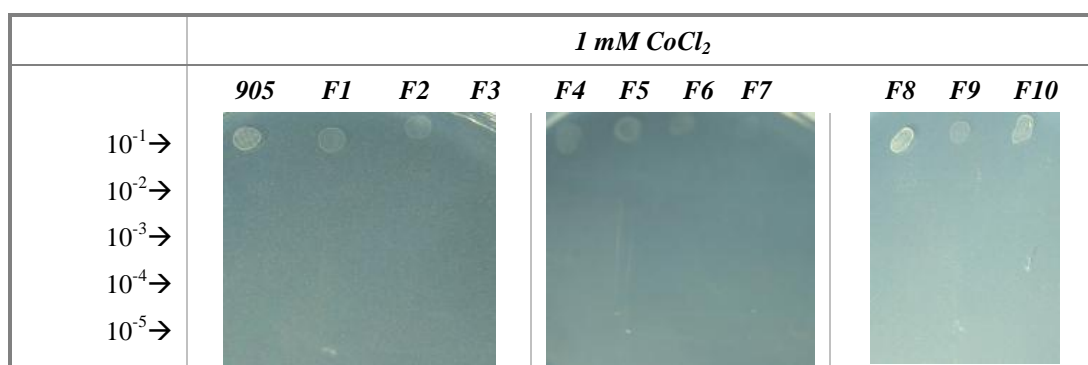
Figure 3.5: 1 mM CoCl$_2$ stress condition images of wild type and individuals after 72 hour incubation.

According to the results indicated in Figure 3.5, 1 mM $CoCl_2$ stress on solid media was highly toxic to all individuals, including wild-type.

The spotting assay images and the cell growth at different dilutions of chromium stress containing plates are indicated in Figure 3.6.
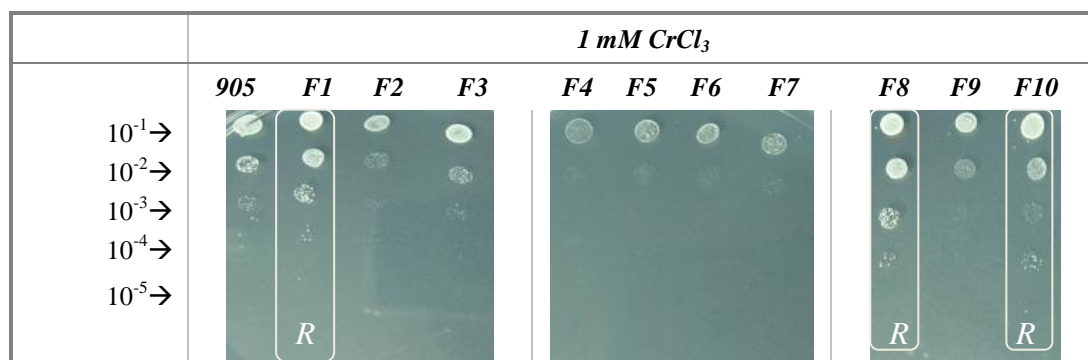
Figure 3.6: 1 mM $CrCl_3$ stress condition images of wild type and individuals after 72 hour incubation.

According to the results indicated in Figure 3.6, *F1*, *F8* and *F10* seem to have a cross-resistance against $CrCl_3$ stress.

The spotting assayimages and the cell growth at different dilutions of zinc stress containing plates are indicated in Figure 3.7.
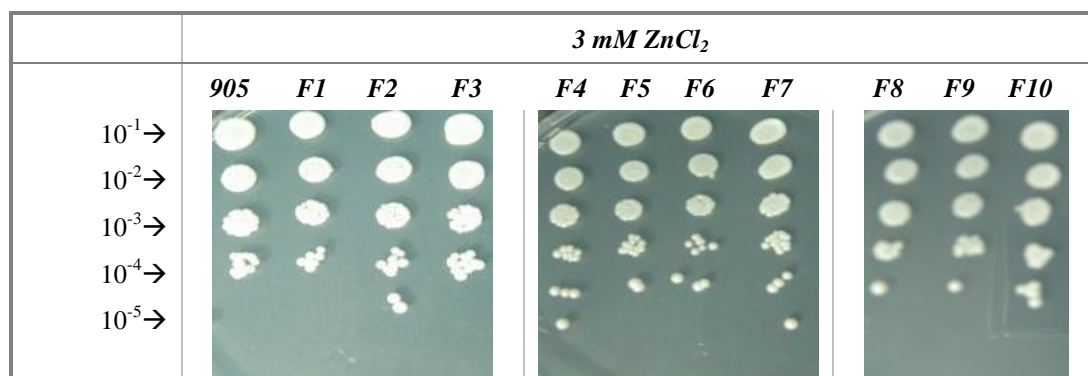
Figure 3.7: 3 mM $ZnCl_2$ stress condition images of wild type and individuals after 72 hour incubation.

According to the results indicated in Figure 3.7, the zinc stress level is not at a highly toxic range for the cells.

The spotting assay images and the cell growth at different dilutions of iron stress containing plates are indicated in Figure 3.8.
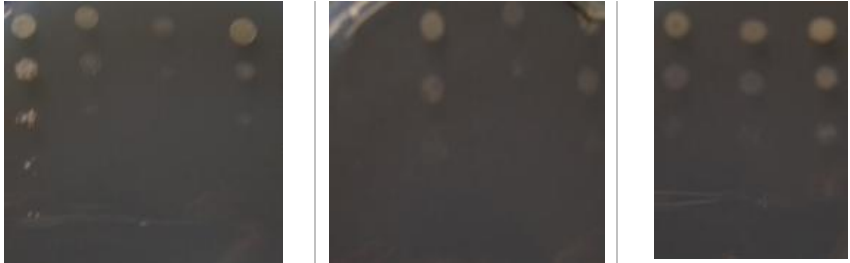
	15 mM $FeCl_2$									
	905	*F1*	*F2*	*F3*	*F4*	*F5*	*F6*	*F7*	*F8*	*F9*	*F10*
10^{-1}→											
10^{-2}→											
10^{-3}→											
10^{-4}→											
10^{-5}→											

Figure 3.8: 15 mM $FeCl_2$ stress condition images of wild type and individuals after 72 hour incubation.

According to the results indicated in Figure 3.8, individuals have no cross-resistance against $FeCl_2$ stress.

The spotting assay images and the cell growth at different dilutions of boron stress containing plates are indicated in Figure 3.9.

	50 mM $B(OH)_3$									
	905	*F1*	*F2*	*F3*	*F4*	*F5*	*F6*	*F7*	*F8*	*F9*	*F10*
10^{-1}→											
10^{-2}→											
10^{-3}→											
10^{-4}→											
10^{-5}→											

Figure 3.9: 50 mM $B(OH)_3$ stress condition images of wild type and individuals after 72 hour incubation.

According to the results indicated in Figure 3.9, freeze-thaw stress resistant individual *F1* is resistant to $B(OH)_3$ when compared to wild type. However, those 50 mM stress level seems too low for the cells.

The spotting assay images and the cell growth at different dilutions of ethanol stress containing plates are indicated in Figure 3.10.
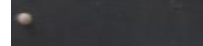
Figure 3.10: 5 % Ethanol stress condition images of wild type and individuals after 72 hour incubation.

According to the results indicated in Figure 3.10, the ethanol stress level is not at toxic range for the cells.

Then, stress levels were rearranged and reapplied to highly freeze-thaw resistant mutant individual *F1* by the same spotting assay method. The cell growth at different dilutions of control and ethanol stress containing plates are indicated in Figure 3.11.


Figure 3.11: Growth images on control, ethanol and cobalt stress containing solid plates.

According to the results indicated in Figure 3.11, *F1* is neither more resistant nor more sensitive to ethanol than the wild-type. *F1* was not different from wild-type and had no cross-resistance or sensitivity to ethanol stress.

The cell growth at different dilutions of zinc, cobalt and magnesium stress containing plates are indicated in Figure 3.12.
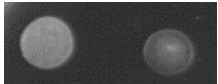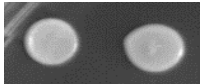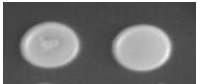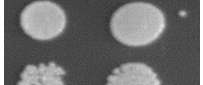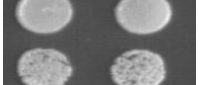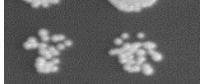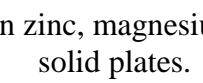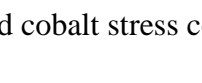
	10 mM ZnCl$_2$		40 mM MgCl$_2$		1 mM CoCl$_2$	
	905	F1	905	F1	905	F1
10^{-1}→						
10^{-2}→						
10^{-3}→						
10^{-4}→						
10^{-5}→						

Figure 3.12: Growth images on zinc, magnesium and cobalt stress containing solid plates.

According to the results indicated in Figure 3.12, cobalt and magnesium stress levels were not at toxic ranges to decide whether *F1* is more resistant or not sensitive than wild-type. However, *F1* seems to be slightly sensitive to zinc stress when compared to wild-type.

The cell growth at different dilutions of control and phenylethanol stress containing plates are indicated in Figure 3.13.
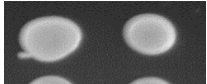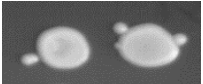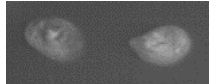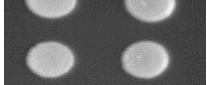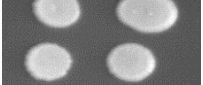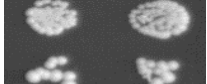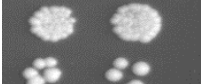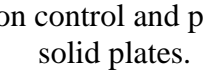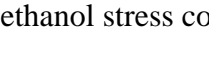
	Control		1 g/l Phenylethanol		3 g/l Phenylethanol	
	905	F1	905	F1	905	F1
10^{-1}→						
10^{-2}→						
10^{-3}→						
10^{-4}→						
10^{-5}→						

Figure 3.13: Growth images on control and phenylethanol stress containing solid plates.

According to the results indicated in Figure 3.13, *F1* has neither sensitivity nor resistance against phenylethanol stress.

- **Cross-resistance analysis via MPN (Most Probable Number) method**

Saccharomyces cerevisiae cells and freeze-thaw resistant mutant individual *F1* were screened at different stress conditions via 5-tube MPN methodology. The cross-resistance analysis were performed by using continuous stress screening strategy.

Wild-type and *F1* were exposed to toxic levels of boron, chromium, nickel, copper and cobalt metal stresses. The MPN results and survival ratios upon those metal stresses are indicated in Table 3.5.

Table 3.5: The MPN results (cell/ml) and survival ratios of wild-type and *F1* after 72 h incubation.

Stress Conditions	*905* (cell/ml)	*F1* (cell/ml)	*905* (survival ratio)	*F1* (survival ratio)
Control	$2.2*10^7$	$5.4*10^7$	1	1
80 mM B(OH)$_3$	$1.7*10^4$	$16*10^4$	$77*10^{-7}$	**$296*10^{-7}$**
3 mM CrCl$_3$	$2.4*10^2$	$24*10^2$	$1.1*10^{-7}$	**$4.4*10^{-7}$**
0.5 mM NiCl$_2$	$24*10^2$	$240*10^2$	$11*10^{-7}$	**$44*10^{-7}$**
0.5 mM CuCl$_2$	$2.4*10^2$	$2.4*10^2$	$1.1*10^{-7}$	$0.4*10^{-7}$
3 mM CoCl$_2$	$24*10^2$	$240*10^2$	$11*10^{-7}$	**$44*10^{-7}$**

Mutant individual *F1* gained cross-resistance to boron, chromium, nickel and cobalt metal ions when compared to wild-type.

Wild-type and *F1* were exposed to toxic levels of iron metal and osmotic (salt) stresses. The MPN results and survival ratios upon those iron and osmotic stresses are indicated in Table 3.6.

Table 3.6: The MPN results (cell/ml) and survival ratios of wild-type and *F1* after 72 h incubation.

Stress Conditions	*905* (cell/ml)	*F1* (cell/ml)	*905* (survival ratio)	*F1* (survival ratio)
Control	$3.5*10^6$	$16*10^6$	1.00	1.00
15 mM FeCl$_3$	$0.46*10^6$	$5.4*10^5$	0.13	0.03
0.25 M NaCl	$9.2*10^6$	$9.2*10^6$	2.63	0.58
Control	$2.2*10^6$	$54*10^6$	1.00	1.00
0.86M NaCl	240	240	$109*10^6$	$4*10^6$

Mutant individual *F1* was sensitive to iron and NaCl when compared to wild-type.

Wild-type and *F1* were exposed to toxic levels of oxidative (hydrogen peroxide) stresses. The MPN results and survival ratios upon those oxidative stresses are indicated in Table 3.7.

Table 3.7: The MPN results (cell/ml) and survival ratios of wild-type and *F1* after 72 h incubation.

Stress Conditions	*905* (cell/ml)	*F1* (cell/ml)	*905* (survival ratio)	*F1* (survival ratio)
Control	$700*10^4$	$170*10^4$	1.00	1.00
0.3 mM H$_2$O$_2$	$70*10^4$	$70*10^4$	0.10	**0.41**
0.4 mM H$_2$O$_2$	$54*10^4$	$92*10^4$	0.08	**0.54**
0.5 mM H$_2$O$_2$	$5.4*10^4$	$92*10^4$	0.01	**0.54**

Mutant individual *F1* gained cross-resistance to oxidative stress when compared to wild-type.

The relative survival ratios of *F1* as fold of wild-type upon those boron, chromium, nickel, cupper, cobalt, iron metal stresses and osmotic (salt) stress are indicated in Figure 3.14.
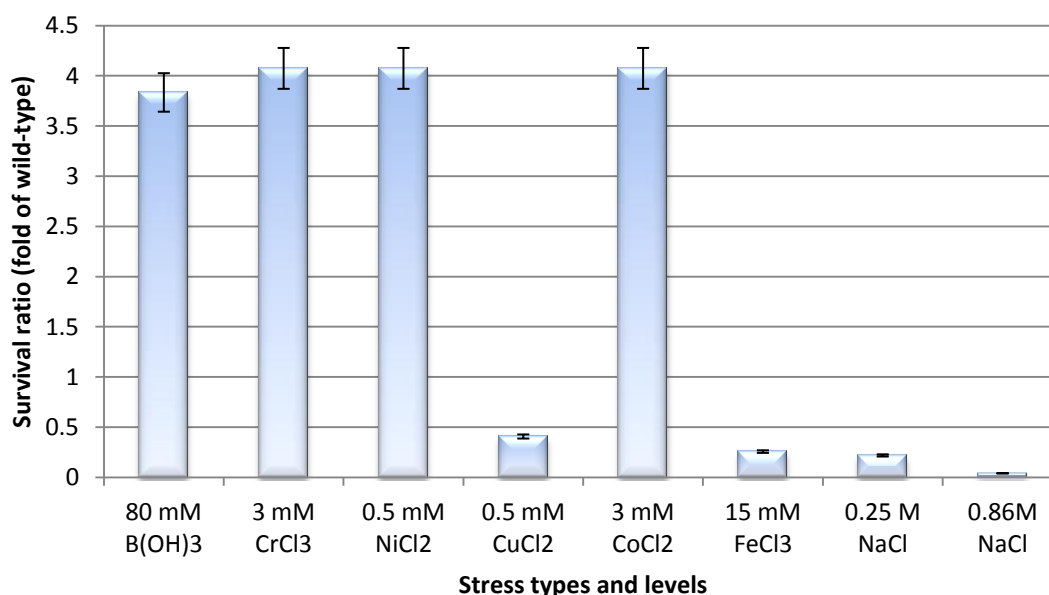
Figure 3.14: Relative survival ratios of *F1* upon metal and osmotic stress after 72 h incubation.

The mutant individual *F1* gained cross-resistance to boron, chromium, nickel, cobalt and oxidative (H$_2$O$_2$) stresses.

The relative survival ratios of *F1* as fold of wild-type upon oxidative stress are indicated in Figure 3.15.
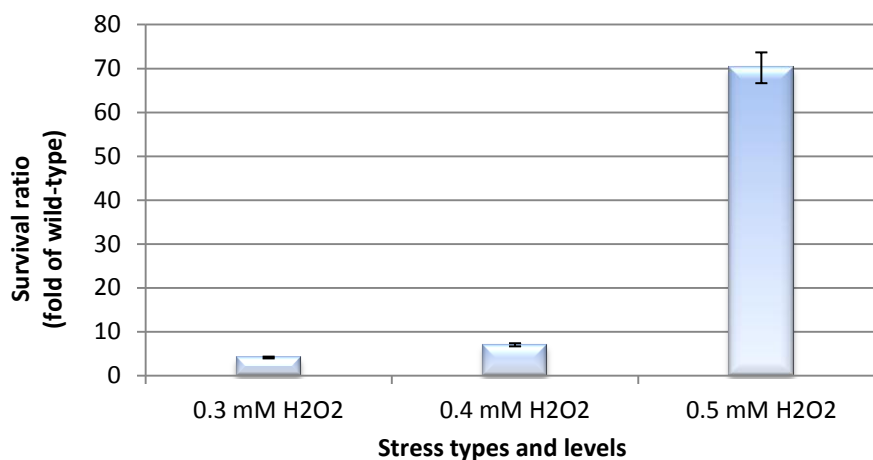
Figure 3.15: Relative survival ratios of *F1* upon oxidative stress after 72 h incubation.

The relative survival ratios of *F1* as fold of wild-type in logarithmic scale upon metal, osmotic and oxidative stresses are indicated in Figure 3.16.
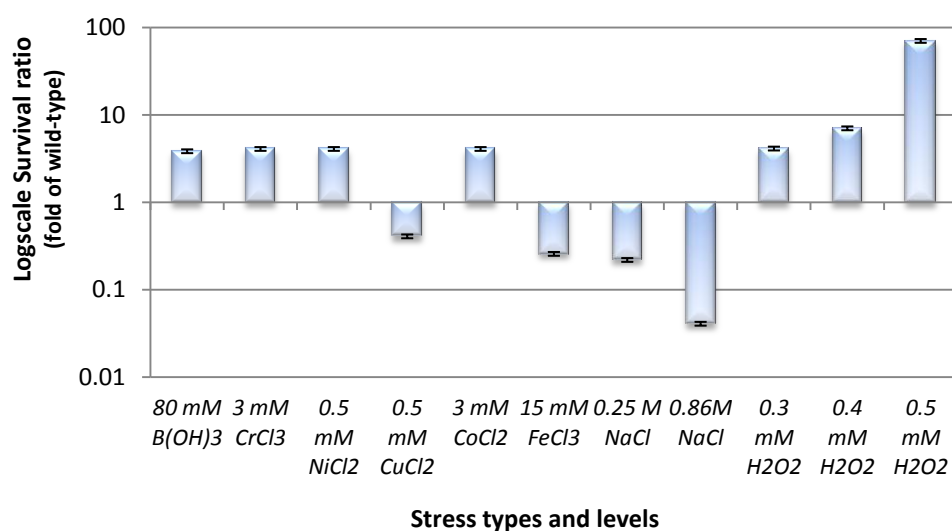
Figure 3.16: Relative survival ratios in logarithmic scale of *F1* upon metal, osmotic and oxidative stresses after 72 h incubation.

3.1.2 Principle component analysis (PCA)

The cross-resistance results of wild-type and mutant individual *F1* were analyzed via PCA. The survival ratio data (72 h) of wild-type and *F1* at different stress conditions were used for the analysis via PCA _MATLAB code. Here, each component score (factor score) is corresponding to a particular data point (signed as different colors).

At this two-dimensional plane we can observe the variance between variables and this data gives us a qualitative conclusion. The similar behaviour between cross-stresses are indicated in Figure 3.17.
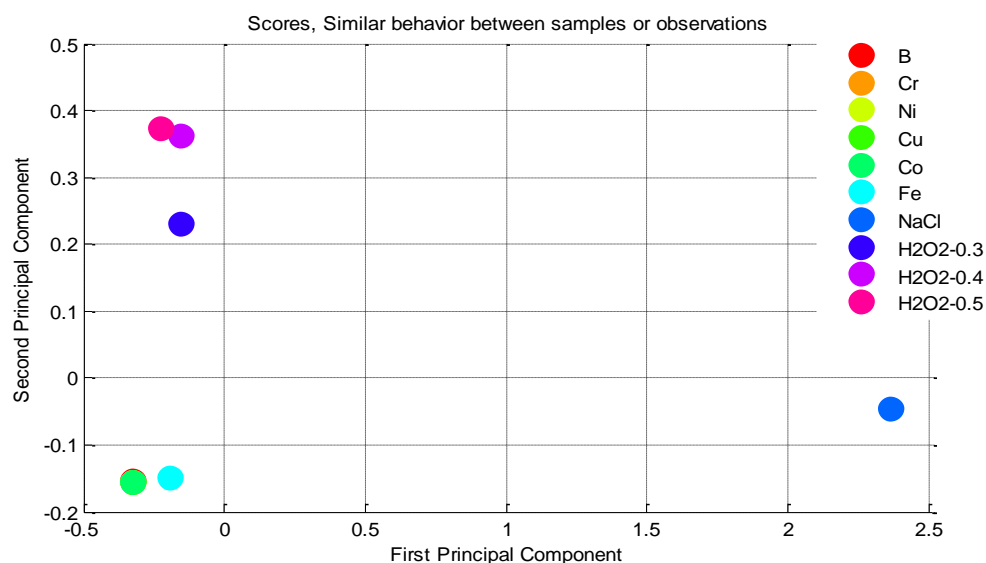
Figure 3.17: PCA results of different stress conditions.

Osmotic and oxidative stresses are indicated difference in response when compared to other cross-stresses. Here, the response is completely related with the distance between the component scores.

The similar behaviour between wild-type and mutant individual *F1* is indicated in Figure 3.18.
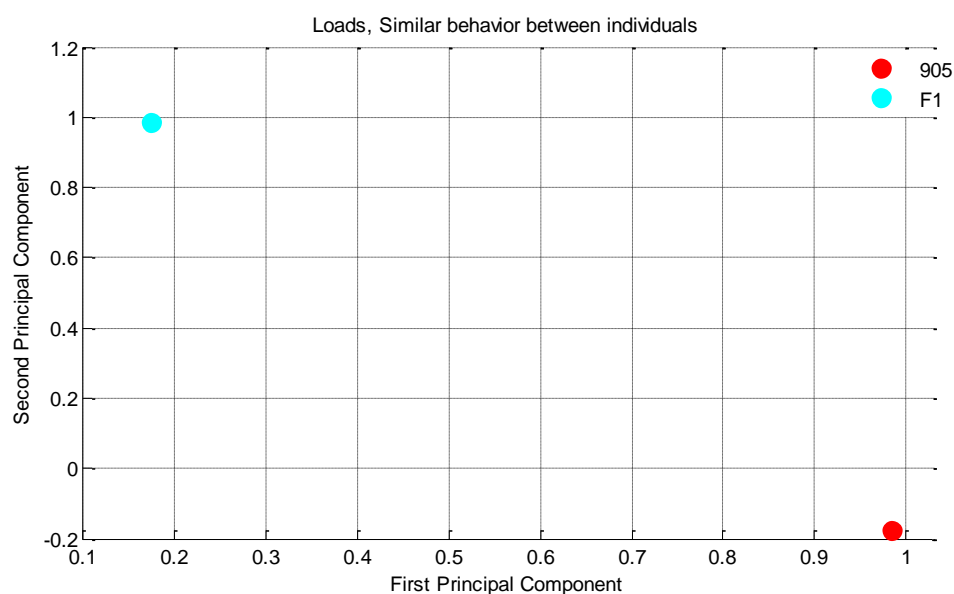
Figure 3.18: PCA results of 72 h incubation at different stress conditions.

It is obvious that there is a high variance between wild-type and *F1* in response to different stress types. Their cross-resistance phenotypes are too different from each other. *F1* showed higher tolerance most of the cross-stresses when compared to wild-type.

As a result, freeze-thaw resistant mutant individual *F1* had different responses to osmotic and oxidative stresses. It has a higher resistance to oxidative stress and higher sensitivity to osmotic stress. Metal stress, osmotic stress and oxidative stress responses had different component scores consistent with the previous analysis.

3.1.3 Genetic characterization of the mutant individual *F1*

To enlighten the genetic basis of the freeze-thaw resistance, real-time PCR analysis were performed with the genes that were related to freeze-thaw resistance. The relative transcriptional changes were analyzed. Wild-type and highly freeze-thaw resistant mutant individual *F1* were used to study molecular characterization of freeze-thaw stress mechanism.

3.1.3.1 Total RNA isolation from yeast cells

Total RNA isolation was performed by following the Roche - High Pure RNA Isolation Kit protocol (Cat no: 11 828 665 001).

3.1.3.2 Measurement of total RNA concentration

Total RNA concentrations were measured by using Qubit® Flourometer and nanodrop.

3.1.3.3 cDNA synthesis

cDNA synthesis was performed by following the Transcriptor High Fidelity cDNA Synthesis Kit protocol (Cat no: 04 379 012 001).

3.1.3.4 Real time-PCR applications

Real time-PCR (Q-PCR) applications were performed by following the Roche-LightCycler® 480 DNA SYBR Green I Master Kit protocol (Cat no: 05 091 284 001).

To identify the relative fold changes of the genes transcriptomic profiles, $2^{(-\text{Delta Delta Ct})}$ method was used (Livak, 2001). The housekeeping gene, beta actin (*ACT1*) was used as the endogenous control gene.

Table 3.8: Efficiency and error values.

	ACT1	*CTT1*	*AQY1*	*AQY2*	*GSH1*	*FPS1*
Error	0.0148	0.0448	0.0214	0.0412	0.090	0.0388
Efficiency	2.012	2.016	1.905	1.959	2.081	2.000

Efficiency and error values of the internal control and the target genes were in the acceptable limit range (Dorak, 2006) (Table 3.8). The efficiency values were between 1.9 - 2.1 and the error values were below 0.2.

- **Expression profiles of *AQY1*, *AQY2*, *CTT1*, *GSH1* and *FPS1* genes**

Expression levels of freeze-thaw stress related genes *AQY1*, *AQY2*, *CTT1*, *GSH1* and *FPS1* were studied by real time-PCR at control and freeze-thaw stress conditions. Relative expression profiles of related genes were normalized to wild-type gene expressions at normal growth conditions and the results are given in Figure 3.19, Figure 3.20, Figure 3.21 and Figure 3.22. The experiments were performed as triplicate to calculate the standard deviations. The variance between expression levels of each gene was emphasized on logarithmic scale graphical format.

Relative expression profiles of wild-type and *F1* for *AQY1* gene under control and freeze-thaw stress conditions are given in Figure 3.19.
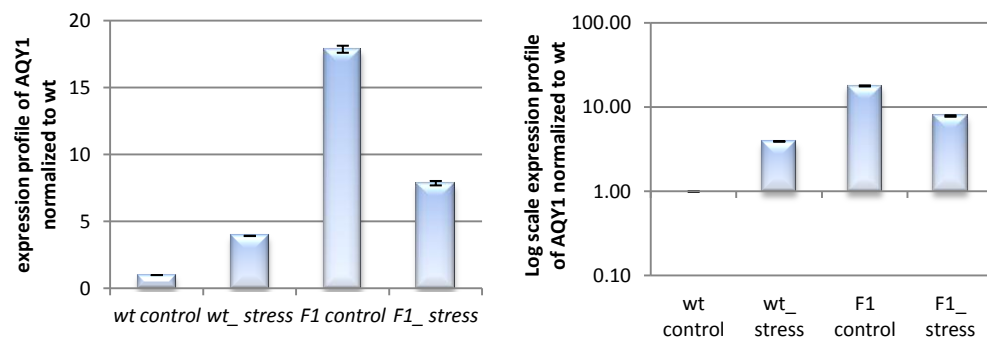
Figure 3.19: Expression level of *AQY1* gene in control and freeze-thaw stress conditions.

The expression level of *AQY1* gene was increased at freeze-thaw stress conditions in wild-type. It is interesting that the relative expression level of *F1* strain was up to 18

fold under control conditions. The expression level of *F1* decreased at stress conditions. However, it is still higher than wild-type. The results were indicated that the expression profile of *AQY1* gene was completely different at mutant individual both control and stress conditions.

Relative expression profiles of wild-type and *F1* for *AQY2* gene under control and freeze-thaw stress conditions are given in Figure 3.20.
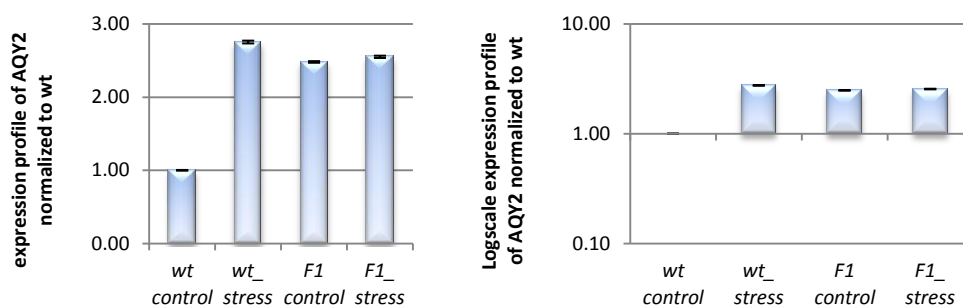
Figure 3.20: Expression level of *AQY2* gene in control and freeze-thaw stress conditions.

The expression level of *AQY2* gene was increased at freeze-thaw stress conditions both wild-type and *F1*. The expression level of *AQY2* at wild-type stress was increased up to 2.5 fold when normalized to wild-type control and the normalized expression level of *F1* stress was slightly lower than the wild-type under stress condition. However, at control conditions the expression level *AQY2* at *F1* was 2.5 fold of wild-type control. The results indicated that the expression profile of *AQY2* gene was completely different at mutant individual for control conditions.

Relative expression profiles of wild-type and *F1* for *CTT1* gene under control and freeze-thaw stress conditions are given in Figure 3.21.
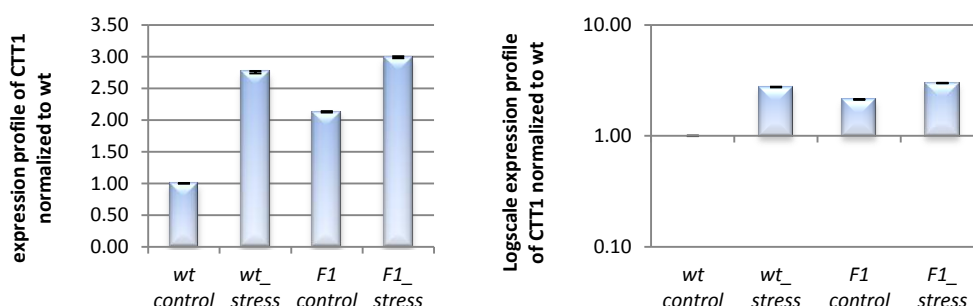
Figure 3.21: Expression level of *CTT1* gene in control and freeze-thaw stress conditions.

The expression level of *CTT1* gene was increased at freeze-thaw stress conditions both wild-type and mutant individual *F1*. The normalized expression level of *F1* was slightly higher than wild-type under stress conditions. The results were indicated that the expression profile of *CTT1* gene was completely different at mutant individual both control and stress conditions.

Relative expression profiles of wild-type and *F1* for *GSH1* gene under control and freeze-thaw stress conditions are given in Figure 3.22.
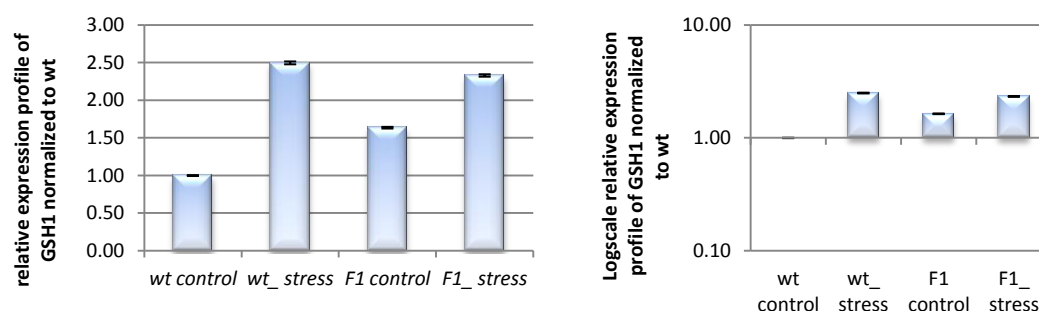
Figure 3.22: Expression level of *GSH1* gene in control and freeze-thaw stress conditions.

The expression level of *GSH1* gene was increased at freeze-thaw stress conditions both wild-type and *F1*. The expression level of *GSH1* at wild-type stress was increased 2.5 fold when normalized to wild-type control and the normalized expression level of *F1* under stress condition was slightly lower than the wild-type stress. In addition, at control conditions the expression level of *GSH1* at *F1* was higher comparing to wild-type control.

Relative expression profiles of wild-type and *F1* for *FPS1* gene under control and freeze-thaw stress conditions are given in Figure 3.23.
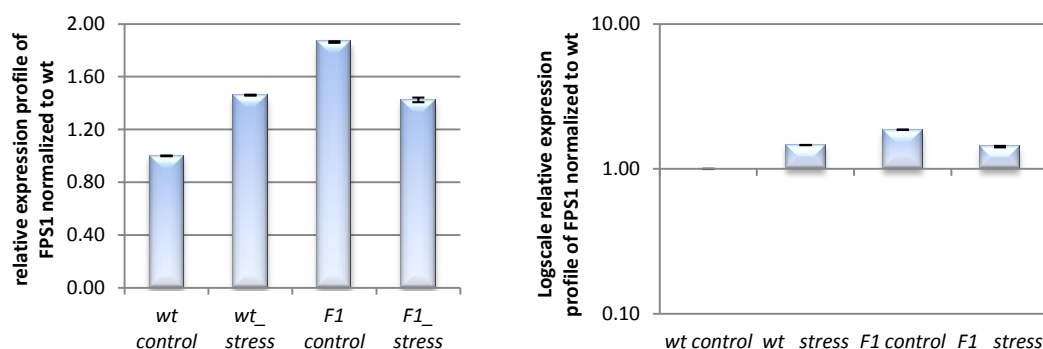
Figure 3.23: Expression level of *FPS1* gene in control and freeze-thaw stress conditions.

The expression level of *FPS1* gene was increased at freeze-thaw stress conditions in wild-type. The normalized expression level of *F1* was decreased under stress conditions when compared to wild-type.

In addition, *FPS1* was upregulated under control conditions. The results were indicated that the expression profile of *FPS1* gene was completely different at mutant individual in control conditions.

3.1.3.5 Whole genome transcriptomic analysis via DNA microarray technology

The whole genom transcriptomic analysis was performed by using highthroughput DNA microarray technology. After obtaining total RNA samples of each triplicate by using "Qiagen RNeasy Mini Kit" (Cat: 74104, Qiagen, USA), "RNA 6000 Nano Assay Kit" (Cat: 5067-1511, Agilent, USA) was used to check the concentrations and the quality of the isolated RNA. The samples were analyzed with Agilent BioAnalyzer 2100 and the RNA integrity numbers (RIN) were calculated.

The optical density (OD_{600}) values, RNA integrity numbers (RIN) and RNA concentrations (ng/µl) are indicated in Table 3.9.

Table 3.9: Optical density (OD_{600}) values, RNA integrity numbers (RIN) and RNA concentrations (ng/µl).

	905				F1		
	1st	2nd	3rd	4th	1st	2nd	3rd
OD_{600}	1.16	1.08	1.09	1.12	0.99	1.02	1.05
RIN	9.90	10.00	9.70	9.60	9.70	9.80	9.90
RNA concentration (ng/µl)	625.00	455.00	595.00	455.00	369.30	295.20	130.30

- **DNA microarray analysis**

The microarray data was analyzed by GeneSpring GX 9.0 software. The mean expression profile of *F1* was normalized to wild-type by this software and then the molecular and functional categorization of up and down regulated genes were done according to FunSpec and Funcat databases [(p-value) < 0.05].

The percentage of upregulated genes with their corresponding functional categories are indicated in Figure 3.24. The analysis were performed with Funcat database.
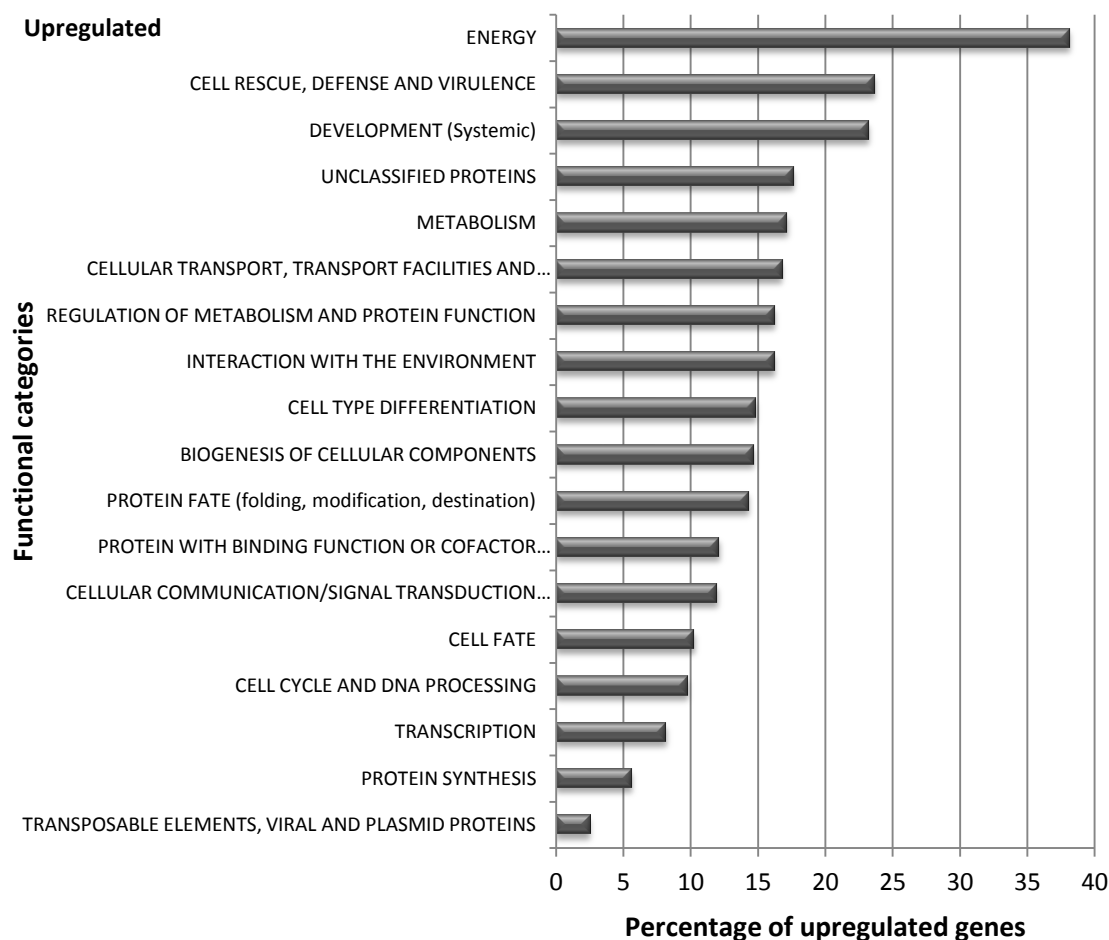
Figure 3.24: The percentage of upregulated genes to the total genes in each category (cut off value is ≥ 2 fold) (Ruepp et al., 2004).

The functional categories of the induced genes of the freeze-thaw resistant mutant individual *F1* under non-stress conditions are similar with the previous study of Odani et al., 2003. After 1 hour pulse freeze-thaw stress treatment, they found out that the genes under energy, cell rescue, metabolism, unclassified proteins, interaction with the environment, cellular transport and protein fate functional categories were upregulated according to the stress (Odani et al., 2003).

The expression levels of 1287 genes were upregulated at freeze-thaw resistant mutant individual *F1*.

Some significantly upregulated genes are listed on Table 3.10. The cut off value is set to ≥ 2 fold.

Table 3.10: Relative upregulated *F1* genes (≥ 2 fold).

	Gene name	Fold change	Gene name	Fold change
Hexose transport	HXT7	68.38	HXT6	62.38
	HXT5	50.67	-	-
Cell rescue, defense and virulence	GPX1	12.91	SGA1	11.75
	PRX1	9.99	RIM4	8.79
	HSP12	263. 60	IME4	7.53
	TSA2	7.44	SPS100	7.15
	EMI2	17.62	SPR3	7.03
	HSP12	263. 60	NCE102	4.08
Eukaryotic plasma membrane	ATG15	2.48	ZEO1	2.53
	YNL194C	146.30	YOP1	3.04
Reticulon protein	RTN2	61.83	-	-
Trehalose biosynthetic process	TPS1	8.30	TSL1	63.02
	TPS2	11.84	PGM2	104.10
	UGP1	12.55	TPS3	4.77
Cellular response to oxidative stress	HYR1	2.51	TSA2	7.44
	GAD1	29.08	GRX2	6.57
	GCY1	15.08	YJR096W	16.35
	GRE3	13.71	HSP12	263.60
	SRX1	13.51	TRX1	2.06
	GPX1	12.91	TRX2	5.76
	PRX1	9.99	CTT1	48.28
	GRX1	8.07	-	-
Oxidative stress response	GAD1	29.08	TSA2	7.44
	SRX1	13.51	FMP46	7.32
	GPX1	12.91	HSP12	263.60
	GRE1	10.61	TRX1	2.06
	PRX1	9.99	TRX2	5.76
	GRX1	8.07	SOD1	2.19
	GRX2	6.57	-	-
Stress response	ALD3	107.30	SSE2	16.15
	DDR2	92.98	MRK1	8.89
	ATH1	6.01	XBP1	17.32
	MGA1	6.60	YGP1	18.29
	HOR7	6.68	SDP1	20.87
	TPS1	8.30	TSL1	63.02
	HSP30	8.71	NTH2	3.61
	UBI4	8.94	DAK1	2.26
	HSP104	9.22	DDR48	4.00
	PAI3	9.52	TPS3	4.77
	TPS2	11.84	CYC7	68.01
	STF2	11.88	YJL144W	20.10
	HSP82	14.88	-	-
Alcohol fermentation	PDC6	3.98	ADH2	3.96
	NDE2	7.28	ALD4	16.65
	ADH1	2.02	ADH5	2.06
	SSA1	9.49	SSA4	57.32
Unclassified proteins	FMP16	68.78	YGR066C	15.83
	FMP43	67.21	YLR149C	15.15
	YNR034W-A	79.45	YMR090W	14.65
	TMA10	112.40	YLR346C	12.78
	BDH2	73.96	YDR374C	23.58
	YER067W	52.72	OM45	10.04
	YMR206W	57.81	RRT8	10.52
	YLR053C	33.39	PNS1	13.38

Table 3.10 (continued): Relative upregulated *F1*genes (≥ 2 fold).

Unclassified proteins	YDR379C-A	22.19	GTO3	20.62
	YBR285W	21.83	RTN2	61.83
	YJL144W	20.10	SPG4	21.84
	YLR312C	19.95	OM14	21.23
	YJR115W	10.14	FMP33	23.22
	YNR014W	10.58	UIP4	27.05
	YKL151C	10.78	PHM7	45.50
	YJL163C	19.32	DCS2	30.79
	YLR162W	17.70	GPM2	27.65
	YNL200C	17.35	RTC3	25.66
	YER121W	17.28	YOR186W	39.06
	YKL091C	16.73	YNL195C	24.27
Carbohydrate metabolic process	HXK1	224.07	PGM2	104.10
	GPH1	133.58	SOL4	51.35
Degradation of arginine	CAR1	2.74	CAR2	4.06
Metabolism of energy reserves (e.g. glycogen, trehalose)	GPH1	133.58	TPS1	8.30
	PGM2	104.10	GIP2	14.60
	UGP1	12.55	HSP82	14.88
	MAL32	14.44	GSY1	15.40
	TPS2	11.84	MAL12	17.81
	GDB1	7.82	GLC3	19.68
	ATH1	6.01	GAC1	24.81
	PIG2	6.80	TSL1	63.02
Glycogen catabolic process	GPH1	133.58	GDB1	7.82
	SGA1	11.75	-	-
Glycogen biosynthetic process	PGM2	104.10	GLC3	19.68
	GSY2	14.77	GAC1	24.81
	GDB1	7.82	GLG1	5.51
	UGP1	12.55	GLG2	4.03
	GSY1	15.40	-	-
Protein folding and stabilization(Takahashi et al., 2009)	HSP26	172.37	SSE2	16.15
	HSP42	15.43	APJ1	17.58
	HSP82	14.88	HSP78	26.52
	HSP104	9.22	SSA4	57.33
	CPR6	6.60	SSA1	9.49
Glycolysis	HXK1	224.07	GLK1	11.94
	GPM2	27.65	TDH1	6.89
	EMI2	17.62		
Response to stress	HSP12	263.60	MRK1	8.89
	SSE2	16.15	HSP30	8.71
	TPS2	11.84	GRE3	13.71
	HSP104	9.22	HSP82	14.88
	FMP45	235.10	CTT1	48.28
	HSP26	172.37	GRE1	10.61
	DDR2	92.98	SSA4	57.33
	TPS1	8.30	TSL1	63.02
	RSB1	41.05	FMP43	67.21
	HOR7	6.68	HSP78	26.52
	HSP42	15.43	XBP1	17.32
	UBI4	8.94	TPS3	4.77
	GPD1	6.47	DDR48	4.00
	ATH1	6.01	DAK1	2.26
glycerol metabolic process	GUT2	7.56	GPD2	2.56
	DAK1	2.26	PGC1	2.02

Environmental stress response (ESR) genes are upregulated or dowregulated against stress conditions to protect cells. Dominantly, expression of most of the ESR genes were related to the growth rate.

The Princeton growth rate/gene expression relationship database was used to analyse our microarray data. When the growth rate decreased due to stress elements, some of the ESR genes were upregulated. Here, the ESR gene expressions were induced in *F1* to adjust growth rate, however there is no stress, evidently.

The genes that are expressed under normal growth conditions in the cell cycle are indicated as a bar chart in the Figure 3.25. The genes that are induced under stress conditions in cell cycle are indicated as a red line and the genes that are repressed under stress conditions in cell cycle are indicated as a green line in the Figure 3.25 (Brauer et al., 2008).

Here, the black line represents our microarray data of upregulated genes.
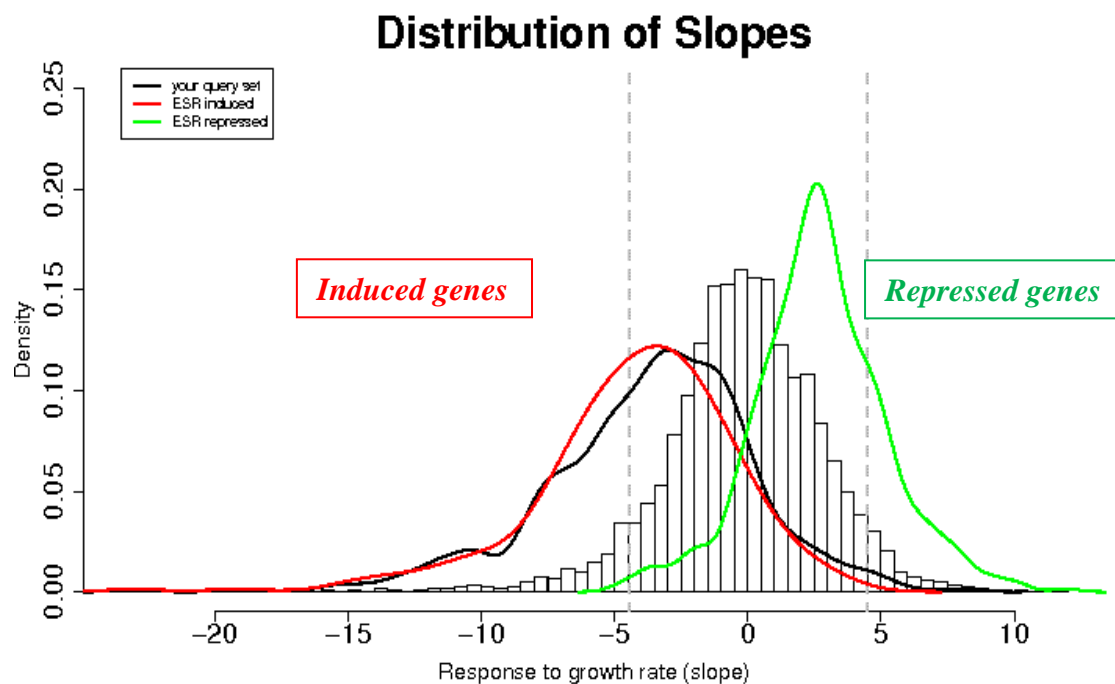
Figure 3.25: The distribution of slopes of up and downregulated ESR genes of yeast. The red line shows induced genes, green line shows repressed genes under environmental stress conditions.Bar chart shows the genes that are expressed under normal growth conditions in cell cycle. The black line shows the upregulated genes of *F1* under normal growth conditions in cell cycle.

Brauer and colleagues, (2008), stated that " ESR genes as defined previously may in fact not be responding directly to stress, but instead are responding to a reduction in growth rate secondary to the stress" (Brauer et al., 2008).

The percentage of downregulated genes with their corresponding functional categories are indicated in Figure 3.26. The analysis were performed with Funcat database.
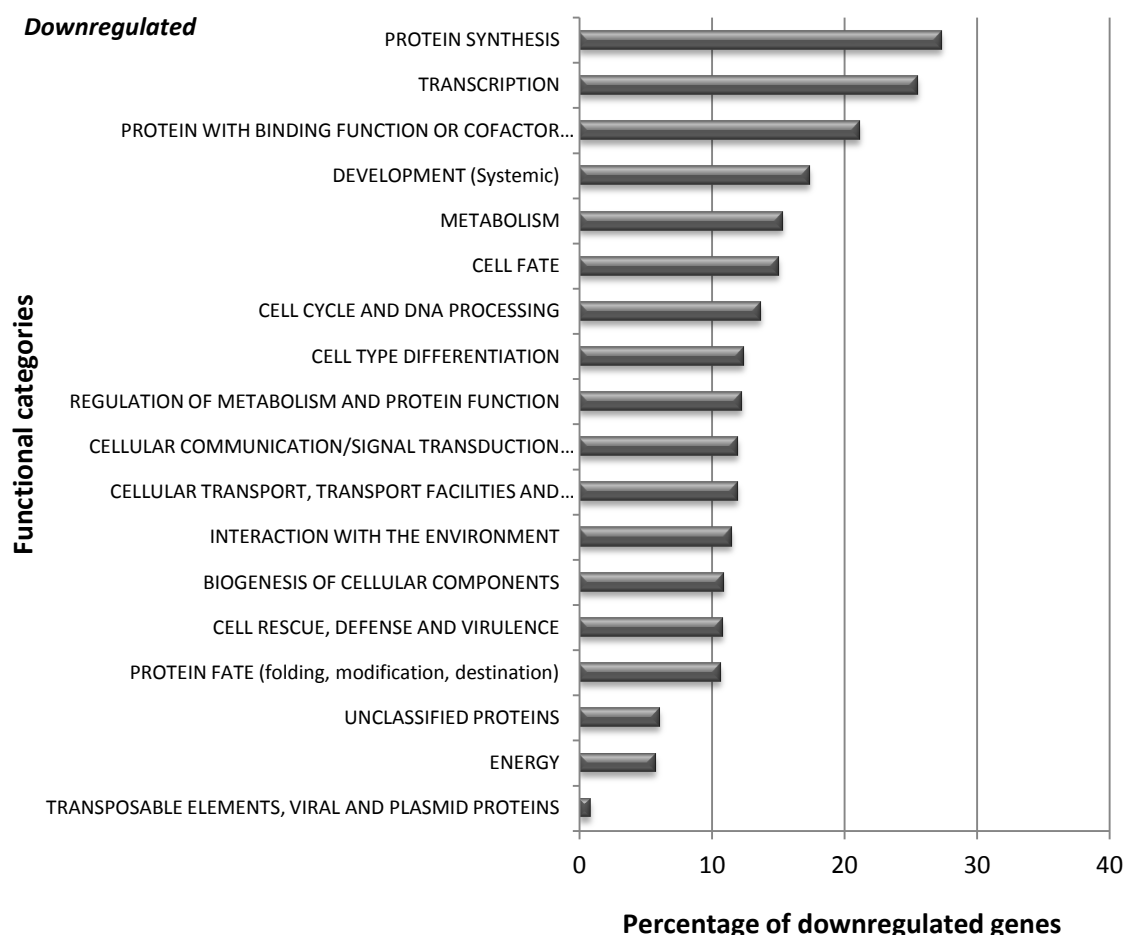
Figure 3.26: The percentage of downregulated genesto total genes in each category (cut off value is ≥ 2 fold) (Ruepp et al., 2004).

The expression levels of 891 genes were downregulated at freeze-thaw resistant mutant individual *F1*. Especially, the genes under protein synthesis and transcription functional categories were downregulated.

Some significantly downregulated genes are listed on Table 3.11. The cut off value is set to ≥ 6 fold.

Table 3.11: Relative downregulated *F1* genes (≥ 6 fold).

	GeneSymbol	*Fold Change*
metal ion binding	*AAH1*	13.91
	PHO84	93.88
transmembrane transport	*YMC2*	7.69
	FCY2	10.01
zinc ion transmembrane transport	*ZRT1*	56.65
nuclear transport	*RIX7*	13.56
catalytic activity	*PDC5*	7.75
methyltransferase activity	*TRM44*	6.94
transferase activity	*ATF2*	6.56
hydrolase activity	*UTR2*	6.30
transferase activity	*SET6*	14.84
aromate anabolism	*ARO3*	13.11
amino acid metabolism	*SUL1*	8.06
ergosterol biosynthetic process	*ERG20*	6.51
purin nucleotide/nucleoside/nucleobase metabolism	*IMD4*	8.40
pyrimidine nucleotide/nucleoside/nucleobase metabolism	*FUI1*	6.48
pyrimidine nucleotide/nucleoside/nucleobase anabolism	*URA7*	6.67
methylation	*HMT1*	10.37
transcription elongation	*ELP2*	7.08
translation initiation	*RPG1*	10.04
mRNA splicing	*DHR2*	15.74
RNA transport	*AIR1*	6.02
tRNA wobble uridine modification	*SAP185*	6.49
rRNA processing Cold-sensitivity	*NSR1*	28.05
tRNA modification	*PUS1*	6.21
	PUS7	6.55
rRNA modification	*SPB1*	11.98
rRNA processing	*NOP58*	6.16
rRNA synthesis	*RPA135*	6.07
	RPA43	7.80
	RPC53	8.94
RNA degradation	*DBP2*	20.63
nucleic acid binding	*GFD2*	7.19
DNA binding	*TOD6*	9.18
RNA binding	*NOP13*	6.25
	TRM1	6.15
	TRM11	6.70
	SSF1	7.00
	VTS1	6.86
	UTP5	8.48
	UTP4	8.69
	NRP1	11.33
	NMD3	8.05
ribosomal large subunit assembly	*YVH1*	6.29
ribosomal large subunit biogenesis	*PUF6*	9.95
	YTM1	7.23
	RRS1	7.47
ribosomal small subunit biogenesis	*KRE33*	9.52
	BUD22	7.55
	SGD1	6.56
ribosomal small subunit export from nucleus	*BUD23*	6.89

Table 3.11 (continued): Relative downregulated *F1* genes (≥ 6 fold).

	GeneSymbol	Fold Change	GeneSymbol	Fold Change
rRNA processing	RSA4	13.84	DIP2	8.73
	REX4	13.50	RIX1	7.90
	MRD1	11.90	NOP53	8.09
	RRP12	11.57	ERB1	8.59
	DBP9	9.94	MAK5	8.50
	DBP7	10.01	PWP1	7.70
	EBP2	9.97	MTR4	7.70
	ECM16	11.11	UTP10	7.42
	BFR2	10.74	RPF2	7.41
	UTP13	10.53	RRP5	7.24
	IPI1	10.52	PNO1	6.82
	NOP9	10.46	IMP3	6.81
	RRP8	9.48	ENP1	6.91
	PWP2	10.10	NUG1	6.86
	NOP8	8.33	HAS1	6.66
	ESF2	8.18	MRT4	6.37
	NOP7	8.30	ENP2	6.36
	NOP2	8.84	DBP8	8.02

	GeneSymbol	Fold Change	GeneSymbol	Fold Change
ribosome biogenesis	LCP5	9.53	IPI3	11.16
	DRS1	9.45	NOP4	13.85
	CIC1	9.37	NSA1	6.34
	RRP9	9.26	UTP8	6.30
	UTP21	9.92	NAN1	6.30
	UTP14	9.91	NOC3	6.27
	DBP3	9.13	LSG1	6.02
	ROK1	9.02	MAK21	7.17
	NSA2	8.67	HCA4	7.19
	NOP14	8.60	UTP23	6.93
	SAS10	8.48	URB2	6.69
	NOC2	8.42	FAF1	6.75
	BMS1	8.73	SDA1	14.92
	RLP24	8.34	NOG2	13.83
	DBP10	7.45	NOG1	13.67
	SOF1	7.44	MAK16	12.28
	RRB1	8.13	ARX1	12.07
	TSR1	7.74	ALB1	11.27
	NOC4	7.76	-	-

			GeneSymbol	Fold Change
Functionally unknown proteins			YLR413W	8.31
			YIL096C	6.28
			YCR087C-A	6.01
			YBL081W	6.55
			YIL091C	7.63
			YBR141C	6.66
			FPR4	9.84

The genes that are expressed under normal growth conditions in the cell cycle are indicated as a bar chart in the Figure 3.27. The genes that are induced under stress conditions in cell cycle are indicated as a red line and the genes that are repressed under stress conditions in cell cycle are indicated as a green line (Brauer et al., 2008). Here, the black line presents our microarray data of downregulated genes. The

Princeton growth rate/gene expression relationship database was used to analyse our microarray data.
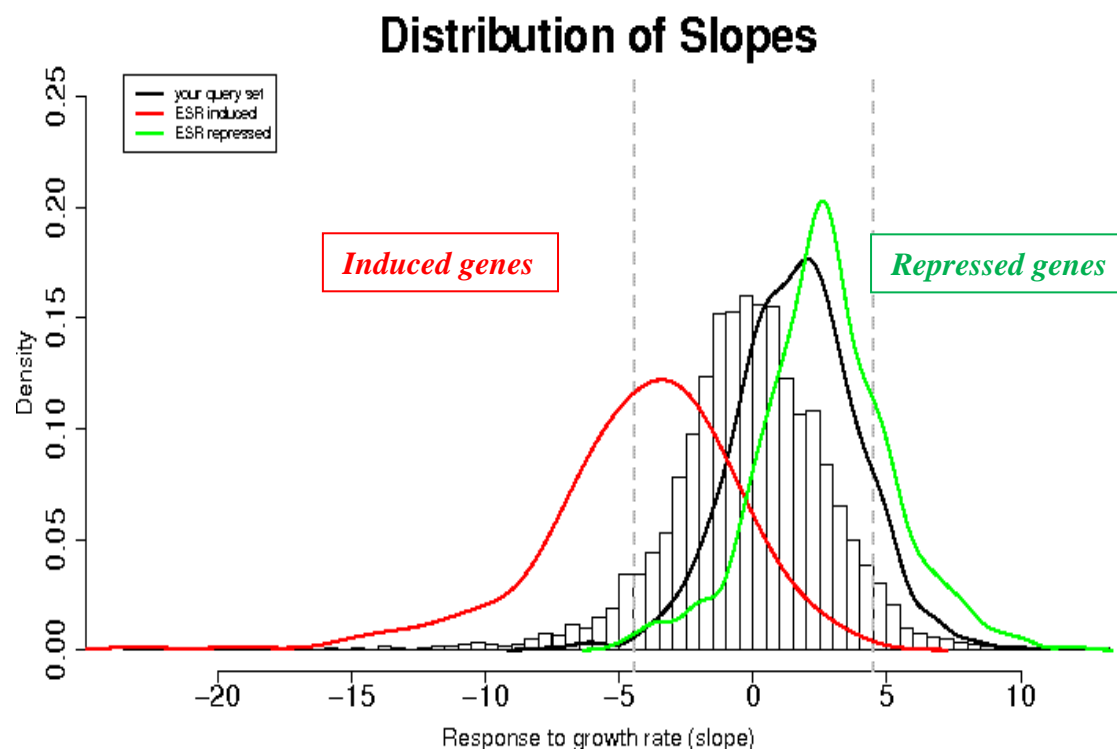
Figure 3.27: The distribution of slopes of up and downregulated ESR genes of yeast. The red line shows induced genes, green line shows repressed genes under environmental stress conditions. Bar chart shows the genes that are expressed under normal growth conditions in cell cycle. The black line shows the downregulated genes of *F1* under normal growth conditions in cell cycle.

When the growth rate decreased due to stress elements, some of the ESR genes were downregulated. Here, the ESR gene expressions were repressed in *F1* to adjust growth rate, however there is no stress, evidently.

3.1.4 Physiological analysis of mutant individual *F1*

Physiological Analysis of Mutant Individual *F1* was performed at normal growth conditions without stress treatment. Growth curve and metabolite analysis was examined with respect to wild-type. Growth curves of wild-type and *F1* was constructed via spectrometric measurements. Metabolite analysis were examined via HPLC and glucose oxidase/peroxidase assay.

3.1.4.1 Growth analysis for mutant individual *F1*

- **Growth analysis via shake flask and bioreactor cultivation**

For the growth analysis, wild-type and *F1* were grown at normal growth conditions without stress treatment. The appropriate volume of samples was taken from each culture for optical density measurements at different time intervals. The optical density results of batch cultivation are indicated in Table 3.12.

Table 3.12: Optical density (OD_{600}) results of shake flask cultivation with respect to time.

Time point	Time (hour)	OD_{600} results of wild-type	OD_{600} results of *F1*
t_0	0.00	0.11	0.09
t_1	1.50	0.12	0.10
t_2	3.00	0.18	0.16
t_3	4.50	0.35	0.40
t_4	6.00	0.57	0.49
t_5	7.00	0.94	0.76
t_6	8.50	1.54	1.28
t_7	10.00	2.22	1.86
t_8	11.50	3.40	2.96
t_9	13.00	3.60	3.50
t_{10}	14.50	4.86	4.44
t_{11}	16.00	4.60	5.23
t_{12}	18.50	5.94	7.28
t_{13}	21.00	5.40	7.81
t_{14}	24.00	5.55	7.95
t_{15}	27.00	6.49	8.40
t_{16}	30.00	4.50	6.90

The optical density results of bioreactor cultivation are indicated in Table 3.13.

Table 3.13: Optical density (OD_{600}) results of bioreactor cultivation with respect to time.

Time point	Time (hour)	OD_{600} results of wild-type	OD_{600} results of *F1*
t_0	0.00	0.23	0.20
t_1	2.00	0.63	0.58
t_2	3.50	1.10	1.05
t_3	5.00	2.11	2.19
t_4	6.50	3.25	2.96
t_5	8.00	5.00	4.46
t_6	9.50	6.20	5.24
t_7	11.00	7.70	7.01
t_8	24.00	9.56	11.93
t_9	30.00	10.77	11.75

The shake flask cultivation optical density (OD_{600}) results of wild-type and *F1* with respect to time are indicated in Figure 3.28.
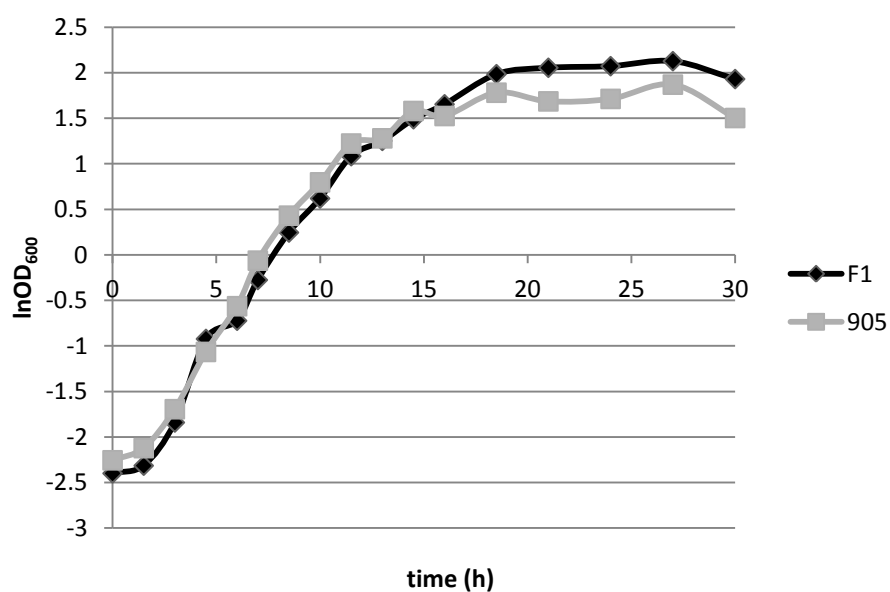
Figure 3.28: Shake flask growth curve of *905* and *F1* with respect to $lnOD_{600}$ /time.

The bioreactor cultivation optical density (OD_{600}) results of wild-type and *F1* with respect to time are indicated in Figure 3.29.
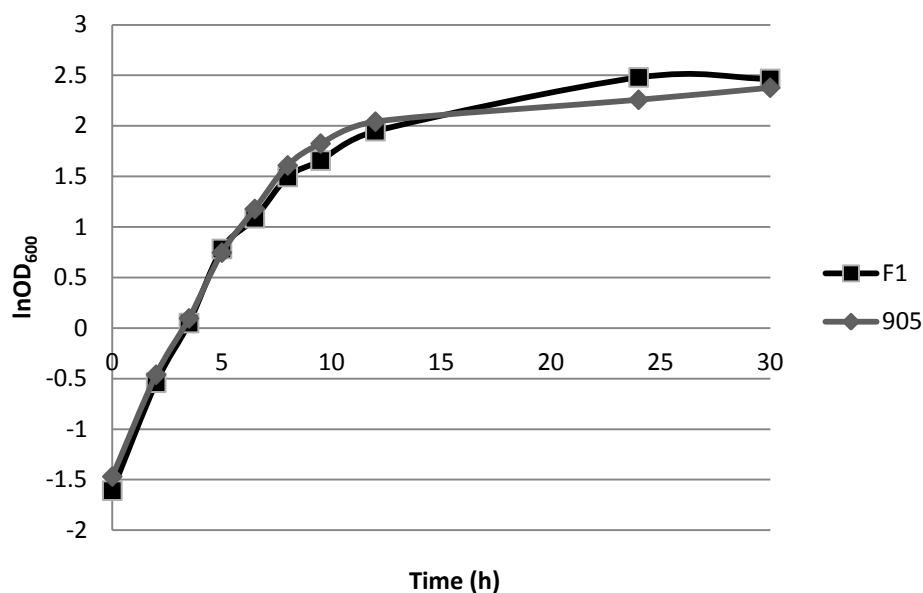
Figure 3.29: Bioreactor growth curve of *905* and *F1* with respect to $\ln OD_{600}$ /time.

The $\ln OD_{600}$ results with respect to time are indicated in Figure 3.28. The specific growth rate (μ) of wild-type was 0.208 h^{-1} and the generation time was calculated as 3.33 h. The growth rate (μ) of mutant strain was 0.186 h^{-1} and the generation time was calculated as 3.73 h. However, after 15 hours wild-type was started to come into stationary phase while *F1* kept growing.

The generation time was calculated according to the following equation;

$$\text{Generation time} = \ln2/\mu$$

The shake flask cultivation specific growth rates (μ) and the generation times are indicated in Table 3.14.

Table 3.14: The specific growth rates (μ) and the generation times of *905* and *F1* in shake flask cultivation.

	Specific growth rates (h^{-1})	Generation Time (h)
905	0.21	3.33
F1	0.19	3.73

The shake flask cultivation growth curve result of wild-type and *F1* with respect to $\ln OD_{600}$-time are indicated in Figure 3.30.
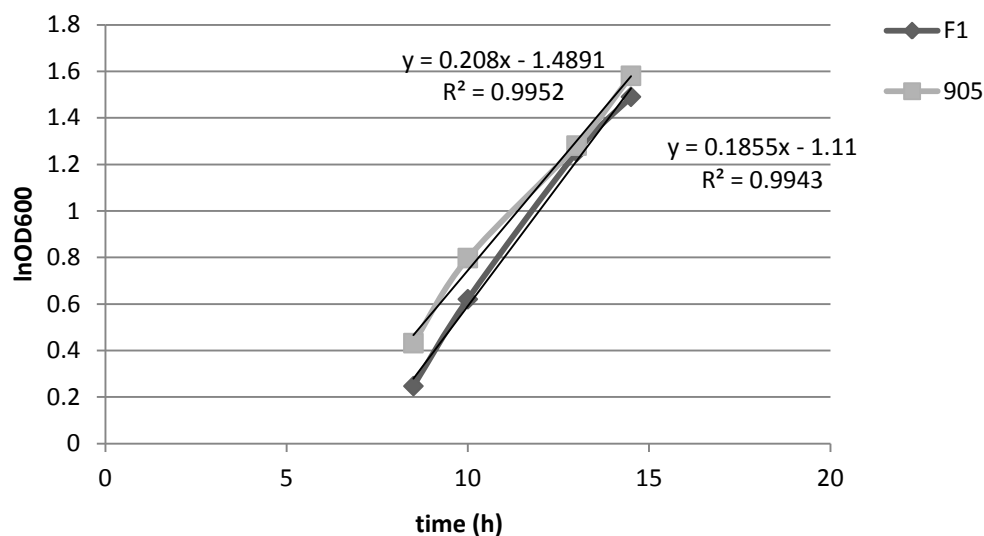
Figure 3.30: Shake flask growth curve of wild-type and *F1* with respect to lnOD$_{600}$-time.

The bioreactor cultivation specific growth rates (μ) and the generation times are indicated in Table 3.15.

Table 3.15: The specific growth rates (μ) and the generation times of *905* and *F1* in bioreactor cultivation.

	Specific growth rates (h^{-1})	**Generation Time (h)**
905	0.44	1.58
F1	0.47	1.48

The bioreactor cultivation growth curve of wild-type and *F1* with respect to lnOD$_{600}$-time are indicated in Figure 3.31.
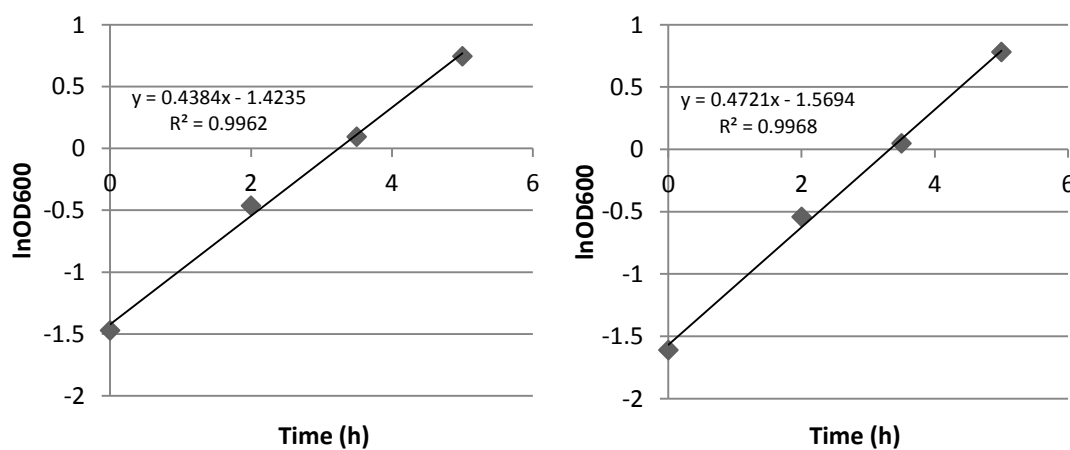
Figure 3.31: Growth curve of wild-type and *F1* with respect to lnOD$_{600}$-time.

66

3.1.4.2 High performance liquid chromatography (HPLC) analysis

Liquid culture samples were taken from *905* and *F1* during the growth curve analysis and extracellular glucose, acetate, glycerol and ethanol concentrations were determined by using high performance liquid chromatography (HPLC). The HPLC measurements were done triplicate for each metabolite and most of the error bars are too small to see.

The shake flask cultivation glucose consumptions of *905* and *F1* during the growth are indicated in Figure 3.32.
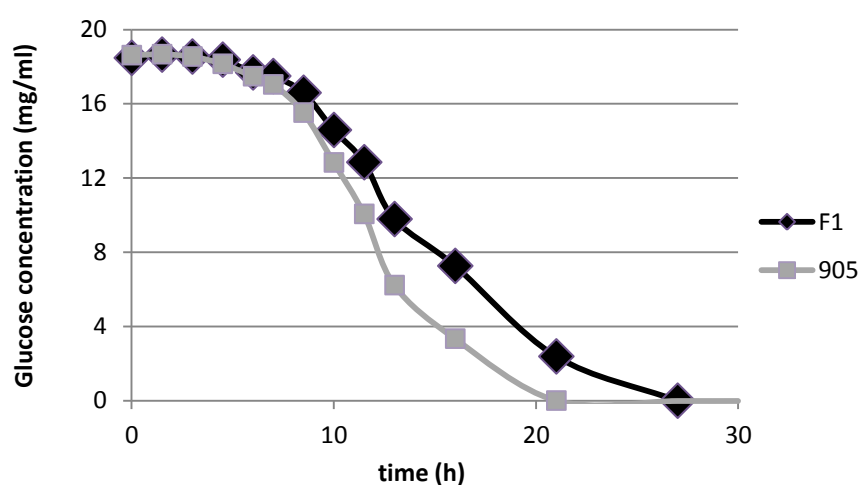
Figure 3.32: Change of glucose concentration during the shake flask growth.

Glucose concentrations decreased normally due to the cellular consumptions during the growth. *F1* was used glucose slower than *905*. The bioreactor cultivation glucose consumptions of *905* and *F1* during the growth are indicated in Figure 3.33.
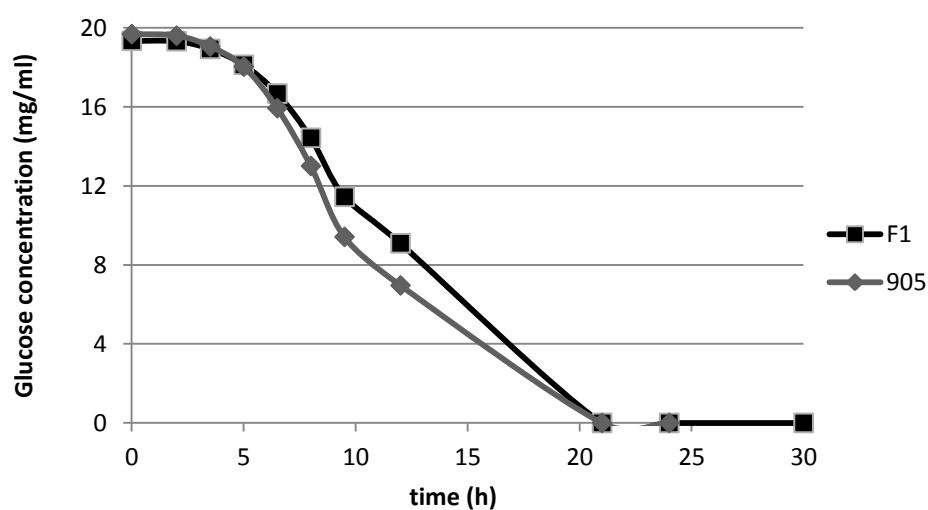
Figure 3.33: Change of glucose concentration during the bioreactor growth.

When we compare the glucose consumption rates of both batch and bioreactor cultivations, they were consistant with the behavior of wild-type and mutant individual *F1*. There is no obvious differences.

The shake flask cultivation glycerol production of *905* and *F1* during the growth are indicated in Figure 3.34.
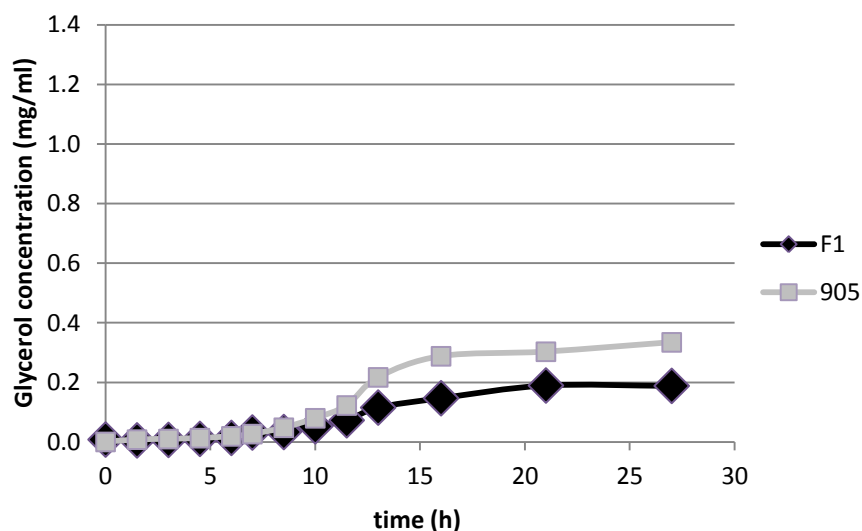
Figure 3.34: Change of glycerol concentration during the shake flask growth.

As shown in Figure 3.34, glycerol productions were observed during the growth. It is obvious that glycerol amount in the exogenous medium of *F1* was lower than *905*.

The bioreactor cultivation glycerol productions of *905* and *F1* during the growth are indicated in Figure 3.35.
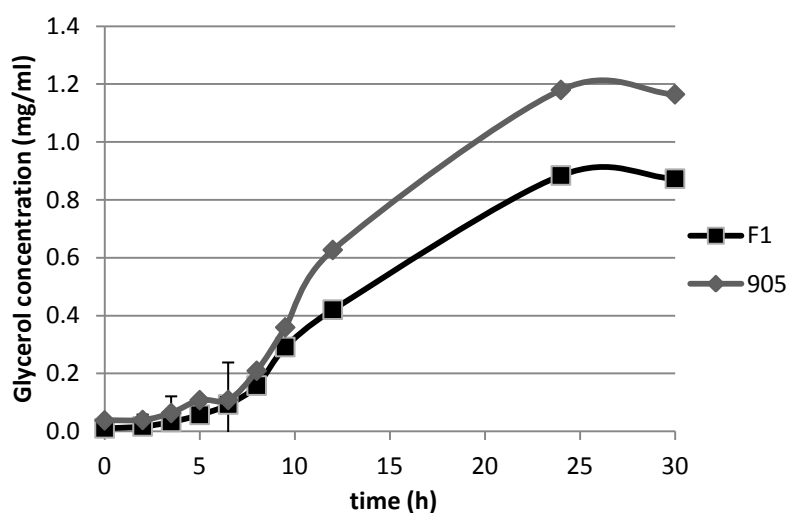
Figure 3.35: Change of glycerol concentration during the bioreactor growth.

In a similar manner and consistent with the shake flask cultivation, glycerol amount in the extracellular culture medium of *F1* was lower than in *905*. On the other hand, the glycerol production rates of wild-type and mutant individual *F1* were higher in the bioreactor cultivation.

The shake flask cultivation acetate production of *905* and *F1* during the growth are indicated in Figure 3.36.
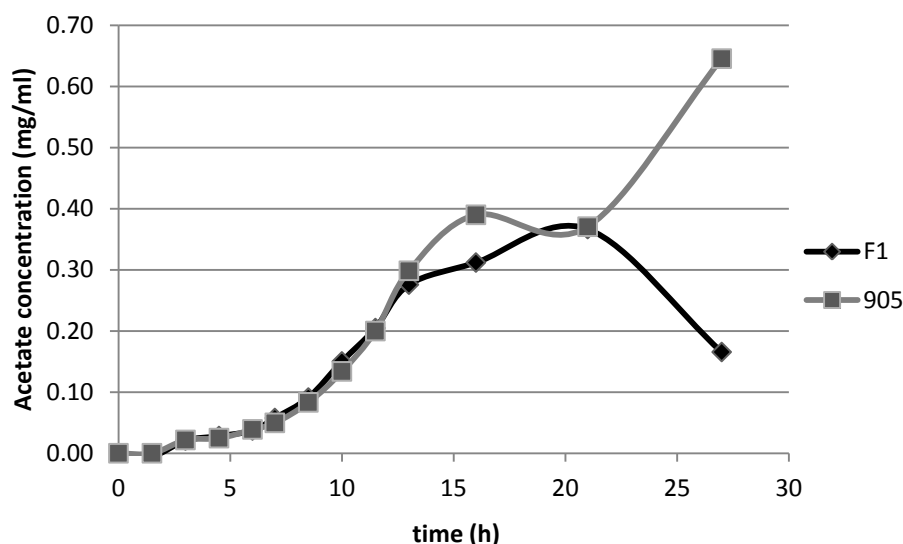
Figure 3.36: Change of acetate concentration during the shake flask growth.

Acetate was produced until the late stationary phase and then started to consume in *F1* different from *905*.

The bioreactor cultivation acetate production of *905* and *F1* during the growth are indicated in Figure 3.37.
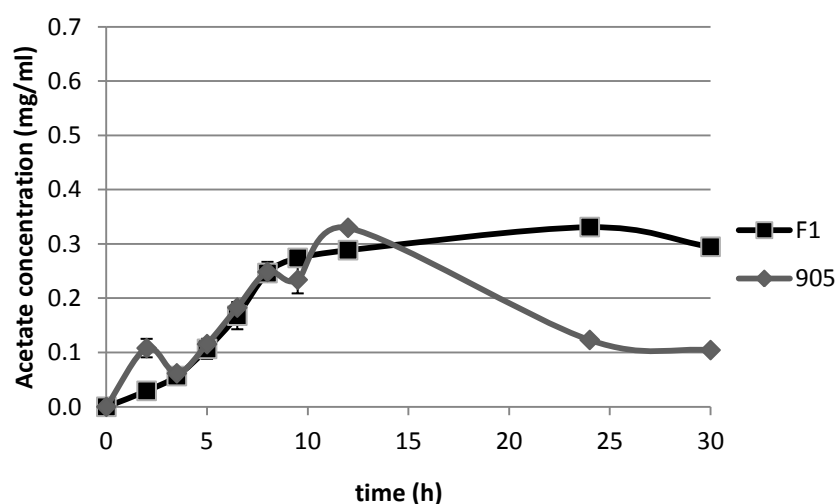
Figure 3.37: Change of acetate concentration during the bioreactor growth.

Acetate was produced during the growth and then started to consume in *905* in stationary phase different from *F1*. The acetate production rates of wild-type and mutant individual *F1* were lower in the bioreactor cultivation. Although the acetate production behavior seems to parallel in both shake flask and bioreactor cultivations, the stationary phase behaviour of wild-type and *F1* were different.

The batch cultivation ethanol productions of *905* and *F1* during the growth are indicated in Figure 3.38.
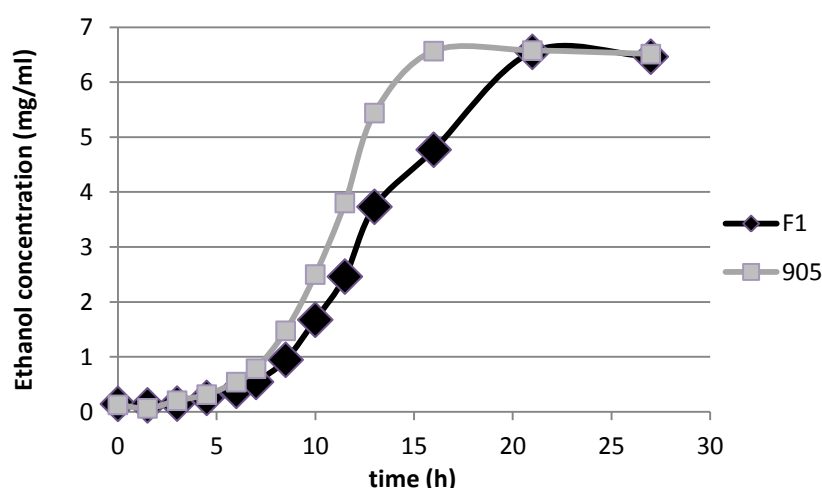
Figure 3.38: Change of ethanol concentration during the shake flask growth.

As shown in Figure 3.15, ethanol was produced during growth. It is obvious that ethanol production rate of *905* was higher than *F1*. The bioreactor cultivation ethanol productions of *905* and *F1* during the growth are indicated in Figure 3.39.
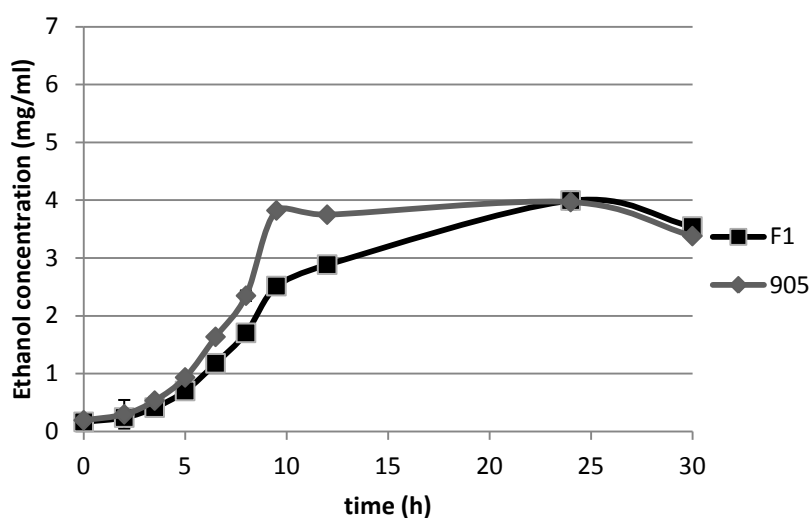
Figure 3.39: Change of ethanol concentration during the bioreactor growth.

The ethanol production behaviour of wild-type and *F1* were consistent with the shake flask cultivation. However, the ethanol production rates were lower than the shake flask cultivation.

Determination of these metabolites was important in order to determine the relationship between growth and exhaustion/production of metabolites.

3.1.4.3 Reserve carbonhydrate analysis of wild-type and mutant individual *F1*

The reserve carbohydrates glycogen and trehalose were analyzed by using glucose oxidase/peroxidase assay. The samples were collected during the growth at spesific time intervals. The intracellular trehalose levels during the growth are indicated for wild-type and *F1* at Figure 3.40.
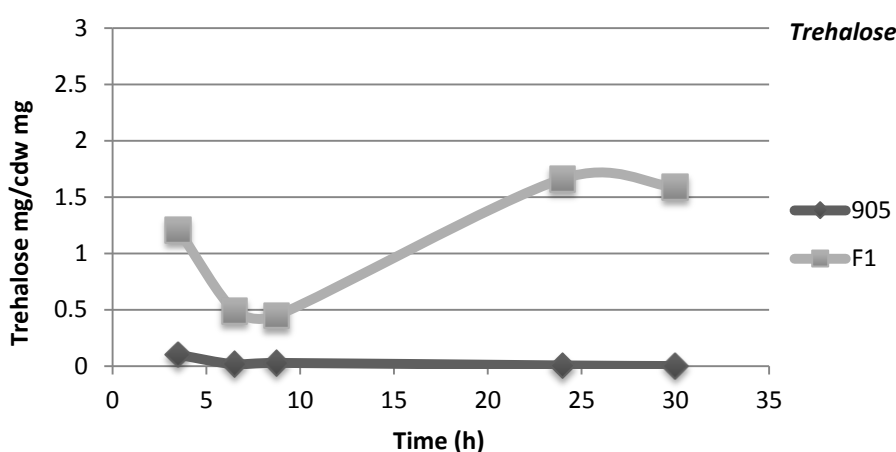
Figure 3.40: Change of intracellular trehalose amount during the growth.

The intracellular glycogen levels during the growth are indicated for wild-type and *F1* at Figure 3.41.
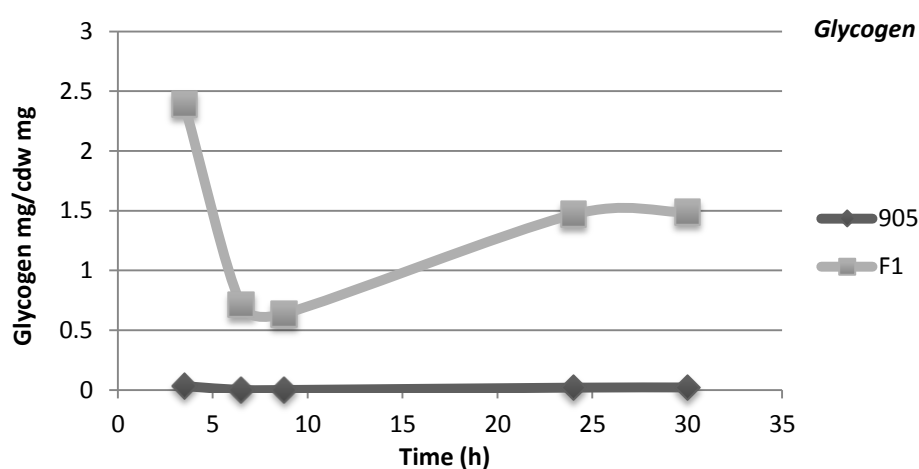
Figure 3.41: Change of intracellular glycogen amount during the growth.

It is obvious that, intracellular reserve carbohydrates trehalose and glycogen were higher in *F1* with respect to wild-type at normal growth conditions without freeze-thaw stress treatment.

3.1.5 Phenotypic characterization of diploid wild-type and diploid *F1*

The diploidization of wild-type and *F1* was performed by using opposite mating type *Saccharomyces cerevisiae* CEN.PK113-1A (matα) strain. After diploidization of wild-type and *F1*, freeze-thaw stress and cross resistance analyses were performed by using spotting assay.

This method was enabled to compare haploid and diploid cells at those different stress conditions.

3.1.5.1 Freeze-thaw stress application

Overnight incubated cell cultures were exposed to three cycles of freeze-thaw stress application. Then, the cultures were analyzed with 5-tube MPN method. Samples were incubated at 30 $^{\circ}$C for 24 hours. The MPN results (cell/ml) and survival ratios of *905*, *2n*, *F1* and *F1_2n* are indicated in Table 3.16.

Table 3.16: The MPN results and survival ratios of *905*, *2n*, *F1* and *F1_2n*.

Wild-type and freeze-thaw resistant mutant individual	*Freeze-thaw stress*		
	Control	3 cycles freeze-thaw stress	Survival ratios
	(cell/ml)	(cell/ml)	
905	16000000	920000	0.06
2n	5400000	3500000	0.65
F1	9200000	9200000	**1.00**
F1_2n	5400000	5400000	**1.00**

The survival ratios of *2n*, *F1* and *F1_2n* as fold of wild-type are indicated in Figure 3.42.
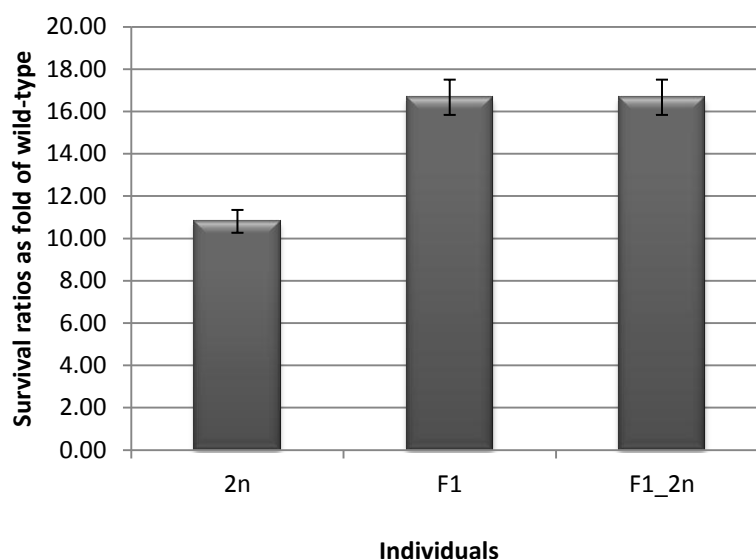
Figure 3.42: Survival ratios of *2n*, *F1* and *F1_2n* as fold of wild-type.

It was seen that, freeze-thaw stress resistant haploid mutant *F1* and diploid *F1_2n* (diploidized with wild-type *934*)was survived upto 16 fold of*905* after three cycles stress application. Here, it is important that there is no survival decline in diploid *F1_2n*, whether it has one copy of wild-type genome. So, the genes that were expressed under freeze-thaw stress conditions were dominant. On the other hand diploid wild-type 2n had upto 10 fold of survival than haploid wild-type. This is because, it has two copy of each stress response genes, whether those genes are not constitutively expressed.

3.1.5.2 Cross-resistance analysis

Cross resistance analysis were performed with 80 mM boron, 0.2 mM nickel and 0.04% acetic acid stresses by using spotting assay. Overnight incubated *F1*, *F1_2n* (diploid form of *F1* and *934*), *905* (mat a), and *2n* (diploid form of *905* and *934*) cell cultures were diluted from 10^{-1} to 10^{-5} and dropped on to YMM w/wo stress factor containing plates. Then the cultures were incubated at 30 $^{\circ}$C for 72 hours.

The growth images of *905*, *2n*, *F1* and *F1_2n* on control plates at normal growth condition without stress treatment are indicated in Figure 3.43.
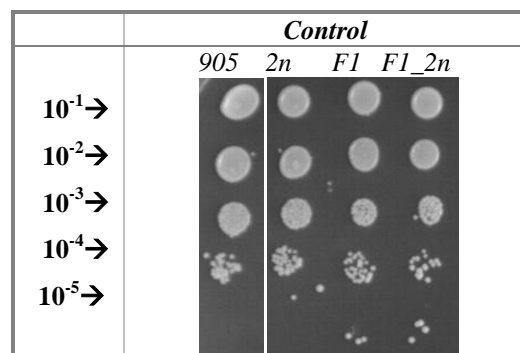
Figure 3.43: Growth images on control plates.

The growth images of *905*, *2n*, *F1* and *F1_2n* on 0.2 mM NiCl$_2$ containing plates are indicated in Figure 3.44.
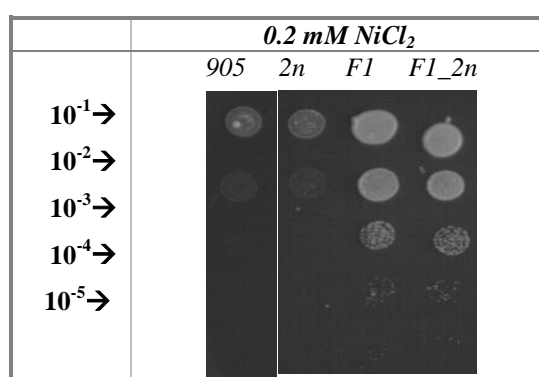
Figure 3.44: Nickel stress results of *F1*, *F1_2n*, *905* and *2n*.

As shown in Figure 3.40, 0.2 mM nickel stress was not fatal on mutant cells. Mutant individual *F1* and its diploid form *F1_2n* that were mated with wild-type *934* was resistant to nickel stress. Haploid and diploid wild-type cells were sensitive to nickel stress.

The growth images of *905*, *2n*, *F1* and *F1_2n* on 80 mM B(OH)$_3$ containing plates are indicated in Figure 3.45.
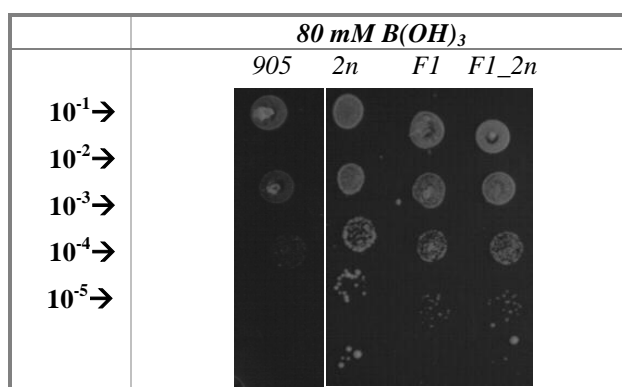
Figure 3.45: Boron stress results of *F1*, *F1_2n*, *905* and *2n*.

As shown in Figure 3.41, 80 mM boron stress was not fatal on mutant cells. Mutant individual *F1* and *F1_2n* were resistant to boron stress. However, diploid wild-type strain *2n* had also great resistance to boron stress. On the other hand, haploid wild-type *905* was sensitive to boron stress when compared to *2n*, *F1* and *F1_2n*.

The growth images of *905*, *2n*, *F1* and *F1_2n* on 0.04 % acetic acid containing plates are indicated in Figure 3.46.
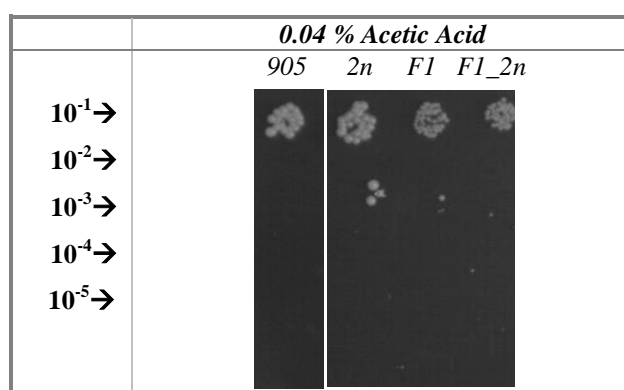
Figure 3.46: Acetic acid stress results of *F1*, *F1_2n*, *905* and *2n*.

As shown in Figure 3.46, diploid wild-type strain *2n* had growth at 10^{-2} dilution on stress containing plate and resistant to acetic acid stress. Wild-type and mutant individuals; *F1* and *F1_2n* had the same result to acetic acid stress.

3.2 Studies with industrial baker's yeast *Saccharomyces cerevisiae R625*

3.2.1 Evolutionary engineering strategy to obtain freeze-thaw resistant industrial baker's yeast mutants

Evolutionary engineering strategy was used to obtain freeze-thaw resistant industrial baker's yeast mutants. For this reason, wild-type industrial *Saccharomyces cerevisiae R625* strain was mutagenized by EMS. The genetically variant population was used to obtain generations and finally the selection of mutant individuals were performed.

3.2.1.1 EMS mutagenesis for industrial baker's yeast *Saccharomyces cerevisiae*

S. cerevisiae R625 cells were mutagenized by applying the ethyl methane sulphonate (EMS) mutagenesis method. *S. cerevisiae R625* cells were exposed to 300 µl, 600 µl and 900 µl EMS for 30 min. The optical density values and the survival ratios of each EMS condition are shown in Table 3.17.

Table 3.17: The optical density results and survival ratios.

EMS Application	OD_{600}	Survival ratio	Incubation time (h)
Contol	4.00	1	24
30' 300 µl	3.40	0.85	24
30' 600 µl	3.10	0.78	24
30' 900 µl	0.76	**0.19**	24

The genetically variant cell population was obtained from the fatal 900 µl EMS application. Then, the mutant population was named as *R625_M*.

3.2.1.2 Screening of industrial baker's yeast *Saccharomyces cerevisiae* and mutant population under freeze-thaw stress conditions

S. cerevisiae R625 cells and genetically variant *S. cerevisiae R625_M* mutant population were screened by applying 1-4 cycle freeze-thaw stress with 5-tube MPN methodology. The MPN results and the survival ratios of *R625* and *R625_M* after 1-4 cycle freeze-thaw stress applications are indicated in Table 3.18.

Table 3.18: MPN results and survival ratios of *R625* and *R625_M* after 24 h incubation.

Freeze-thaw Stress Application	*R625* Cell/ml	*R625_M* Cell/ml	*R625* Survival ratio	*R625_M*
Control	$7*10^6$	$35*10^5$		
1 cycle	$24*10^5$	$24*10^4$	0.34	0.07
2 cycle	$92*10^4$	$24*10^4$	0.13	0.07
3 cycle	$54*10^4$	$24*10^4$	0.08	0.07
4 cycle	$54*10^4$	$35*10^3$	0.08	0.01

The survival ratios of *R625* and *R625_M* was determined according to the MPN results by dividing the cell/ml numbers of stress applied ones to the cell/ml numbers of its control one. The survival ratios of *R625* and *R625_M* after 1-4 cycle freeze-thaw stress applications are indicated in Figure 3.47.
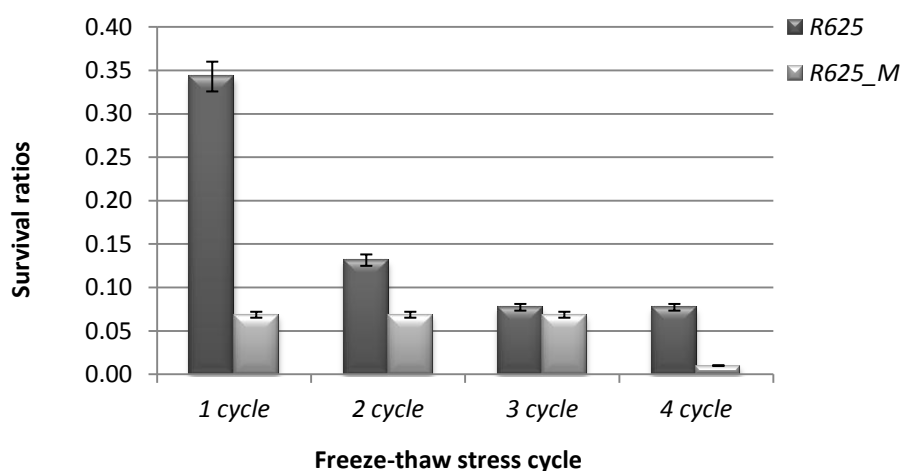
Figure 3.47: The survival ratios of *R625* and *R625_M* after 24 h incubation.

According to the MPN results, genetically variant *S. cerevisiae R625_M* mutant population was sensitive to freeze-thaw stress when compared to wild-type *S. cerevisiae R625* cells.

3.2.1.3 Obtaining freeze-thaw resistant industrial baker's yeast generations

To obtain the freeze-thaw resistant generations, pulse increasing stress selection strategy was adopted. The MPN results and the survival ratios of the mutant generations are indicated in Table 3.19.

Table 3.19: MPN results and survival ratios of generations after 24 h incubation.

Generations	Control (cell/ml)	Stress (cell/ml)	Survival ratio	% Survival ratio
R625_FG1	3500000	9200	0.0026	0.26
R625_FG2	2200000	5400	0.0025	0.25
R625_FG3	1600000	3500	0.0022	0.22
R625_FG4	3100000	2400	0.0008	0.08
R625_FG5	3500000	1700	0.0005	0.05
R625_FG6	16000000	24000	0.0015	0.15
R625_FG7	5400000	35000	0.0065	0.65
R625_FG8	3500000	24000	0.0069	0.69
R625_FG9	3500000	24000	0.0069	0.69
R625_FG10	2400000	3300	0.0014	**0.14**

The stress level was increased one cycle at each increasing numbered generation. Ten generations were obtained and the final generation was named as *R625_FG10*. The final generation was exposed to 10 repetative cycles of freeze-thaw stress

application. The graphical representation of the percent survival ratios of the mutant generations are indicated in Figure 3.48.
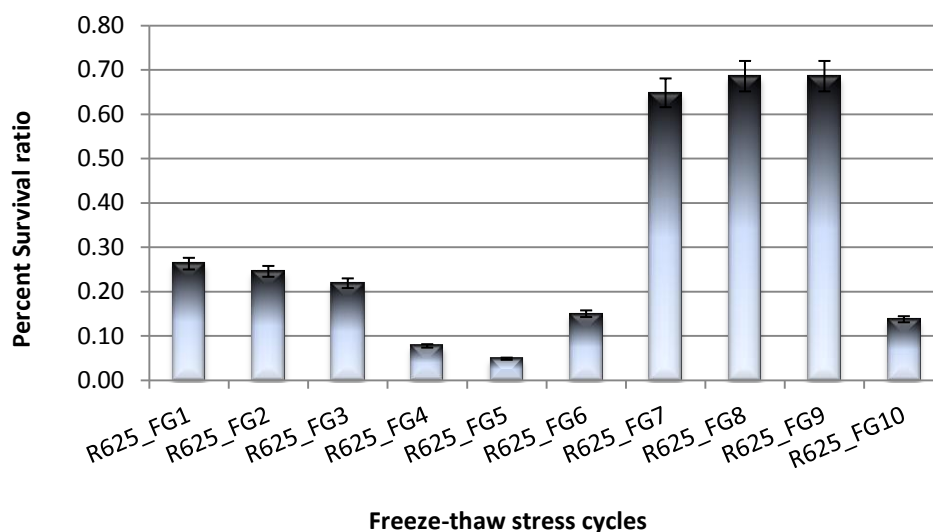
Figure 3.48: MPN results and survival ratios of generations after 24 h incubation.

3.2.1.4 Selection of the mutant individuals from the final mutant generation

Selection of individual mutants was performed randomly from the final freeze-thaw stress resistant generation *R625_FG10*. Ten mutant individuals were selected from *R625_F10G* final heterogeneous mutant population. The nomenclature, for the pulse increasing stress mutant individuals, which obtained from the final freeze-thaw stress generation are indicated in Table 3.20.

Table 3.20: Nomenclature of mutant individuals, selected from pulse increasing freeze-thaw stress final population (*F10G*).

Freeze-thaw resistant mutant individuals	Code of pulse increasing application individuals
1st mutant individual	R625_P1
2nd mutant individual	R625_P2
3rd mutant individual	R625_P3
4th mutant individual	R625_P4
5th mutant individual	R625_P5
6th mutant individual	R625_P6
7th mutant individual	R625_P7
8th mutant individual	R625_P8
9th mutant individual	R625_P9
10th mutant individual	R625_P10

The randomly selected individuals were labeled and coded as freeze-thaw resistant mutant individuals.

3.2.1.5 Screening of Freeze-thaw resistant industrial baker's yeast mutant individuals

After obtaining pulse increasing stress final generation, selection of the most resistant mutant individuals were performed via spotting assay and MPN method.

- **Screening of freeze-thaw resistant industrial baker's yeast mutant individuals via spotting assay**

After obtaining pulse increasing stress final generation, selection of mutant individuals was performed. Thereafter, screening of freeze-thaw resistance of mutant individuals was performed after one and two cycles of freeze-thaw stress application.

The growth images of freeze-thaw resistant mutant individuals *P1*, *P2*, *P3*, *P4*, *P5*, *P6*, *P7*, *P8*, *P9*, *P10*, *R625* (wild-type) and *10FG* (*R625_10FG*) on control plates without stress are indicated in Figure 3.49.
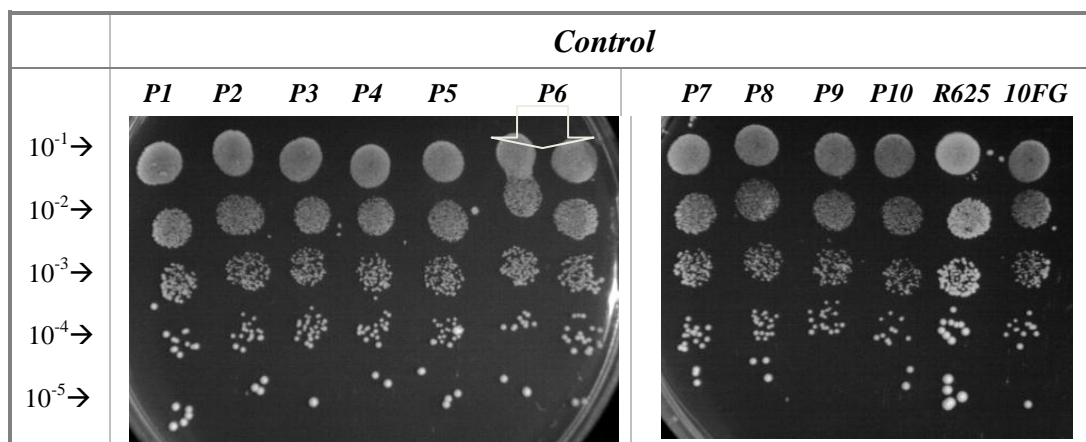
Figure 3.49: Non-stress (control) application growth images of individuals, wild type and final generation after 48 hour incubation.

The growth images of freeze-thaw resistant mutant individuals *P1*, *P2*, *P3*, *P4*, *P5*, *P6*, *P7*, *P8*, *P9*, *P10*, *R625* (wild-type) and *10FG* (*R625_10FG*) after one cycle freeze-thaw stress application are indicated in Figure 3.50.
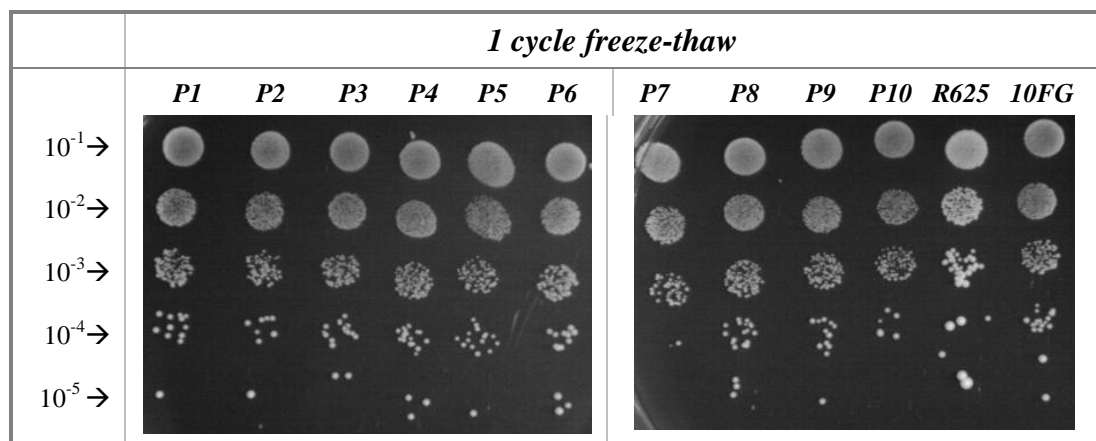
Figure 3.50: One cycle freeze-thaw stress application growth images of individuals, wild type and final generation after 48 hour incubation.

As shown in Figure 3.50, one cycle of freeze-thaw stress application was not fatal on wild-type and mutant cells.

The growth images of freeze-thaw resistant mutant individuals *P1*, *P2*, *P3*, *P4*, *P5*, *P6*, *P7*, *P8*, *P9*, *P10*, *R625* (wild-type) and *10FG* (*R62510FG*) after two cycle freeze-thaw stress application are indicated in Figure 3.51.
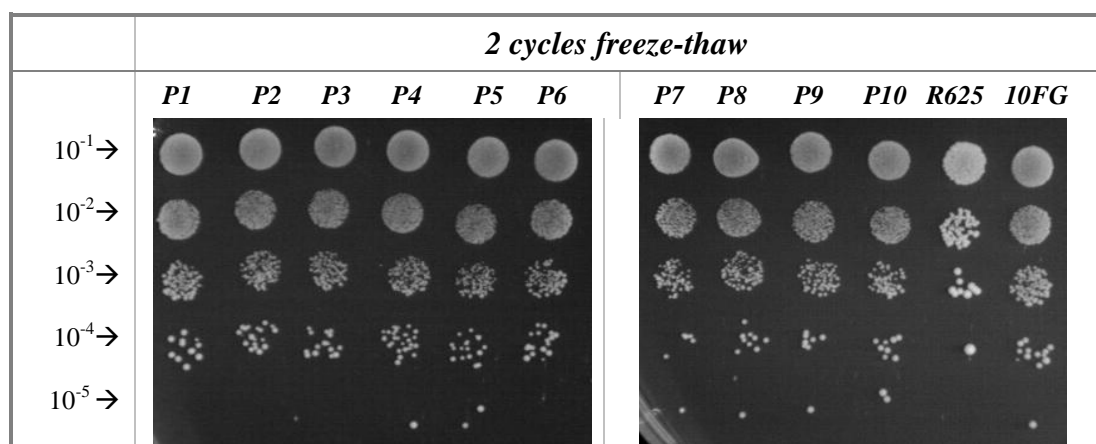
Figure 3.51: Two cycles freeze-thaw stress application growth images of individuals, wild type and final generation after 48 hour incubation.

As shown in Figure 3.51, two cycles of freeze-thaw stress application was effective on wild-type, *P1*, *P2*, *P3* and *P6*. The other mutant individuals *P4*, *P5*, *P7*, *P8*, *P9*, *P10* and final generation *R625_10FG* seems to have 10 fold higher survival than the wild-type.

- **Screening of freeze-thaw resistant industrial baker's yeast mutant individuals via MPN method**

In order to determine the freeze-thaw stress responses of the mutant individuals, survival ratios of two, three and four cycles freeze-thaw stress application were obtained from the five tube-MPN data. The MPN results of two, three and four cycle freeze-thaw stress applications are indicated in Table 3.21.

Table 3.21: MPN results (cell/ml) of freeze-thaw stress application (24 h).

Wildtype and mutant individuals	Control (cell/ml)	2_cycle freeze-thaw stress application (cell/ml)	3_cycle freeze-thaw stress application (cell/ml)	4_cycle freeze-thaw stress application (cell/ml)
R625_P4	3500000	1600000	350000	350000
R625_P5	3500000	2400000	540000	350000
R625_P7	3500000	240000	240000	24000
R625_P8	2400000	1600000	540000	350000
R625_P9	3500000	920000	350000	350000
R625_P10	2400000	540000	240000	240000
Wild-type	5400000	240000	35000	35000
R625_10FG	3500000	920000	920000	240000

The survival ratios of freeze-thaw resistant mutant individuals, wild-type (*R625*) and final generation (*R625_10FG*) after corresponding freeze-thaw stress applications are indicated in Table 3.22.

Table 3.22: Survival ratios after freeze-thaw stress application (24 h).

Wildtype and mutant individuals	Survival ratios of 2_cycle freeze-thaw stress application	Survival ratios of 3_cycle freeze-thaw stress application	Survival ratios of 4_cycle freeze-thaw stress application
R625_P4	0.46	0.10	0.10
R625_P5	0.69	0.15	0.10
R625_P7	0.07	0.07	0.01
R625_P8	**0.67**	**0.23**	**0.15**
R625_P9	0.26	0.10	0.10
R625_P10	0.23	0.10	0.10
Wild-type	0.04	0.01	0.01
R625_10FG	0.26	0.26	0.07

The % survival ratios of wild-type and mutant individuals with their corresponding freeze-thaw stress cycles, after 24 h incubation are indicated in Figure 3.52.
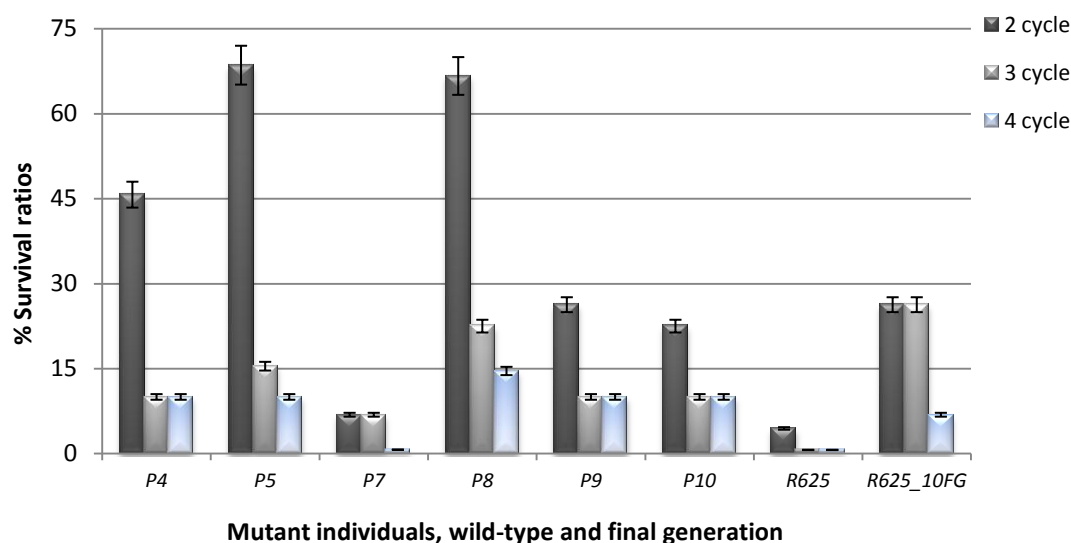
Figure 3.52: Survival ratios of wild-type and freeze-thaw resistant mutant individuals.

The survival ratios as fold of wild-type values of the individual mutants / freeze-thaw stress cycles, after 24 h incubation are indicated in Figure 3.53.
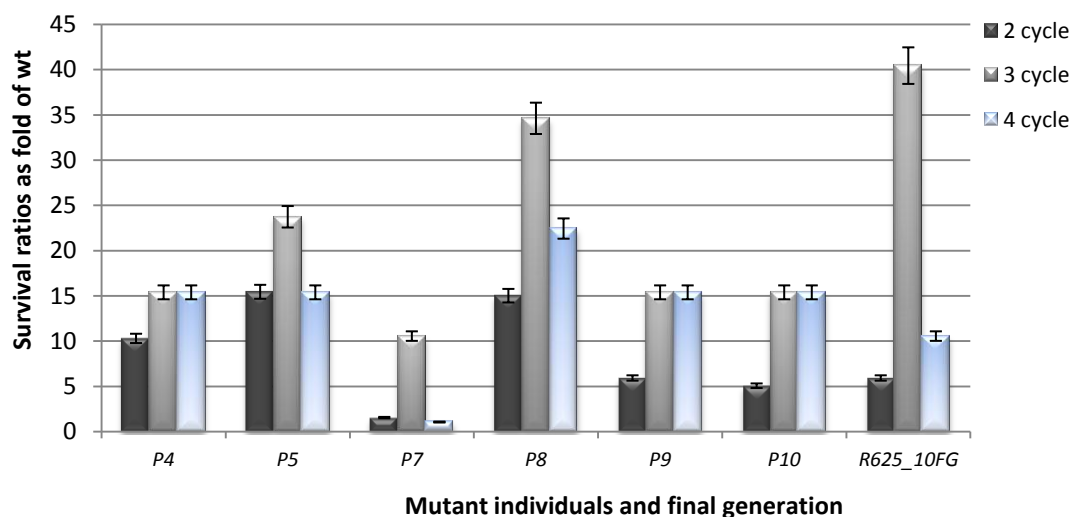
Figure 3.53: The survival ratios as fold of wild-type.

3.2.1.6 Cross-resistance analysis

Cross-resistance analysis were performed by using spotting assay and MPN (Most Probable Number) method.

- **Cross-resistance analysis via spotting assay**

Industrial *S. cerevisiae R625* cells and freeze-thaw resistant mutant individuals; *P3*, *P4*, *P7*, *P8*, *P9* and *P10* were screened at different stress conditions via spotting assay. The cross-resistance analysis were performed by using continuous stress screening strategy.

Wild-type and freeze-thaw resistant mutant individuals; *P3*, *P4*, *P7*, *P8*, *P9*, *P10* were exposed to toxic levels of boron, chromium, nickel, copper, magnesium, cobalt, zinc metal stresses and ethanol stress.

The stress levels are indicated in Table 3.23.

Table 3.23: Stress factors and concentrations for cross resistance analysis.

Stress factors	*NiCl₂*	*CoCl₂*	*CrCl₃*	*ZnCl₂*	*MgCl₂*	*Acetic acid*
Stress levels	0.2 mM 0.5 mM	1 mM 3 mM	3 mm	10 mM	40 mM	0.04 %

The spotting assay images of the cell growth at control (no stress factor) conditions are indicated in Figure 3.54.
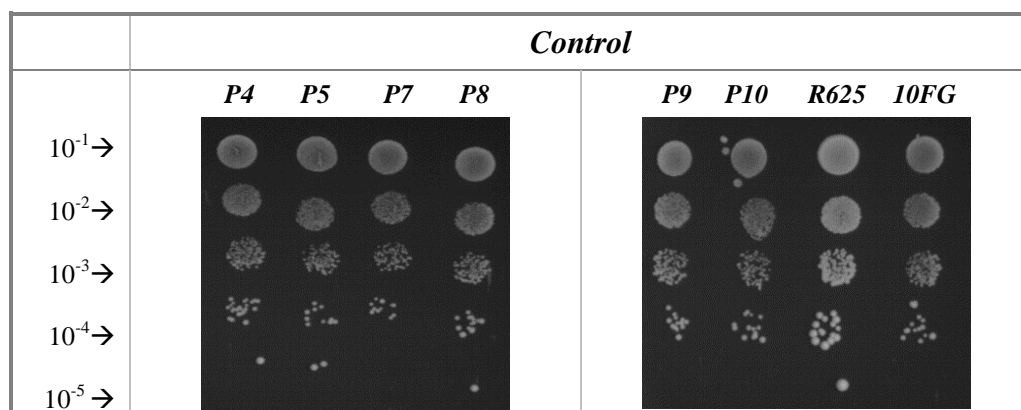
Figure 3.54: Growth images of individuals, wild type and final generation after 48 hour incubation at control conditions.

The spotting assay images of the cell growth at 40 mM MgCl₂ stress conditions are indicated in Figure 3.55.
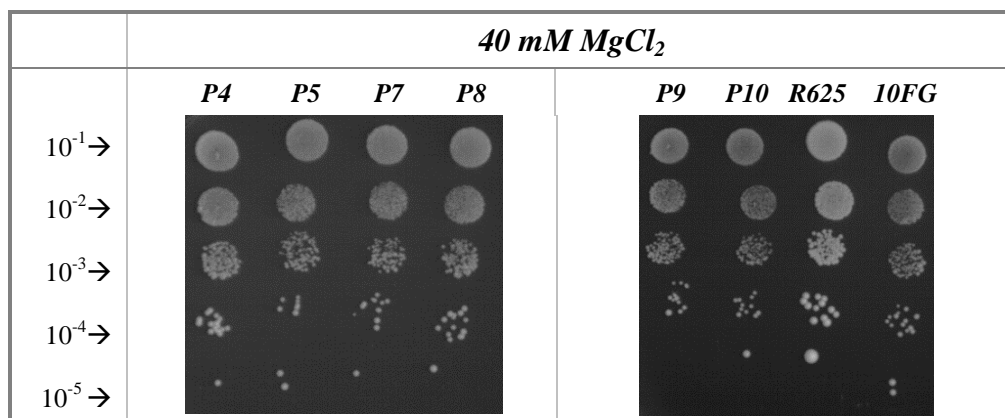
Figure 3.55: Growth images of individuals, wild type and final generation after 48 hour incubation at magnesium stress conditions.

The spotting assay images of the cell growth at 10 mM $ZnCl_2$ stress conditions are indicated in Figure 3.56.
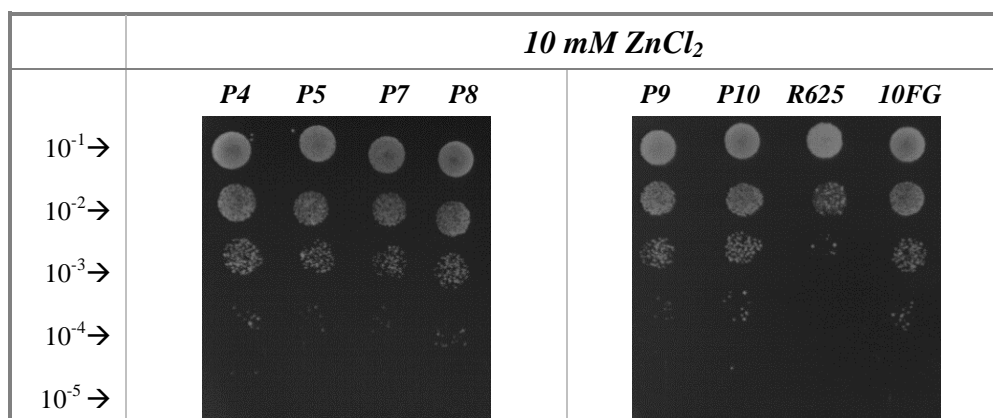
Figure 3.56: Growth images of individuals, wild type and final generation after 48 hour incubation at zinc stress conditions.

The spotting assay images of the cell growth at 1mM and 3 mM $CoCl_2$ stress conditions are indicated in Figure 3.57.
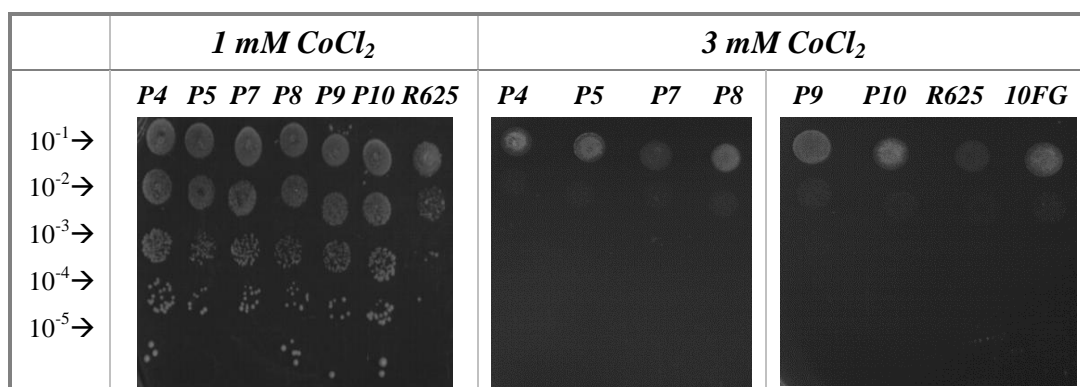
Figure 3.57: Growth images of individuals, wild type and final generation after 48 hour incubation at cobalt stress conditions.

The spotting assay images of the cell growth at 3 mM CrCl$_3$ stress conditions are indicated in Figure 3.58.
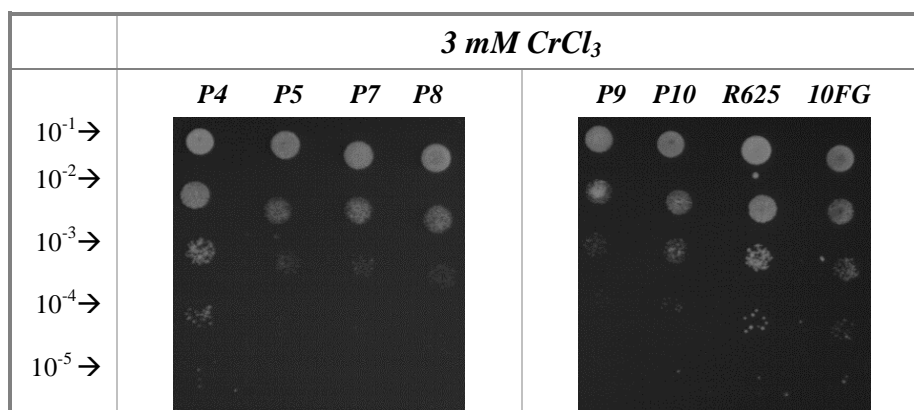
Figure 3.58: Growth images of individuals, wild type and final generation after 48 hour incubation at chromium stress conditions.

The spotting assay images of the cell growth at 0.5 mM CuCl$_2$ stress conditions are indicated in Figure 3.59.
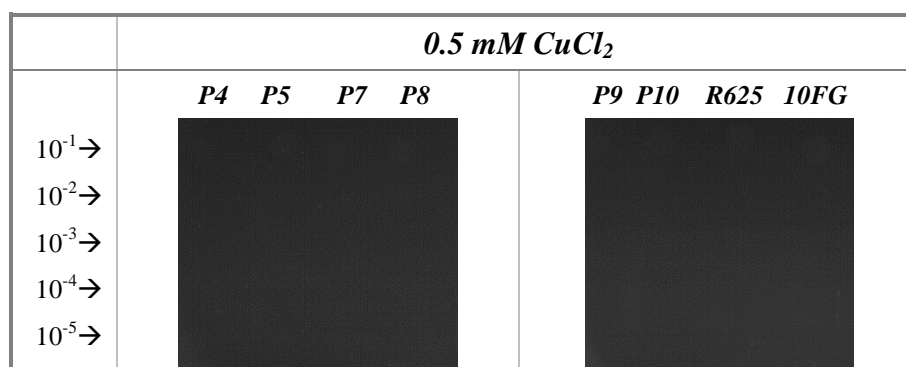
Figure 3.59: Growth images of individuals, wild type and final generation after 48 hour incubation at cupper stress conditions.

The spotting assay images of the cell growth at 0.2 and 0.5 mM NiCl$_2$ stress conditions are indicated in Figure 3.60.
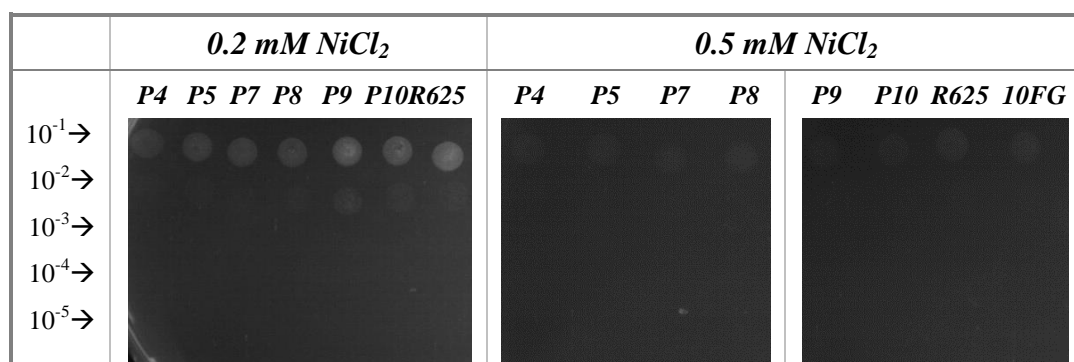
Figure 3.60: Growth images of individuals, wild type and final generation after 48 hour incubation at nickel stress conditions.

The spotting assay images of the cell growth at 0.04 % Acetic acid stress conditions are indicated in Figure 3.61.
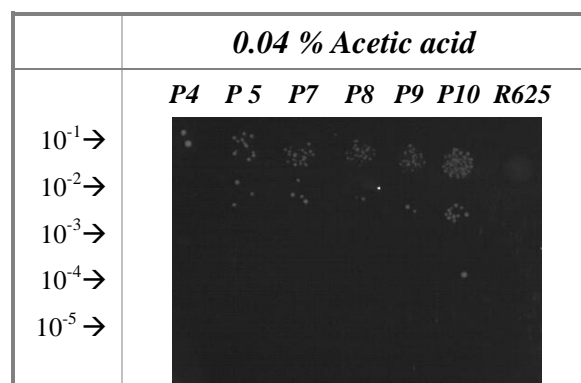
Figure 3.61: Growth images of individuals, wild type and final generation after 48 hour incubation at acetic acid stress conditions.

Freeze-thaw resistant mutant individuals were resistant to acetic acid when compared to wild-type strain.

- **Cross-resistance analysis via MPN (Most Probable Number) method**

Industrial *S. cerevisiae R625* cells and freeze-thaw resistant mutant individuals; *P3*, *P4*, *P7*, *P8*, *P9* and *P10* were screened at different stress conditions via 5-tube MPN methodology. The cross-resistance analyses were performed by using continuous stress screening strategy.

Wild-type and freeze-thaw resistant mutant individuals; *P3*, *P4*, *P7*, *P8*, *P9*, *P10* were exposed to toxic levels of boron, chromium, cobalt, zinc metal stresses, osmotic and ethanol stresses. The stress levels are indicated in Table 3.24.

Table 3.24: Stress factors and concentrations for cross resistance analysis.

Stress factors	$CoCl_2$	$CrCl_3$	$ZnCl_2$	$B(OH)_3$	$FeCl_2$	NaCl	Ethanol	H_2O_2
Stress levels	3 mM	3mm	10mM	50mM	15mM	5 %	7 % 10 %	0.5 mM

The MPN results (cell/ml) andthe survival ratios upon boron and ironstress conditionsare indicated in Table 3.25.

86

Table 3.25: MPN results (cell/ml) and survival ratios after 72 h incubation.

İndividuals	Control (cell/ml)	50 mM Boron (cell/ml)	Survival Ratios	Control (cell/ml)	15 mM Iron (cell/ml)	Survival Ratios
P4	5400000	1400000	0.26	5400000	2400000	0.44
P5	9200000	460000	0.05	9200000	2400000	0.26
P7	3500000	540000	0.15	3500000	1600000	0.46
P8	3500000	1700000	**0.49**	3500000	9200000	**2.63**
P9	2400000	2200000	**0.92**	2400000	5400000	**2.25**
P10	9200000	1100000	0.12	9200000	9200000	1.00
R625	2400000	540000	0.23	920000	540000	0.59

The MPN results (cell/ml) and the survival ratios upon cobalt and zinc stress conditions are indicated in Table 3.26.

Table 3.26: MPN results (cell/ml) and survival ratios after 72 h incubation.

İndividuals	Control (cell/ml)	3 mM Cobalt (cell/ml)	Survival Ratios	10 mM Zinc (cell/ml)	Survival Ratios
P4	9200000	540000	0.06	350000	0.04
P5	9200000	540000	0.06	1100000	0.12
P7	540000	110000	0.20	92000	0.17
P8	110000	220000	**2.00**	2200000	**20.00**
P9	350000	540000	**1.54**	700000	**2.00**
P10	3500000	350000	0.10	540000	0.15
R625	2200000	920000	0.42	2400	0.00

The MPN results (cell/ml) and the survival ratios upon ethanol stress conditions are indicated in Table 3.27.

Table 3.27: MPN results (cell/ml) and survival ratios after 72 h incubation.

İndividuals	Control (cell/ml)	10 % Ethanol (cell/ml)	Survival Ratios	Control (cell/ml)	7 % Ethanol (cell/ml)	Survival Ratios
P4	1700000	350000	0.21	5400000	1700000	0.32
P5	1700000	350000	0.21	9200000	9200000	1.00
P7	130000	2300	0.02	3500000	2400000	0.69
P8	1600000	170000	0.11	3500000	1600000	0.46
P9	3500000	110000	0.03	2400000	920000	0.38
P10	1600000	46000	0.03	9200000	5400000	0.59
R625	920000	920000	1.00	2400000	1600000	0.67

The MPN results (cell/ml) and the survival ratios upon oxidative stress conditions are indicated in Table 3.28.

Table 3.28: MPN results (cell/ml) and survival ratios after 72 h incubation.

İndividuals	Control (cell/ml)	0.5 mM H_2O_2 (cell/ml)	Survival Ratios
P4	5400000	2400000	0.44
P5	3500000	3500000	1.00
P7	5400000	3500000	0.65
P8	3500000	5400000	**1.54**
P9	9200000	1700000	0.18
P10	2400000	3500000	**1.46**
R625	5400000	1700000	0.31

The MPN results (cell/ml) and the survival ratios upon osmotic stress conditions are indicated in Table 3.29.

Table 3.29: MPN results (cell/ml) and survival ratios after 72 h incubation.

İndividuals	Control (cell/ml)	5 % NaCl (cell/ml)	Survival Ratios
P4	9200000	3500000	0.38
P5	5400000	160000	0.03
P7	540000	1600000	**2.96**
P8	110000	920000	**8.36**
P9	3500000	240000	0.07
P10	3500000	920000	0.26
R625	2200000	540000	0.25

The MPN results (cell/ml) and the survival ratios upon heat stress conditions are indicated in Table 3.30.

Table 3.30: MPN results (cell/ml) and survival ratios after 48 h incubation.

İndividuals	Control (cell/ml)	60 °C Heat (cell/ml)	Survival Ratios
P4	7000000	11000	0.0016
P5	2400000	3500	0.0015
P7	3500000	94000	**0.0269**
P8	3500000	24000	0.0069
P9	5400000	35000	0.0065
P10	3500000	35000	0.0100
R625	5400000	92000	0.0170

The survival ratios as fold of wild-type upon boron, iron, cobalt and H_2O_2 stress conditions are indicated in Figure 3.62.
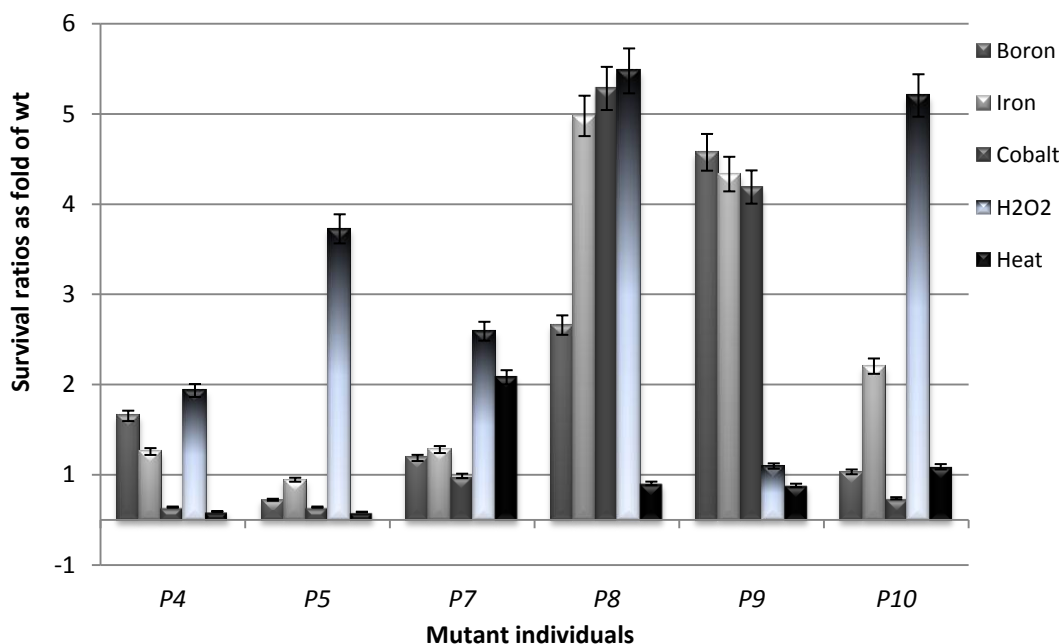
Figure 3.62: The survival ratios as fold of wild-type after 72 h incubation.

The logarithmic scale results of survival ratios as fold of wild-type upon boron, iron, cobalt, oxidative, heat, osmotic and zinc stress conditions are indicated in Figure 3.63.
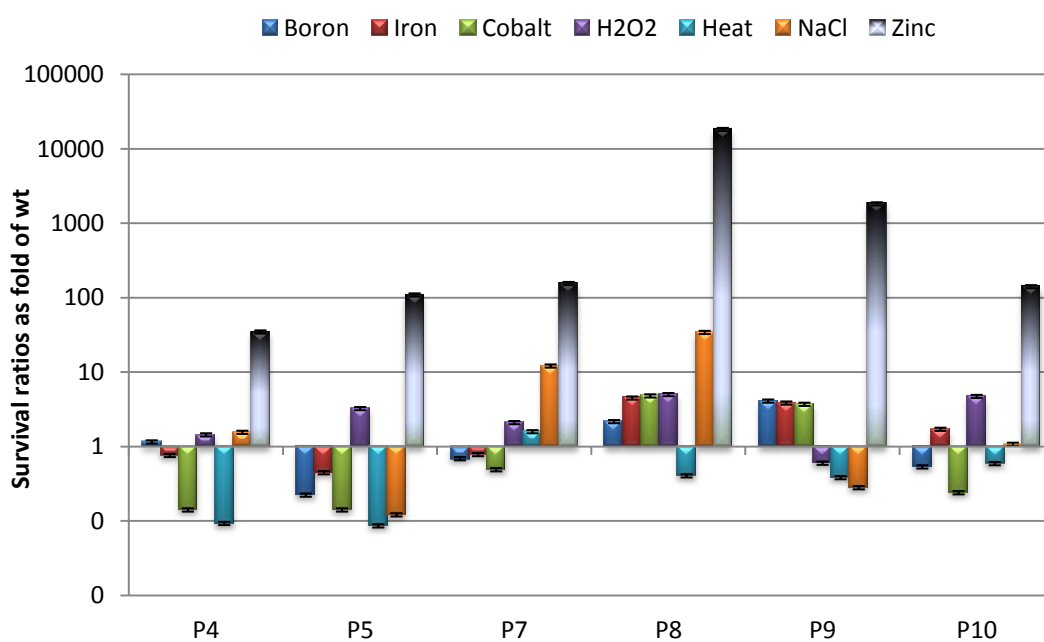
Figure 3.63: The logarithmic scale results of survival ratios as fold of wild-type after 72 h incubation.

The survival ratios as fold of wild-type upon ethanol stress conditions are indicated in Figure 3.64.
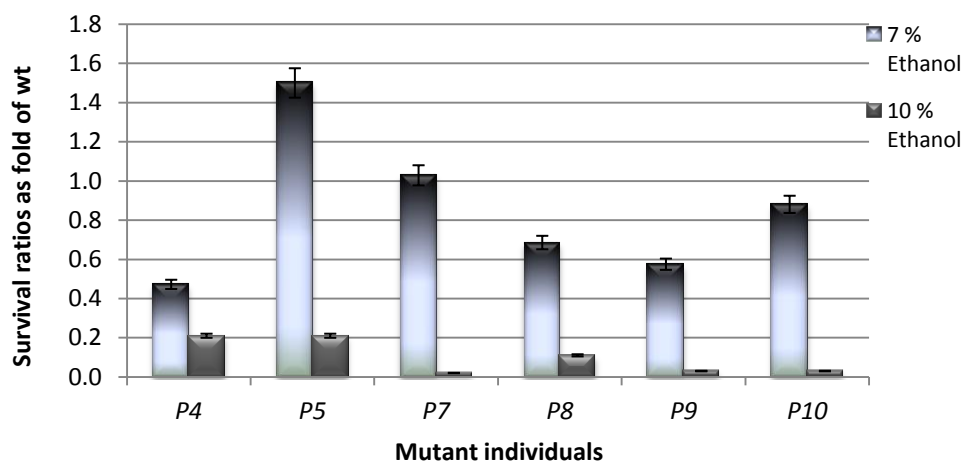
Figure 3.64: The survival ratios as fold of wild-type after 72 h incubation.

3.2.1.7 Principle component analysis (PCA)

The cross-resistance results of wild-type and mutant individuals were analyzed via PCA. The survival ratio data (72 h) of wild-type and mutant individuals at different stress conditions were used for analysis via PCA MATLAB code. Here, each component score (factor score) is corresponding to a particular data point (signed as different colors). At this two-dimensional plane we can observe the variance between variables and those data give us a qualitative conclusion.

The similar behaviour between individuals are indicated in Figure 3.65.
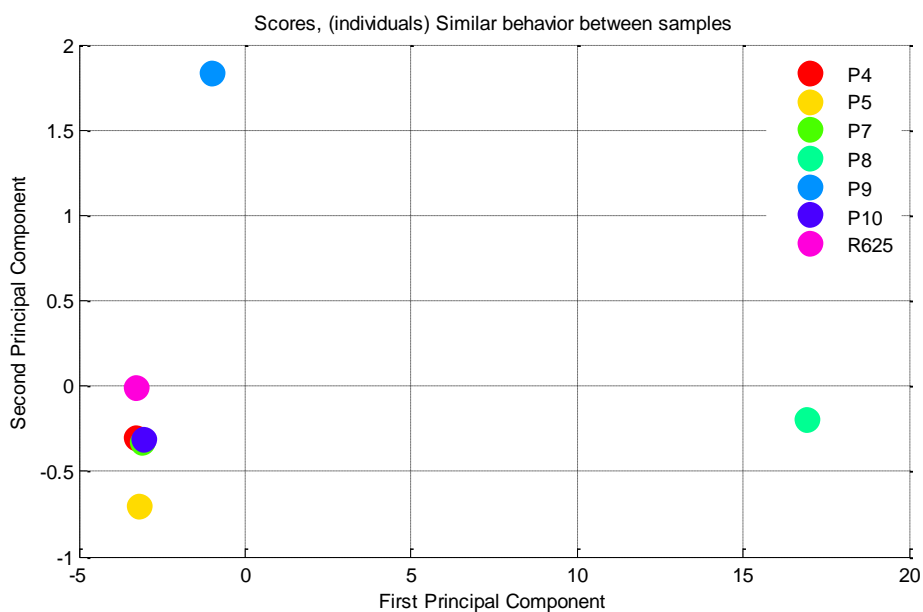
Figure 3.65: PCA results of different stress conditions.

Industrial mutant individuals *P9* and especially, *P8* are indicated difference in response when compared to wild-type and the other mutant individuals. Here, the response is completely related with the distance between the component scores. It is obvious that *P8* had the highest resistance and the variability.

The similar behaviour between different type of cross-stresses are indicated in Figure 3.66.
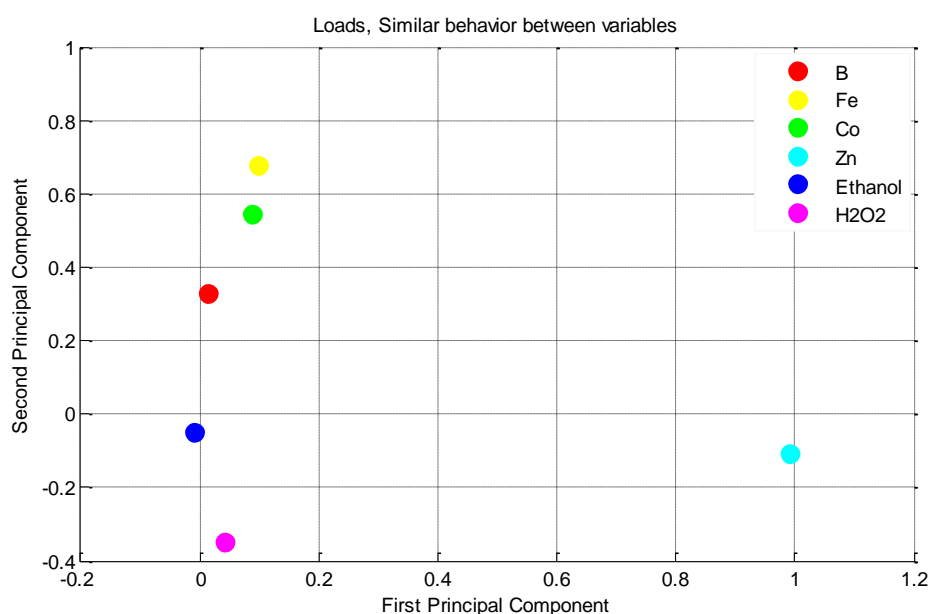
Figure 3.66: PCA results of different stress conditions.

It is obvious that there is a high variance between wild-type and mutant individuals in response to different cross-stresses. The cross-resistance phenotypes are too different from each other at different cross-stresses, especially at zinc metal stress condition.

As a result, freeze-thaw resistant mutant individual *P8* had different responses to all stresses. It has a higher resistance to oxidative stress, cobalt and iron stresses.Metal stress and oxidative stress responses had different component scores consistent with the previous analysis.

3.2.1.8 Physiological analysis of mutant individual *P8*

- **Growth analysis for mutant individual *P8***

For the growth analysis, wild-type and *P8* were grown at normal growth conditions without stress treatment at the controlled state of 30 °C, 150 rpm. Here the certain state of growth parameters are important to lead the optimal growth curve for each

strain. The appropriate volume of samples was taken from each culture for optical density measurements at different time intervals for both shake flask and bioreactor cultivations.

The shake flask cultivation optical density (OD_{600}) results of *R625* and mutant individual *P8* with respect to time are indicated in Table 3.31.

Table 3.31: Optical density (OD_{600}) results of shake flask cultivation with respect to time.

Time point	Time (hour)	OD_{600} results of wild-type	OD_{600} results of P8
t_0	0.00	0.35	0.38
t_1	2.00	0.45	0.57
t_2	3.50	0.83	0.88
t_3	5.00	1.52	1.34
t_4	6.50	1.99	1.49
t_5	8.00	2.08	2.20
t_6	9.50	2.90	2.75
t_7	11.00	4.25	3.88
t_8	24.00	5.19	4.66
t_9	27.00	5.03	4.56

The bioreactor cultivation optical density (OD_{600}) results of *R625* and mutant individual *P8* with respect to time are indicated in Table 3.32.

Table 3.32: Optical density (OD_{600}) results of bioreactor cultivation with respect to time.

Time point	Time (hour)	OD_{600} results of wild-type	OD_{600} results of P8
t_0	0.00	0.22	0.19
t_1	2.00	0.51	0.52
t_2	3.50	1.16	0.90
t_3	5.00	2.40	1.40
t_4	6.50	3.40	2.15
t_5	8.00	4.40	3.07
t_6	9.50	5.02	4.00
t_7	12.00	5.54	4.19
t_8	24.00	6.13	5.96
t_9	30.00	5.54	5.45

The shake flask cultivation $lnOD_{600}$ results of wild-type and *P8* with respect to time are indicated in Figure 3.67.
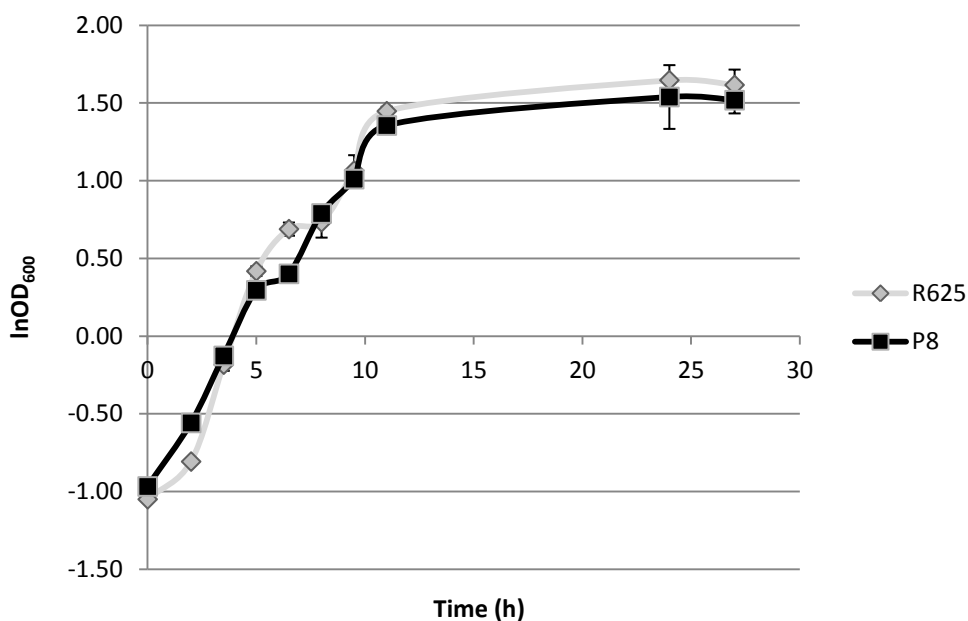
Figure 3.67: Shake flask growth curve of *R625* and *P8* with respect to $lnOD_{600}$.

The bioreactor cultivation $lnOD_{600}$ results of wild-type and *P8* with respect to time are indicated in Figure 3.68.
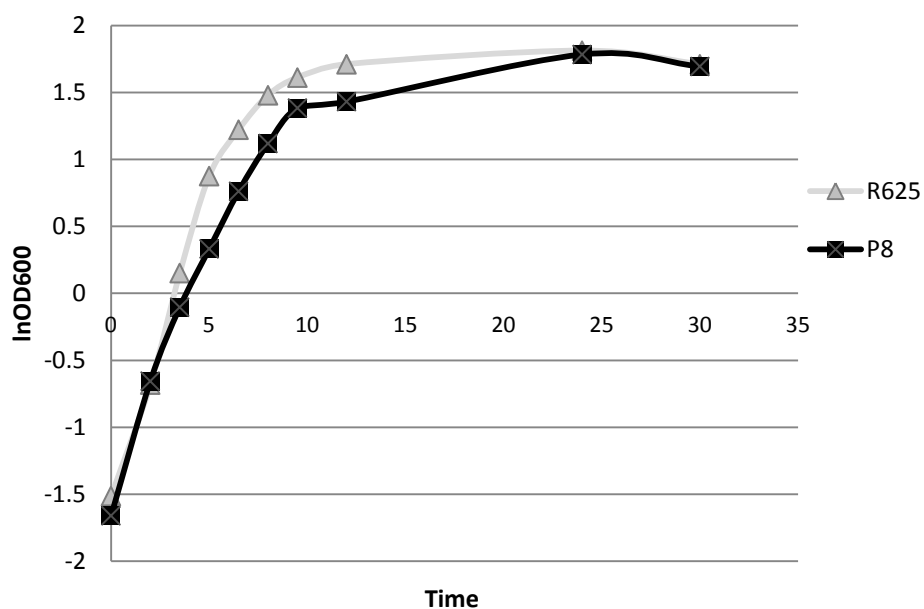
Figure 3.68: Bioreactor growth curve of *R625* and *P8* with respect to $lnOD_{600}$.

The specific growth rates (μ) were calculated according to the $\ln OD_{600}$ graphs (Figure 3.66) and the generation times were calculated according to the following equation;

$$\text{Generation time} = \ln 2/\mu \quad (3.1)$$

To determine the specific growth rates of individuals lineer model was used to exponential growth phase.

The shake flask cultivation growth results of *R625* and *P8* with respect to $\ln OD_{600}$/time are indicated in Figure 3.69. Here, the slope gives the rate of growth.
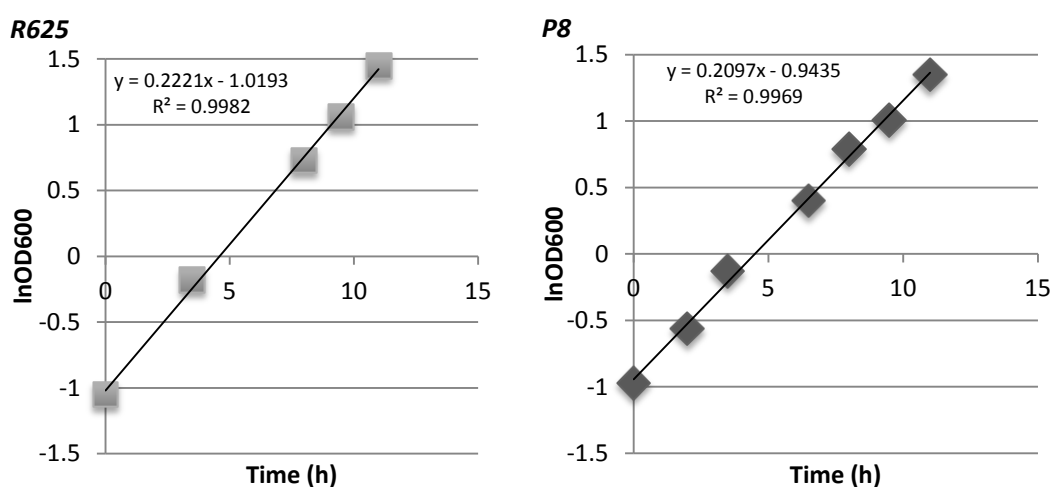
Figure 3.69: Shake flask growth result of wild-type and *P8* with respect to $\ln OD_{600}$-time.

The specific growth rates (μ) and the generation time times are indicated in Table 3.33.

Table 3.33: The specific growth rates (μ) and the generation times of wild-type and *P8* in shake flask cultivation.

	Specific growth rates (h^{-1})	Generation Time (h)
R625	0.222	3.12
R625_P8	0.210	3.30

The bioreactor cultivation growth results of wild-type *R625* and mutant individual *P8* with respect to $\ln OD_{600}$/time are indicated in Figure 3.70.
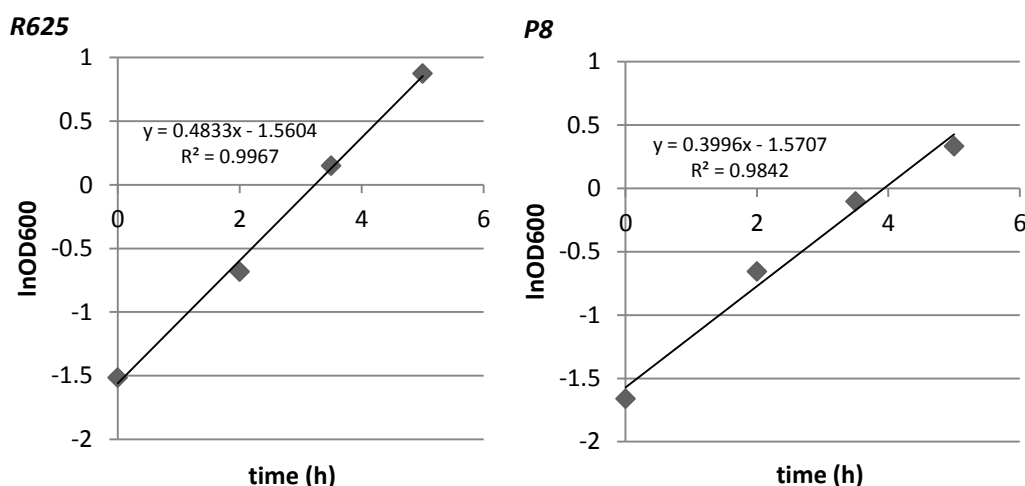
Figure 3.70: Bioreactor growth result of *R625* and *P8* with respect to $\ln OD_{600}$-time.

The specific growth rates (μ) and the generation time times are indicated in Table 3.34.

Table 3.34: The specific growth rates (μ) and the generation times of wild-type and *P8* in bioreactor cultivation.

	Specific growth rates (h^{-1})	Generation Time (h)
R625	0.48	1.44
R625_P8	0.40	1.73

- **High performance liquid chromatography (HPLC) analysis**

Exogenous culture medium samples were taken from *R625* and *P8* during the growth curve analysis and exogenous glucose, acetate, glycerol and ethanol were determined by using high performance liquid chromatography (HPLC).

The shake flask cultivation glucose consumption (mg/ml) of *R625* and *P8* during the growth are indicated in Figure 3.71.
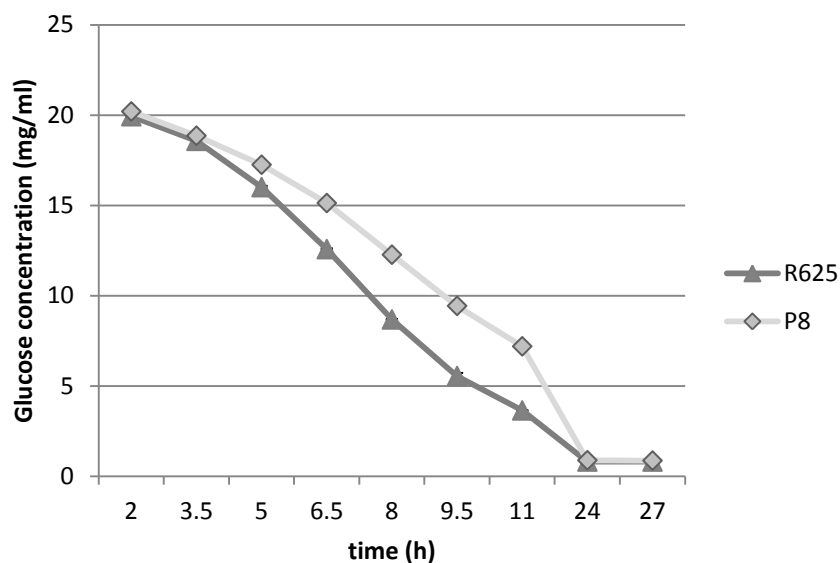
Figure 3.71: Change of glucose concentration during the shake flask growth.

Glucose concentrations were decreased normally due to the cellular consumptions during the growth. *P8* was used glucose slower than *R625*.

The bioreactor cultivation glucose consumptions (mg/ml) of *R625* and *P8* during the growth are indicated in Figure 3.72.
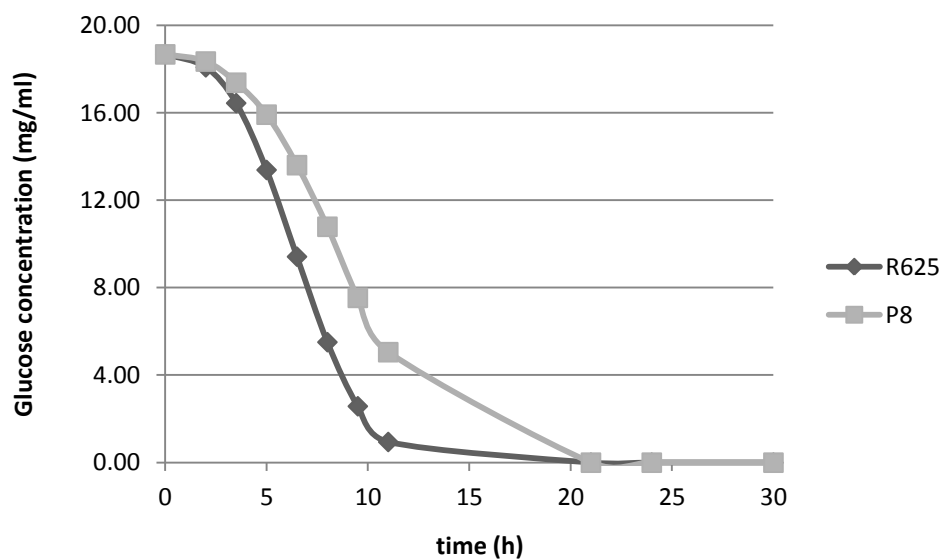
Figure 3.72: Change of glucose concentration during the bioreactor growth.

The glucose consumption was consistent with the shake flask cultivation.

The batch cultivation glycerol productions (mg/ml) of *R625* and *P8* during the growth are indicated in Figure 3.73.
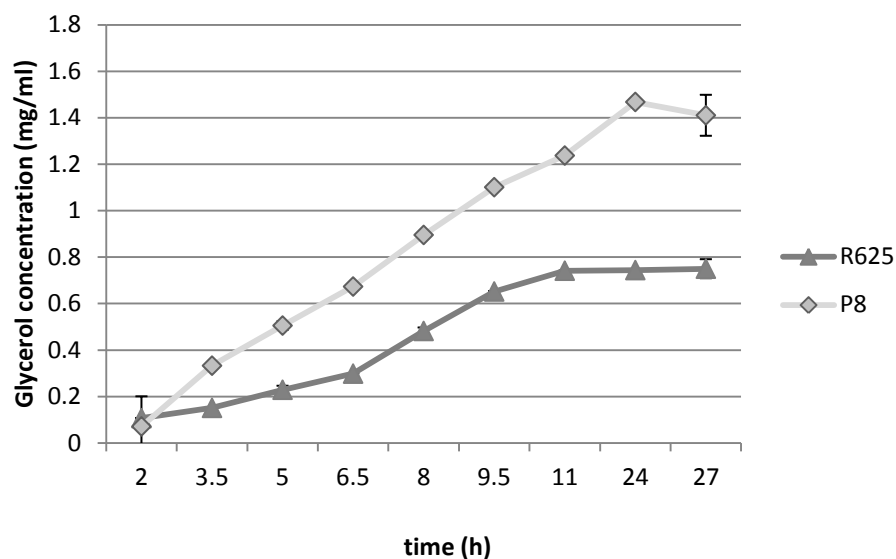
Figure 3.73: Change of glycerol concentration during the shake flask growth.

As shown in Figure 3.73, glycerol production were observed during the growth. It is obvious that glycerol amount in the culture supernatant of *P8* was higher than *R625*.

The bioreactor cultivation glycerol production (mg/ml) of *R625* and *P8* during the growth are indicated in Figure 3.74.
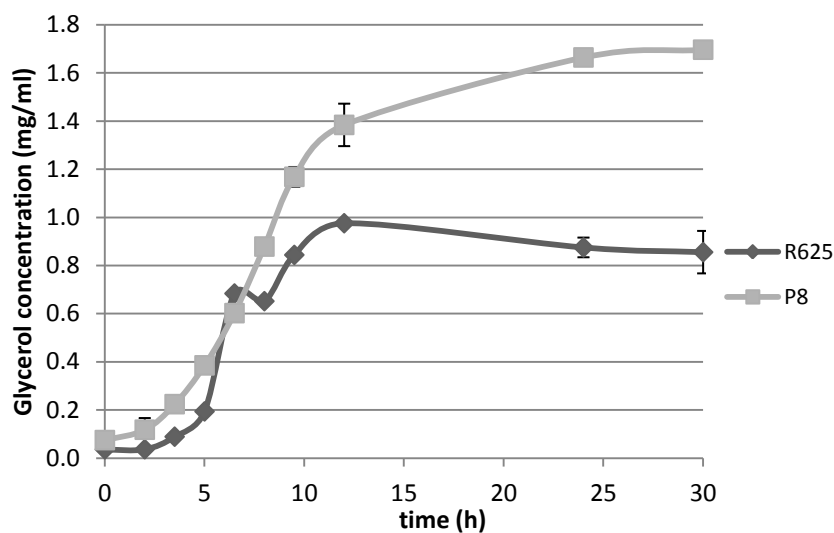
Figure 3.74: Change of glycerol concentration during the bioreactor growth.

The glycerol production was consistent with the shake flask cultivation. In addition the glycerol production was slightly higher in bioreactor cultivation in both *R625* and *P8*.

The shake flask cultivation acetate productions (mg/ml) of *R625* and *P8* during the growth are indicated in Figure 3.75.
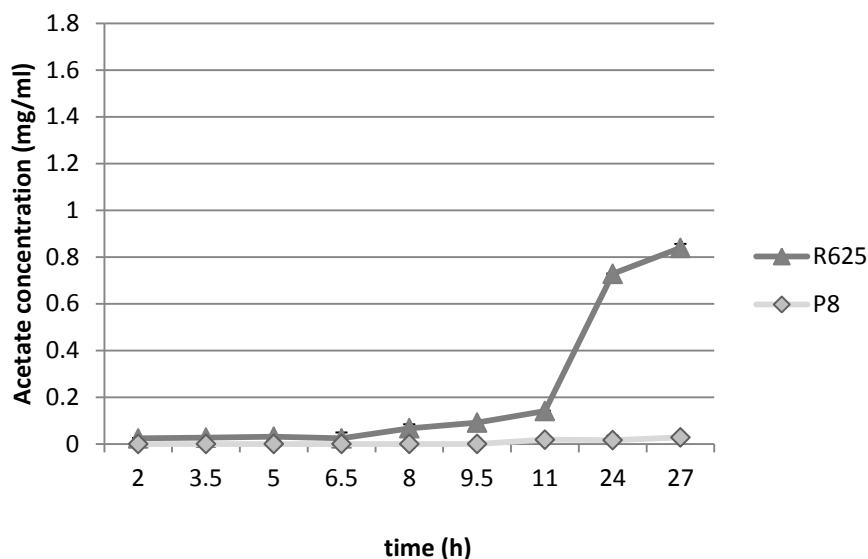
Figure 3.75: Change of acetate concentration during the shake flask growth.

The acetate amount in the exogenous medium of *R625* was higher at the stationary phase. However, it is still too low for *P8*.

The bioreactor cultivation acetate production (mg/ml) of *R625* and *P8* during the growth are indicated in Figure 3.76.
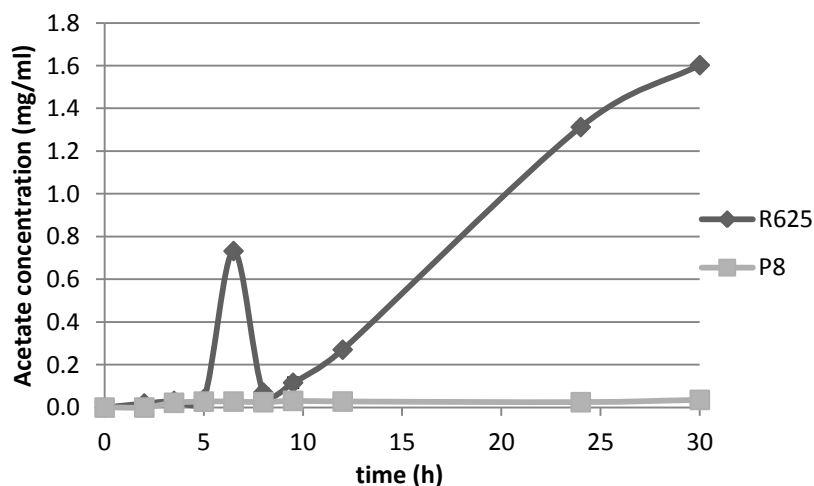
Figure 3.76: Change of acetate concentration during the bioreactor growth.

The acetate production was consistant with the batch cultivation. On the other hand, the acetate production was higher in bioreactor cultivation in *R625*.

The shake flask cultivation ethanol productions (mg/ml) of *R625* and *P8* during the growth are indicated in Figure 3.77.
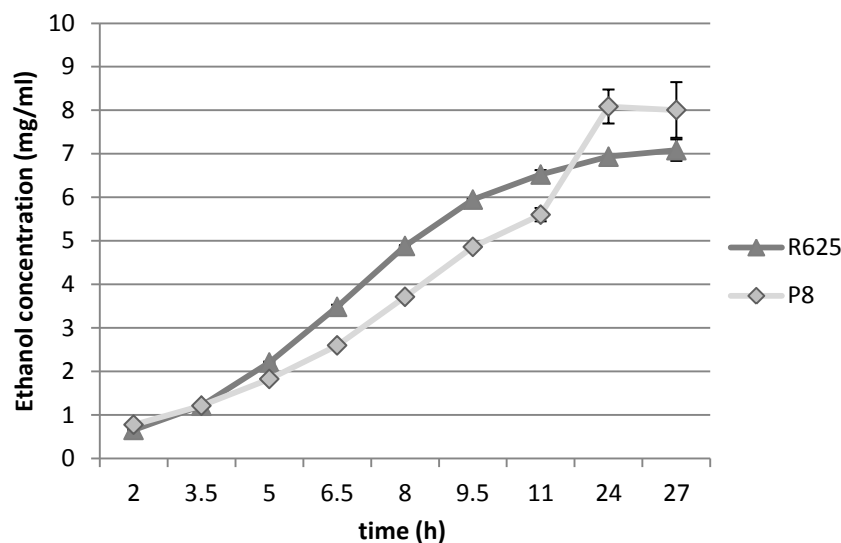
Figure 3.77: Change of ethanol concentration during the shake flask growth.

As shown in Figure 3.77, ethanol was produced during the growth of *R625* and *P8*.

The bioreactor cultivation ethanol production (mg/ml) of *R625* and *P8* during the growth are indicated in Figure 3.78.
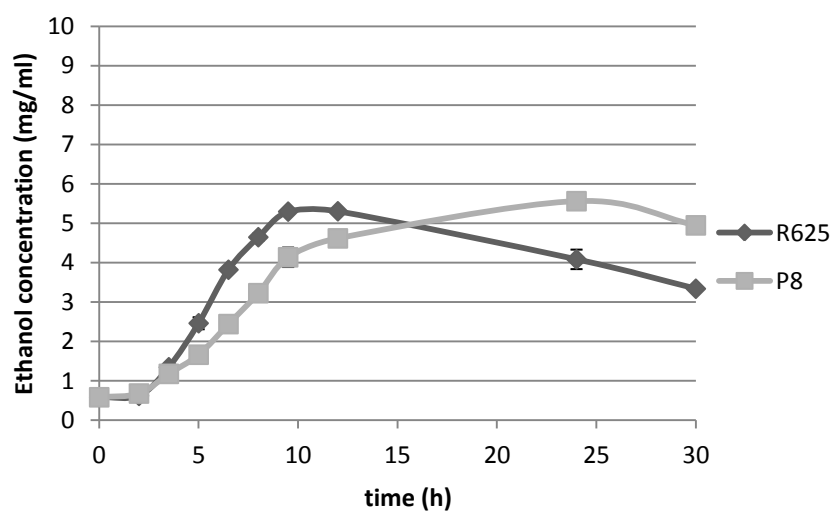
Figure 3.78: Change of ethanol concentration during the bioreactor growth.

The ethanol production was consistent with the shake flask cultivation. However, the ethanol production was lower in bioreactor cultivation for both *R625* and *P8*.

Determination of these metabolites was important in order to determine the relationship between growth and consumption / production of metabolites.

- **Reserve carbohydrate analysis of wild-type and mutant individual *P8***

The reserve carbohydrates glycogen and trehalose were analyzed by using glucose oxidase/peroxidase assay. The samples were collected during the growth at specific time intervals.

The intracellular trehalose levels during the growth are indicated for wild-type and *P8* at Figure 3.79.
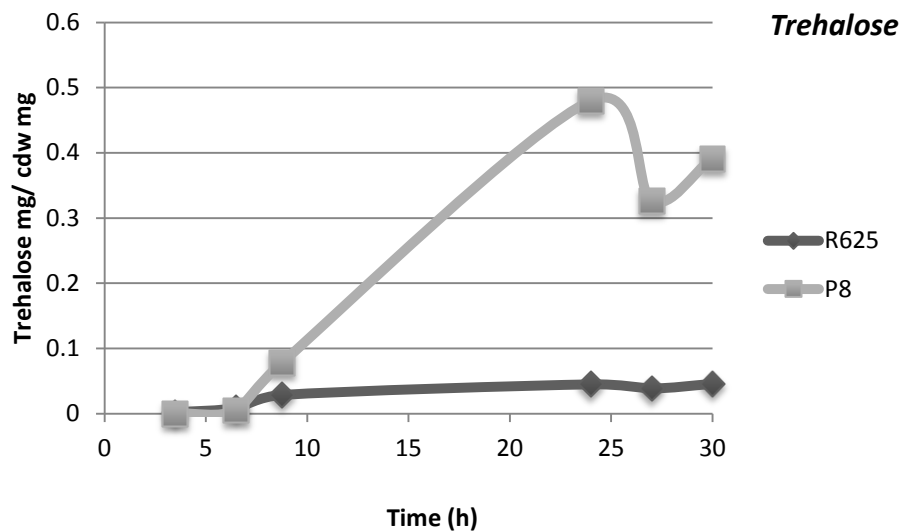
Figure 3.79: Change of intracellular trehalose amount during the growth.

The intracellular glycogen levels during the growth are indicated for wild-type and *P8* at Figure 3.80.
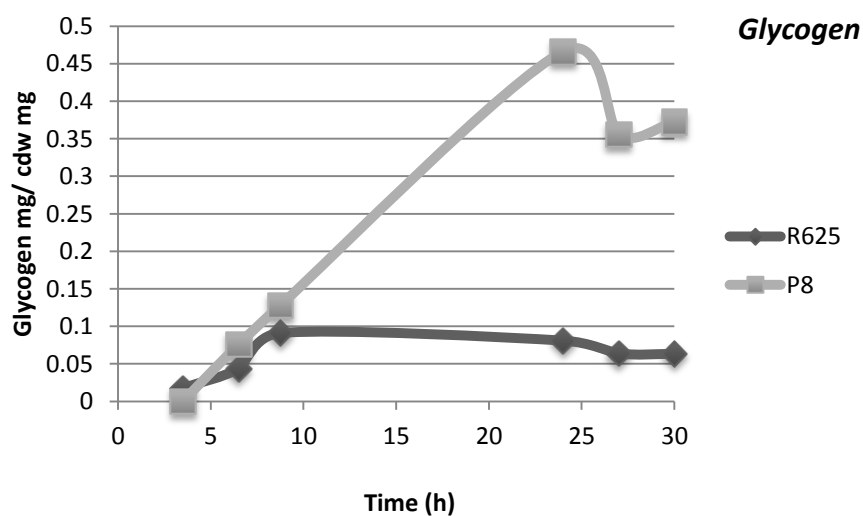
Figure 3.80: Change of intracellular glycogen amount during the growth.

100

It is obvious that, intracellular reserve carbohydrates trehalose and glycogen were higher in *P8* with respect to wild-type at normal growth conditions without freeze-thaw stress treatment.

4. DISCUSSION AND CONCLUSION

4.1 Studies with the Yeast *Saccharomyces cerevisiae CEN.PK113-7D*

In this thesis project, evolutionary engineering strategy was performed to obtain freeze-thaw resistant mutant yeast strains. Ten freeze-thaw cycles were applied to chemically mutagenized variant mutant population of *Saccharomyces cerevisiae* (*906*). Due to its high damage to cells and lethal effect, we applied 10 cycles of freeze-thaw stress and obtained final mutant generation (*F10G*). The survival ratio was 0.31 %, after ten cycles of freeze-thaw stress application. As a result of iterative cycles of selective freeze thaw stress, the last generation contains heterogeneous population of freeze-thaw tolerant strains.

Ten random mutant individuals were selected from *F10G* final heterogeneous mutant population. Thereafter phenotypic, physiological and genetic analysis were performed, respectively.

To analyze the phenotypic response upon freeze-thaw stress of each mutant individual, five tube-MPN method was performed. After one and two cycles of freeze-thaw stress application mutant individual *F1* had survived upon 7 and 700 fold normalized to wild-type, respectively. Other mutant individuals' survival ratio *F3*, *F8*, *F9* and *F10* were also remarkable. Mutant individual *F1* was selected for detailed analysis and the genetic stability was also confirmed by MPN assay (Figure 3.2 or Table 3.3).

Spotting assay and five tube-MPN method were performed to analyze potential cross resistances to other industrial and metal stresses. Ten mutant individuals were examined with magnesium, chromium, zinc, iron, boron and ethanol via spotting assay. *F1* and *F8* seem to have a cross-resistance against $CrCl_3$ stress and individuals have no cross-resistance against $FeCl_2$ stress. Magnesium concentration (3 mM) was too low and cobalt concentration (3 mM) was too high to decide whether cross-resistance has present or not (Figure 3.4).

For the detailed phenotypic analysis, mutant individual *F1* was tested with rearranged concentrations of stresses via spotting assay and MPN. Mutant individual *F1* was resistant to boron, chromium, cobalt, nickel and oxidative (hydrogen peroxide) stresses and sensitive to iron, copper and osmotic (NaCl) stresses. 40 mM magnesium stress concentration had no toxic effect on *F1* and wild-type (Figure 3.12). Osmotic stress sensitivity of the freeze-thaw resistant mutant *F1* is an unusual case. Previous studies emphasize that freeze-thaw tolerance exist together with the osmotic stress tolerance. However, cellular response to NaCl-related and freeze-thaw-related osmotic (turgor and water loss) stress have different mechanisms (Shima and Takaghi, 2009). NaCl induced osmotic stress includes Na^+ ion toxicity beside osmotic stress (Ren et al., 2012).

The cross-resistance results of wild-type and mutant individual *F1* were also analyzed via principle component analysis (PCA). By adapting the multiple cross-resistance data on two dimensional plane, the variance between variables could be observed and this data provided a qualitative conclusion. The response is completely related with the distance between the component scores. Here, similar behaviour between observation, according to the first principal component at the x-axis, metal and oxidative stresses are indicated difference in response when compared to osmotic stress. Iron sensitivity have a distance besides other metal stresses that the mutant individual have cross-resistance to them (Figure 3.17). Similar behaviour between individuals, according to the first principal component at the x-axis, there is a high variance between wild-type and mutant individual *F1* in response to different stress types. Their cross-resistance phenotypes are too different from each other. *F1* showed higher tolerance most of the cross-stresses when compared to wild-type (Figure 3.18).

As a result, freeze-thaw resistant mutant individual *F1* had different responses to osmotic and oxidative stresses. It has a higher resistance to oxidative stress and higher sensitivity to osmotic stress. Metal stress, osmotic stress and oxidative stress responses had different component scores consistent with the previous analysis.

MATa type *S. cerevisiae* (*905*) and mutant individual *F1* cells were diploized by using an opposite mating type *S. cerevisiae* (*934, MATα*) cells. The tetrad formation was visualized on 2 % potassium acetate, pH 7.0 medium to confirm diploidization process. After diploidization of wild-type and mutant cells, cross resistance analyses

were performed. *F1*, *F1_2n* (diploid form of *F1* and *934*), *905* (*MATa*) and *2n* (diploid form of *905* and *934*) cell cultures were used. After 3 cycles of freeze-thaw stress application *F1* and *F1_2n* survived with no loss of viability. On the other hand, diploid obtained from the cross of opposite mating type wild-type cells had a higher survival rate while the wild-type did not cope with the harsh effects of freeze-thaw stress treatment (Figure 3.42). This is because, it has two copy of each stress response genes, whether those genes are not constitutively expressed. Here, it is important that diploidization of freeze-thaw resistant mutant individual with wild-type had no negative effect on freeze tolerance which can be explained by the dominant nature of freeze-thaw resistance related genes.

Physiological analysis of freeze-thaw resistant mutant individual *F1* and wild-type was performed at normal growth conditions in a batch culture without stress treatment. Growth curve and metabolite analysis were examined.

The specific growth rate (μ) of wild-type was 0.208 h^{-1} and the generation time was calculated as 3.33 h. The growth rate (μ) of mutant strain was 0.186 h^{-1} and the generation time was calculated as 3.73 h (Figure 3.30). The specific growth rate of *F1* was 0.9-fold of wild-type. It is common that the mutant organisms have generally slow growth phenotype (Çakar et al., 2011). On the other hand, F1 has not a slow growth phenotype, the lag phase of growth was not long with respect to wild-type besides, after 15 hours incubation, wild-type was started to come into stationary phase while *F1* kept growing. There is an evidence about a *S. cerevisiae* mutant organism with the double copy of *COX5B* gene have the ability to grow faster than its wild-type strain. *COX5B* encodes the subunit Vb of cytochrome c oxidase, it is generally induced in anaerobic growth of the cells (Trueblood and Poyton, 1988). Similarly, *COX5B* gene was 10.47 fold upregulated in mutant individual *F1* when compared to wild type. Another study was referred that cAMP-dependent protein kinase pathway have the role in increased growth phenotype and also freeze-thaw resistance. Thereafter, upregulation of *TPK2*, *TPK3*, *RAS2*, *GPA2*, *GPB1*, *GPB2*, *PDE2*, *SHR5* and *IRA1* genes resulted in cell fitness (Breslow et al., 2008; Park et al., 1997). *TPK2* and *SHR5* genes were upregulated in mutant individual *F1*.

During the growth curve analysis samples were taken for metabolite analysis via HPLC and glucose oxidase/peroxidase assay. Exogenous glucose, acetate, glycerol

and ethanol concentrations (mg/mL) were determined by using high performance liquid chromatography (HPLC).

Glucose concentrations were decreased parallel with the growth. However, *F1* used glucose slower than wild-type opposite to its growth rate. After 21 hour incubation, wild-type consumed the glucose thoroughly (Figure 3.31). On the other hand, *F1* consumed glucose, after 27 h of incubation and kept growing. Thus, the diauxic shift of *F1* was not seen on the growth curve results (Figure 3.30). Glycerol productions were increase during the growth for both wild-type and *F1*. The glycerol amount in the exogenous medium of *F1* was clearly lower than wild-type in exponential growth phase (Figure 3.32). The acetate productions were increased similarly with glycerol during the growth. The acetate amount in the exogenous medium of *F1* was close to the wild-type in exponential growth phase. Mutant individual *F1* was started to consume acetate after glucose consumption. On the other hand wild-type was not (Figure 3.33). The ethanol productions were increased during the growth. Ethanol production rate of *905* was higher than *F1* (Figure 3.34). The glucose consumption of *F1* in exponential growth phase was lower than that of the wild-type. Thus the production of metabolite rates were lower in *F1* than the wild-type. However, the acetate levels were nearly parallel with wild-type. It is because of the production of acetate was increased due to slower consumption of glucose in *F1*. On the other hand, the ethanol concentrations were considerably lower in *F1*. This is because of the metabolic pathway goes through the acetate rather than ethanol production (Eglinton et al., 2002). When the F1 cells started to consume acetate at stationary phase, the ethanol production was increased and came near to the wild-type levels. The succinate productions were started after 10th hour of incubation. The succinate amount in the exogenous medium of *F1* was clearly higher than the wild-type (Figure 3.35).

The reserve carbohydrates, glycogen and trehalose were analyzed by using glucose oxidase/peroxidase assay. The samples were collected during the growth at specific time intervals. The intracellular reserve carbohydrates, trehalose and glycogen were higher in *F1* with respect to wild-type under the normal growth conditions without freeze-thaw stress treatment (Figure 3.36 and Figure 3.37). Trehalose, glycogen, glycerol and ethanol are the cryoprotectant agents for the cells and increase tolerance to freeze-thaw stress (Sasano et al., 2012c; Schade et al., 2004; Lewis et al., 1993). It

is obvious that freeze-thaw resistant mutant individual *F1* had higher amount of reserve trehalose and glycogen. Previous studies have shown that glycogen and trehalose productions are increased under cold, hyperosmotic and oxidative stresses (Schade et al., 2004). In addition, trehalose seriously conserves microsatellite nuclear DNA from damage beside its protection effect against freeze-thaw stress via protection against autolysis, role in stabilization of membranes and facilitation of protein folding with Hsp104 heat-shock protein (Todorova et al., 2012; Schade et al., 2004). Intracellular cryoprotectors seriously important to cope with the mutative recombinogenic effect of freeze-thaw stress on nuclear DNA and centromeres (Todorova et al., 2012). It is worth to emphasize that, higher trehalose levels of the mutant individual F1 along with its growth is important for industrial frozen dough applications and trehalose accumulating yeasts were patented before (Van-Dijck et al., 1995; European patent application 91200686.3, 1991; International patent application PCT/FI93/00049, 1993). Additionally, the heat-shock protein Hsp104 was 9.22 fold of wild-type.

In order to understand the development and genetic background of high levels of freeze-thaw resistance in *S. cerevisiae* along with the multiple stress resistance characteristics, transcriptomic analysis were performed by using quantitative real time-PCR methods. The expression levels were determined in mutant individual *F1* and compared to the wild-type. The relative transcriptional changes of freeze-thaw stress related genes *AQY1*, *AQY2*, *CTT1*, *GSH1* and *FPS1* were studied at control and freeze-thaw stress conditions.

Aquaporins are integral membrane proteins function on water and glycerol transport activity across cell membranes. There are two identified aquaporin-encoding genes which are *AQY1* and *AQY2* in yeast. Overexpression of aquaporin genes resulted in freeze-thaw stress tolerance (Tanghe et al., 2005; Tanghe et al., 2002). Especially, the upregulation of aquaporin genes under rapid freezing conditions are important to efflux water out of the cell to reduce intracellular ice-crystal formation to survive. Yeast cells have high osmolarity resistance, so they freeze later than the extracellular media and gain time to cells overexpress aquaporins (Tanghe et al., 2004). Relative expression profile of *AQY1* gene was increased at freeze-thaw stress conditions both wild-type and *F1* (Figure 3.19). It is remarkable that expression level of *F1* strain was up to 20 fold while the wild-type below 5 fold at freeze-thaw stress conditions

and the expression level of *F1* at control condition was up to 25 fold of the wild-type control. The expression profile of *AQY1* gene was completely different at mutant individual for both control and stress conditions. Relative expression profile of *AQY2* gene was increased at freeze-thaw stress conditions both for the wild-type and *F1*. The relative expression level of *AQY2* at wild-type stress was increased up to 2.5 fold and the expression level of *F1* under stress was slightly lower than the wild-type stress. However, the relative expression of mutant individual *AQY2* gene at control conditions was 2.5 fold of the wild-type control. Those results were also consistent with the microarray analysis data.

CTT1 gene encodes cytosolic catalase T enzyme, has a role to protect cells against oxidative damage by hydrogen peroxide. It is also reported that the expression levels are upregulated under oxidative and freeze-thaw stresses (Odani et al., 2003). Relative expression profile of *CTT1* gene was increased at freeze-thaw stress conditions both wild-type and *F1*. The relative expression level of *CTT1* at wild-type stress was increased upon 2.5 fold and upto 3 fold for mutant individual. The relative expression of mutant individual *CTT1* gene at control conditions was 2-fold of that of wild-type control. Those results were also consistent with the microarray analysis data.

GSH1 gene encodes a g-glutamylcysteine synthetase enzyme for glutathione (GSH) biosynthesis (Park et al., 1998). Glutathione (Q-glutamylcysteinylglycine; GSH) is an oxidative stress defender molecule that is a free radical scavenger and a cofactor of antioxidant enzymes in the cells (Lee et al., 2001). The expression levels of *GSH1* are induced under freeze-thaw and oxidative stress conditions (Park et al., 1998). Relative expression profile of *GSH1* gene was increased under freeze-thaw stress conditions for both wild-type and *F1*. The expression level of *GSH1* at wild-type stress was increased 2.5 fold when normalized to the wild-type control and the normalized expression level of *F1* stress was slightly lower than wild-type stress, similar to the response of *AQY2* gene. However, the relative expression of mutant individual *GSH1* gene at control conditions was upon 1.5 fold of wild-type control.

FPS1 gene encodes a plasma membrane channel protein for passive intracellular glycerol efflux out of the cell. It is important in controlling the turgor pressure by adjusting the intracellular glycerol and enables rapid efflux of glycerol under hypo-osmotic pressure. Previous studies have shown that *FPS1* repressed or deleted strains

had the ability to accumulate glycerol that resulted in freeze-thaw tolerance (Beese-Sims et al., 2011; Izawa et al., 2004b). Relative expression profile of *FPS1* was increased at freeze-thaw stress condition in wild-type. However, the relative expression of mutant individual *FPS1* gene at control conditions was 1.7-fold higher than that of the wild-type control, there is a low expression tendency of *F1* at stress conditions, up to 1.5 fold. That low expression tendency consistent with the response of freeze-thaw stress.

Table 4.1: Expression profiles of mutant individual *F1* normalized to wild-type according to Q-PCR and microarray results.

	AQY1	*AQY2*	*FPS1*	*GSH1*	*CTT1*
MICROARRAY	8.39 (up)	1.25 (up)	1.22 (down)	1 (same)	48.28 (up)
Q-PCR	17.86 (up)	2.48 (up)	1.86 (up)	1.64 (up)	2.13 (up)

The Q-PCR analysis were performed under mid-log growth conditions of the cultures. On the other hand, microarray analysis were performed under initial-log phase of growth, so there is some differences between expression profiles (Table 4.1).

The results indicated that the expression profiles of *AQY1*, *AQY2*, *CTT1*, *GSH1* and *FPS1* genes under control conditions were completely different from the wild-type.

To enlight the genetic basis underlying the freeze-thaw resistance mechanism, whole genome transcriptomic analysis was performed by using high throughput DNA microarray technology. The microarray data was analyzed by GeneSpring GX 9.0 software. The mean expression profile of *F1* was normalized to the wild-type by this software and then the molecular and functional categorization of up and down regulated genes were done according to FunSpec and Funcat databases [(p-value) < 0.05). It is remarkable that 1287 genes were upregulated and 891 genes were downregulated at freeze-thaw stress resistant mutant individual *F1*, respectively. Those of the high numbered, differential regulated genes resulted in multiple-stress tolerance (Wei et al., 2007).

The percentage of upregulated genes with their corresponding functional categories were analyzed with Funcat database (Figure 3.26). The functional categories of the induced genes of the freeze-thaw resistant mutant individual *F1* under non-stress

conditions are similar with the previous study of Odani et al., 2003. After 1 hour of pulse freeze-thaw stress treatment, they found out that the genes under energy, cell rescue, metabolism, unclassified proteins, interaction with the environment, cellular transport and protein fate functional categories were upregulated according to the stress (Odani et al., 2003). The subcellular localization of the upregulated genes were analyzed with Funspec database. According to the Funspec database subcellular localization results; mitochondria, mitochondrial inner membrane, peroxisome, peroxisomal matrix, cytoplasm and integral membrane / end membranes genes were determined upregulated in *F1*.

Freeze-thaw stress leads to extreme vital danger to yeast cells. This stress did not threat the survival in a one problematic way it causes variety of problems in the cell including low internal pH, imbalance of metabolites, dehydration, ionic toxicity, oxidative damage to proteins, lipids, DNA and membrane damage (Wei et al., 2007).

Basicly, freeze-thaw and cold stress induce a variety of mechanisms to cope with the adverse effects of the stresses. These mechanisms include the induction of carbohydrate metabolism, glycogen metabolism, heat shock proteins, oxidative stress related processes, adaptation of membrane fluidity and environmental stress response (ESR) mechanism such as reserve carbohydrate accumulation and glutathione/glutaredoxin system (Schade et al., 2004).

The hexose transporters (*HXT5*, *HXT6*, *HXT7*, *HXT14*, *HXT15*, *HXT16*) were highly upregulated in mutant individual *F1*. It was shown that high affinity hexose transporters *HXT6* and *HXT7* is upregulated in the second stage of fermentation in metabolically active non-growing cells (Berthels et al., 2008). However, in mutant individual *F1*, the hexose transporters *HXT6* and *HXT7* was upregulated 62 and 68 fold of wild-type, respectively in the early log phase. After the glucose uptake inside the cell, the metabolic processes are started with phosphorylation process via Hxk1, Hxk2 and Glk1 kinases. *HXK1* and *GLK1* are upregulated in the second stage of fermentation in metabolically active non-growing cells. This might be the result of nitrogen starvation (Berthels et al., 2008). Whereas, the total RNA of mutant individual *F1* was isolated in early logharithmic phase of growth, besides Yvhlp phosphatase which is upregulated under nitrogen starvation conditions (Dong-Park et al., 1996) was 6.3 fold downregulated when compared to the wild-type. *GLK1*, which encodes a glucose phosphorylating enzyme glucokinase and *HXK1* which encodes a

glucose/fructose phosphorylating enzyme hexokinase were upregulated 12 and 224 fold of the wild-type, respectively, at mutant individual *F1*. Especially, *HXK1* was dramatically upregulated in mutant individual *F1* as 224 fold of wild-type.

Another interesting case is that the upregulation of *FBP1* gene encoding a key regulatory enzyme in gluconeogenesis; Fructose-1,6-bisphosphatase (Santt et al., 2008). In the presence of glucose *FBP1* is downregulated because there is no need of gluconeogenesis, however it was 5.48 fold upregulated with respect to wild-type. This may be the reason of upregulation of high affinity glucose/hexose transporter genes and limited transfer of glucose as if the mutant individual stand in nutrient limiting conditions. On the other hand genes encoding Vid 24, Vid28 and Vid30 proteins that have a role in vacuolar import (Santt et al., 2008) and degradation of FBPase were upregulated 1.40, 1.78 and 4.26 fold maybe to equalize the overexpression in glucose containing growth media. Although the presence of glucose represses the expression of *FBP1*, it is overexpressed in mutant individual *F1*.

One of the stress mechanisms against freeze-thaw stress is the induction of heat shock proteins to prevent protein aggregation (Wei, 2007). Most of the studies were demonstrated the positive effects of heat shock proteins among other defence mechanisms (Sahara et al., 2002; Schade et al., 2004; Aguilera et al., 2007). Heat-shock protein encoding genes *HSP12*, *HSP26*, *HSP42*, *HSP104*, *SSA4*, *SSE2* and *YRO2* are significantly upregulated in mutant individual *F1*. The heat shock protein Hsp12 (YFL014W) have a role to stabilize plasma membrane under heat shock stress conditions and the disaccharide molecule trehalose in the same manner. Those two molecules act as cryoprotectants and were considerably upregulated in *F1*. Previous studies were shown that upregulation of the genes inside the trehalose production pathway, molecular chaperons and the lipid composition of the cell membrane that were related to the membrane robustness provides freeze-thaw resistance (Park et al., 1997; Dang and Hincha, 2011; Tanghe et al., 2002).

Previous studies have shown that genes encoding heat shock proteins Hsp12 and Hsp26 were upregulated in the presence of ethanol and the Etp1 is a transcriptional activator for those heatshock proteins. High concentrations of Nha1 results in ethanol sensitivity on *ETP1* deleted strain and Etp1 controls the levels of Nha1 under ethanol stress conditions (Snowdon et al., 2009). The analysis of microarray data revealed

that *HSP12* and *HSP26* were dramatically upregulated as 263.60 and 172.37 fold of wild-type, respectively. It is interesting that the transcriptional level of *ETP1* was 2.61 fold upregulated and *NHA1* was 2.45 fold downregulated with respect to wild-type under normal growth conditions without ethanol stress. The dramatic upregulation of *HSP12* and *HSP26* may not fully related to the upregulation of *ETP1*, but may have a role.

S. cerevisiae has two defence systems, that are enzymatic and non-enzymatic mechanisms, to cope with the oxidative stress and detoxifying reactive oxygen species (ROS) to maintain the steady state redox balance (Jamieson, 1998).

Non-enzymatic defence system includes glutathione (*GSH1* and *GSH2*), metallothioneins (*CUP1* and *CRS5*), thioredoxins (*TRX1*, *TRX2*) and glutaredoxins (*GRX1* and *GRX2*). Glutaredoxin encoding genes *GRX1* is effected on superoxide anion and *GRX2* is effected on hydrogen peroxide. The thioredoxin encoding genes *TRX1* and *TRX2* deoxidize the GSH for redox balance (Luikenhuis et al., 1998). The expression levels of *TRX1*, *TRX2*, *CUP1*, *CRS5*, *GRX1* and *GRX2* were upregulated in mutant individual *F1*.

Enzymatic defence system includes catalase (*CTT1* encodes catalase A, *CTA1* encodes catalase T) and superoxide dismutase (*SOD1, SOD2*) enzymes. Catalase enzyme breaks down the hydrogen peroxide molecule into oxygen and water. Superoxide dismutase protects cells against oxgen toxicity. There is two common forms located in mitocondria and cytoplasma in yeast cells. The expression levels of *CTT1, CTA1, SOD1* and *SOD2* were upregulated in mutant individual *F1*.

There are various antioxidant mechanisms in *S. cerevisiae*. *SOD1* and *SOD2* encoding superoxidedismutase metalloenzyme disrupted cells can be survive via expression of *ATX1* gene, encoding a copper homeostasis factor that acts on both superoxide anion and hydrogen peroxide. However, it can only upregulated under excess levels of manganese or copper (Lin and Culotta, 1995). In mutant individual *F1*, *SOD1, SOD2* and *ATX1* levels were 2.19, 3.56 and 3.00 fold of wild-type, respectively.

Another oxidative stress related gene *IMP2* encodes a transcriptional activator for ion homeostasis inside the cell (Masson and Ramotar, 1998) was also upregulated 1.71 fold of wild-type in mutant individual *F1*.

Oxidative stress response genes *CTT1, SOD2* molecular chaperoning genes *HSP12, HSP104* and trehalose synthesis genes *TPS1, TPS2* are under the control of *MSN2* transcriptional factor. Overexpression *MSN2* induce those genes and upregulate them. This is important in frozen dough industry and the survival of the yeast in frozen dough (Sasano et al., 2012a). Previous studies showed that oxidative stress response genes were induced under freeze-thaw stress conditions. Especially, *HSP12* (263.60 fold), *CTT1* (48.28 fold) *GAD1*, (29.08) and *SOD1* (2.19) were highly upregulated in *F1* (Takahashi et al., 2009; Odani et al., 2003). Mitochondrial *SOD2* (3.56 fold) was highly upregulated in the presence of cytosolic *SOD1* and contribute to freeze-thaw resistance of *F1* (Park et al., 1998). Besides, the regulation of *CTT1* and *HSP12* is controlled by intracellular cAMP levels, so the freeze-thaw stress too (Jamieson, 1998; Park et al., 1997).

As expected, stress response genes; *DDR* (292.98), *ALD* (3107.30), *HSP82* (14.88), *MRK1* (8.89), *NTH2* (3.61), *YJL144W* (20.10), *HSP30* (8.71), *ATH1* (6.01), *UBI4* (8.94), *TPS2* (11.84) (Momose et al., 2010; Takahashi et al., 2009; Odani et al., 2003; Shima and Takagi, 2009), Stress related metabolism of the energy reserve (e.g. glycogen, trehalose) genes are induced in response to freeze-thaw stress (Shima and Takagi, 2009; Aguilera et al., 2007). Trehalose metabolism genes; *ATH1* (6.01), *TPS1* (8.30), *TPS2* (11.84), *TSL1* (63.02), glycogen metabolism genes; *GLG1* (5.51), *GSY1* (15.40), *GDB1* (7.82), *GPH1* (133.59), *GLC3* (19.68), *GAC1* (24.81) and carbohydrate metabolic process genes; *HXK1* (224.07), *GPH1* (133.59), *PGM2* (104.10), *SOL4* (51.35) were dramaticaly upregulated in mutant individual *F1*. It was previously shown that carbohydrate metabolic process genes were also induced under cold stress (Schade, 2004), so in mutant individual *F1*.

TPS1, TPS2, TPS3, UGP1, TSL1, PGM2 genes that were responsible in trehalose biosynthetic process and *CAR1, CAR2* genes that were responsible in degradation of arginine were found to be related with freeze-thaw stress (Momose et al., 2010; Shima and Takagi, 2009). On the other hand, *NTH1* gene, encodes a neutral trehalase enzyme that is responsible for the degradation of trehalose in the yeast cells. Freeze-thaw resistant mutant *F1* had high concentrations of trehalose when compared to wild-type yeast cells (Sasano et al., 2012b; Van Dijck et al., 2000). According to the microarray data it is interesting that the expression of *NTH1* gene was upregulated in

mutant *F1* cells. However, the trehalose accumulation of mutant individual *F1* was significantly high.

Membrane channel protein aquaporins have the role to transport water and glycerol. It was shown that upregulation of aquaporins induce freeze-thaw resistance (Tanghe et al., 2002). Especially two of them *AQY1* and *YFL054c* (homologue to *FPS1*) were upregulated at mutant individual *F1*. The results are consistant with the QPCR and microarray data.

Hydrophillin protein encoding genes have a role in dessication stress by acting as an antioxidant molecules against the accumulation of ROS in the cells (Lopez-Martinez et al., 2012). In *S. cerevisiae* there are 12 hydrophilin genes and 5 of them are related with dessication stress. Two uncharacterized hydrophilin genes that are *YJL144W* and *YMR175W* (Sip18) have a role in dessication stress and considering our microarray data, those two genes were 20 and 10.74 fold upregulated at freeze-thaw resistant mutant individual *F1* compared to wild-type. Likewise, other cytoplasmic hydrophilin genes; *GRE1, STF2* were also upregulated in mutant individual *F1*, 10.6 and 11.9 fold of wild-type, respectively (Dang and Hincha, 2011; Lopez-Martinez et al., 2012). On the other hand, another hydrophilin gene *NOP6* was 3.65 fold downregulated when compared to wild-type.

The cell wall integrity (CWI) signalling pathway is important in morphogenesis during the cellular growth and also the stress conditions against cell wall and cell membrane integrity. Under stress conditions, the sensors receive the signal and transfer it to the downstream signal transduction pathway to get quick response and remodelling of the cell wall / membrane structure (Heinisch et al., 2010). The yeast cell wall architecture composed of ß-1,3- glucan, ß-1,6-glucan, mannoproteins and chitin (Lagorce et al., 2003). Freeze-thaw stress causes extreme changes on the ratios of ß-1,3/ß-1,6-glucan, mannoproteins and chitin in the cell wall structure.

The integrity pathway of the cell wall is vital for the yeast cells. The yeast cell wall has not a distinct composition and easily changed due to growth phase and stress conditions. The PKC1-SLT2 cell wall integrity pathway is induced under stress conditions and the deletion of *FKS1* encoding beta_1,3-glucan synthase or *GAS1* encoding glycosylphosphatidylinositol-anchor cell-wall protein resulted in chitin synthesis (induction of *CHS1* and *CHS3* genes) in the cells (Lagorce et al., 2002),

however in *F1* those pathways were downregulated different from the wild-type. On the other hand, upregulation of *HSP12* and *GSY2* (glycogen synthase) is evident under stress conditions.

According to Takahashi and colleagues, 2009 alcohol fermentation genes; *NDE2*, *ADH2* and unclassified proteins; *FMP16*, *YLR149C*, *YNL195C* were upregulated after freeze-thaw stress treatment in yeast cells (Takahashi et al., 2009). The alcohol fermentation genes; *NDE2* (7.28), *ADH2* (3.96) and unclassified proteins; *FMP16* (68.77), *YLR149C* (15.15), *YNL195C* (24.27) were upregulated in mutant individual *F1*.

Glycerol increases tolerance to freeze stress (Sasano et al., 2012c). However, the production rate of glycerol in *F1* seems to low when compared to wild-type. By the way, it is interesting that plasma membrane glycerol proton symporter *STL1* (17.35) and the genes *GUT2* (7.56), *DAK1* (2.26), *GPD2* (2.56), *PGC1* (2.02) that were responsible for glycerol assimilation in the cell were upregulated at *F1*. Previous studies have shown that overexpression of *STL1* gene resulted in glycerol accumulation and important in freeze-thaw stress resistance (Tulha et al., 2010). However, the expression of *STL1* is under the control of glucose repression and only induced under stress conditions such as heat shock (Ferreira and Lucas, 2007). Mutant individual *F1* seems to overcome those glucose repression and the expression levels of *STL1* was 17.35 fold of wild-type. Beside the *STL1* upregulation, *FPS1* expression was 1.22 fold downregulated, so the glycerol import increased and export reduced. According to the HPLC results, the mutant *F1* seem to have lower levels of extracellular glycerol in the media, maybe the reason is that the accumulation and also assimilation inside the cell.

Cellular cAMP levels regulates freeze-thaw stress responces and downregulation of *CYR1* leads to low levels of cAMP that causes freeze-thaw resistance. The *CYR1* is upregulated 3.10 fold of wild-type. Cellular cAMP levels induce most of the stress related genes under the control of Msn2p and/or Msn4p transcriptional activators (Jamieson, 1998). Msn2p/Msn4p general stress transcription factors controls the Environmental Stress Response (ESR) genes and negatively regulated by protein kinase A (PKA) and TOR signalling pathways. ESR genes induced and repressed in response to level of the suboptimal conditions. The quick response is important for the cell protection and survive so, the ESR promramme started in the cellular system.

ESR genes includes carbohydrate metabolism, oxidative stress defence mechanisms, protein metabolism, intracellular signalling and DNA-damage, defence and repair mechanisms. The environmental stress response genes are differentially induced or repressed in different kind of stresses such as heat shock, oxidative stress, osmotic shock, nutrient starvation, DNA damage and extreme pH (Gasch et al.,2000; Gasch, 2007; Wei, 2007)**.**

It is also important to mention that, cell wall mutations also cause the induction of ESR genes. Lagorce and colleagues 2003, stated that the mutations in cell wall, change the transcriptomic profile of cells same as the ESR mechanism and those results are also correlated with the expression profile of mutant individual *F1* (Lagorce et al., 2003). Here, some of the cell wall organization (*ECM15, ECM8, FMP45, SED1, SPR28, ECM11, ZRG8, MTL1, SPR3, ROM1, SKN1, ECM12, YPS6, MHP1, TAX4, SOD1, CWP1, MYO3, ECM4, CCW12, ECM19, UBC7, AVO2, LST8, ZEO1, HPF1, CSR2*) and cell wall biogenesis genes (*PKH1, SDP1, PKH2*) were upregulated in *F1*. In addition, chitin synthesis gene *CHS3* and *CHS1* were 2.27 and 2.06 fold downregulated, ß-glucan remodeling genes; *CRH1, SCW10* and *EXG1* were downregulated, respectively 1.45, 3.00 and 3.05 fold of wild-type, cell wall strengthening genes; *PIR3* and *CWP1* were upregulated, respectively 1.46 fold and 10.83 fold and lastly the cell surface protection genes; *SPI1* and *SED1* were upregulated, respectively 24.01 and 3.22 fold of wild-type. Mannoproteins are the other cell wall components and both *CWP1* and *CWP2* were upregulated 10.83 and 1.67 fold of wild-type.

So, it is important that cell wall stress related pathways were dramatically changed in *F1* and the molecular architecture of the cell wall of mutant individual *F1* seems to remodelled with respect to wild-type.

There are 5 cell surface stress sensors that are Wsc1, Wsc2, Wsc3, Mid2 and Mtl1 in yeast plasma membrane (Heinisch et al., 2010). Those sensors have a role to detect cell wall integrity and transfer the signal to Rho1p under stress conditions (Levin, 2005). The cell surface stress sensor gene *MTL1* and the GDP/GTP exchange protein Rom1p for Rho1p activation against cell wall stress (Lewin, 2005) were upregulated in mutant individual *F1*, however the transcriptional factors Swi4 and Skn7 that were related to upregulation of those genes were downregulated.

Unsaturated/saturated fatty acid and lipid/protein ratios are vital for yeast survival under those stress conditions. High unsaturated/saturated fatty acid ratio is the result of yeast fatty acid desaturase enzyme activity that is encoded by *OLE1* gene. To cope with the harsh conditions of freeze-thaw stress *OLE1* expression is induced and the ratio of unsaturated/saturated fatty acid is increased and the rigidity is increased. However, under normal growth circumstances, Ole1 is toxic to the cells and the unsaturated fatty acids have increased lipid peroxidation rates via ROS (Rodrıguez-Vargas et al., 2007; Landolfo et al., 2010; Jendretzki et al., 2011). *OLE1* was downregulated in mutant individual *F1*, maybe to protect itself against lipid peroxidation under optimal growth conditions but, it maybe induced under freeze-thaw stress conditions. On the other hand, most of the ergesterol biosysnthetic genes were upregulated in the mutant individual and ergesterol is a protector molecule against oxidative damage (Landolfo et al., 2010). Temperature shift to low degrees leads to membrane fluidity in yeast cells. Membrane fluidity is the result of increased levels of unsaturated fatty acids in the membrane via *OLE1* gene (Schade et al., 2004). Under freeze-thaw stress conditions, the increased membrane fluidity gives Na+ tolerance to cells, however, we did not observe Na+ tolerance in mutant individual *F1*. This case can be explained by the freeze-thaw induced osmotic resistance (Wei, 2007).

Plasma membranes are vital for cells to communicate with the environment and transport of nutrients, minerals, water etc. Thus, the composition of the membranes are important feature for cellular viability. Yeast plasma membranes have particular protein and lipid compositions and eiosomes which are the large protein complexes, have a big role in protein and lipid organizations at plasma membranes of the yeast cells. Eisosomes contain two important proteins Pil1 and Lsp1 (Karotki et al., 2011). The expression pattern of those two genes were upregulated in mutant individual *F1*, so the membrane organization seemed to change. Not only the eisosomes in plasma membrane, but also the other factors that are related to plasma membrane was changed in mutant individual.

The ESR genes were regulated via three different evolutionary-tuned signaling pathways and transcriptional factors, according to the stress types. Those are cAMP-PKA, HOG and TOR (target of rapamycin) signal transduction pathways. To prevent the induction of stress response elements in both cAMP-PKA and TOR (target of

rapamycin) signal transduction pathways upon cold shock, *RAS1* and *YVH1* genes (Aguilera et al., 2007) were down regulated to inhibit the promotion of MSN2/MSN4 transcription factors at mutant individual *F1*. However, it is interesting that without any up/down regulation of *MSN4* transcription factor, the expression of stress response element genes of *SSA4, TPS1, TPS2* and *HSP12* were highly upregulated in mutant individual *F1*. That maybe related with the upregulation of *MSN2* 1.34 fold of the wild-type. The similar results were also obtained for the HOG signal transduction pathway, without any change of the *HOG1* expression levels *GPD1, GRE1, GLO1* and *HSP12* genes were highly upregulated in mutant individual *F1*.

To understand the nutrient sensing signaling pathways, we indicated up and down regulated genes of mutant individual *F1* with arrows in Figure 4. 1. Under optimal growth conditions the environmental stress response related genes were up and down regulated as if cells were in a stress condition in mutant individual F1. To understand the differentially expressed ESR genes in F1, we construct the signaling mechanisms that are responsible for the ESR gene expressions. However, the results seem to be conflicting.
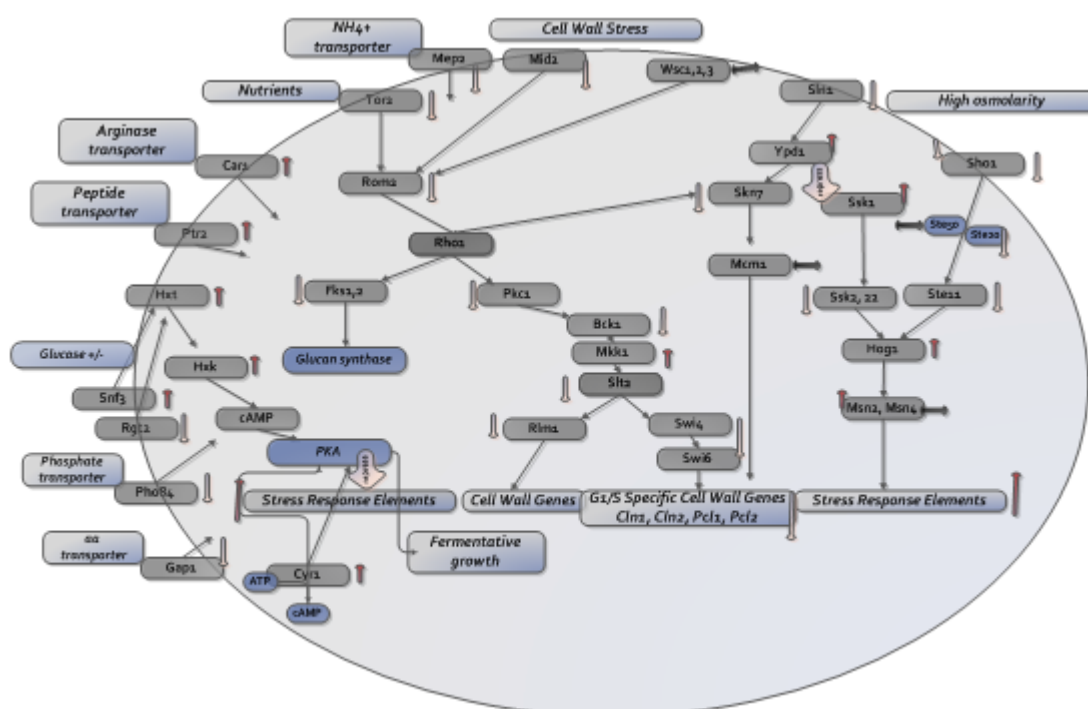
Figure 4.1: Glucose, amino acids, phosphate and ammonium signaling pathways on cellular membrane. The arrows near the boxes indicate upregulation and downregulation of those genes in mutant individual *F1* (Rubio-Texeira et al., 2009; Belinchon and Gancedo, 2007).

Gasch and colleagues (2000) stated that yeast cells detect stress signals and responses to that signals via adjusting the genomic expression programme (Gasch et al., 2000; Gasch, 2007). So, *F1* was adjusted its genomic expression programme with an unknown stress signaling pathways.

There are three types of sensors; G protein-coupled receptors (GPCRs), transporting and non-transporting tranceptors (Rubio-Texeira et al., 1998). Glucose sensors, Snf3 and Rgt2 are non-transporting tranceptors and have a role in induction of *HXT* genes expressions which are responsible for glucose and hexose transport (Özcan et al., 1998). Although the expression of *SNF3* gene is repressed by glucose, here, the expression levels of *SNF3* was upregulated 2.13 fold of wild-type at mutant individual *F1* in the presence of glucose and then the signal was induced the hexokinase transporter genes that mentioned before. Interestingly, Mth1, the repressor protein and the glucose-responsive transcription factor Rgt1 that are blocking the expressionof *HXT* genes was upregulated 9.96 and 1.32 fold of wild-type, respectively. However, those upregulated genes did not repress *HXT* genes in *F1* (Rubio-Texeira et al., 1998). Another glucose sensor *RGT2* is a constitutively expressing gene, but, it was downregulated 1.63 fold of wild-type in an interesting kind of way (Forsberg and Ljungdahl, 2001a).

In *S. cerevisiae*, in the presence of glucose Rgt2 non-transporting glucose sensor senses the glucose signal and activates Yck1 (casein kinase I). Then, Yck1 kinase enzyme phosphorilates *HXT1* gene repressors; Mth1 and Std1 to recognize by Grr1 for degredation. So, the *HXT1* gene derepressed and expresses hexose transporters for uptake of the glucose. In mutant individual *F1*, *HXT1* gene expression was downregulated by the action of upregulated Mth1 repressor protein, downregulation of Rgt2 sensor and the downregulation of all the genes (*YCK1, YCK2* and *GRR1*) related to the derepression mechanism of the *HXT1* gene. The other non-transporting glucose sensor Snf3 was 2.13 fold upregulated but maybe not enough (Moriya and Johnston, 2004).

G protein-coupled receptors (GPCRs) sense the glucose and transfer the answer to carbon signaling Ras/cAMP/PKA pathway that is responsible nutrient control, growth and glucose stress response of the cell (Rubio-Texeira et al., 1998). The Ras/cAMP/PKA pathway is induced in the presence of glucose and suppresses the stress resistance mechanisms. Glucose make cells fragile to stress conditions and

decreases the replicative lifespan. However, in the presence of glucose mutant individual *F1* acts very different. It is remarkable that the Ras/cAMP/PKA pathway did not repress the expression of stress related *ADR1, FBP1, RIM15* and *MSN2* genes, besides those genes were 6.16, 5.48, 1.46 and 1.34 fold upregulated with respect to wild-type. This situation also maybe the result of the downregulation of hexose transporters. Thus, slow uptake of glucose is realized and the suppression of Ras/cAMP/PKA pathway on stress responsive genes were prevented. In addition, *PDE1* gene that has a role in cAMP breakdown was 2.56 fold upregulated and maybe related to overcome Ras/cAMP/PKA repression (Verstrepen et al., 2004).

In amino acid starvation the Ptr3 sensor cannot induce the Ssy1 mediated signals, so the transcription levels of those genes are downregulated (Forsberg and Ljungdahl, 2001a). In mutant individual *F1* those two genes were downregulated and the *PTR2* encoding peptide transporter and *CAR1* encoding arginase transporter was upregulated 1.53 and 2.74 fold of wild-type, respectively.

The sporulation genes are induced under starvation conditions. Especially in diploid cells IME4 is induced to control mating-type locus for meiosis. However, *IME4* cannot induced in haploid yeast cells because of the ncRNA-mediated regulation (antisense repression) of this gene. *RME2* (Regulator of Meiosis 2) is repressed *IME4* gene mRNA product by *RME2* encoding anti-sense RNA only in haploid cells (Shah and Clancy, 1992; Gelfand et al., 2011). It is interesting that *IME4* was 7.5 fold upregulated as when compared to wild-type and the expression level of *RME2* was the same as wild-type. Normally, this case of *IME4* expression is impossible for haploid cells. So, there may be some mutations that were effected on repressor antisense mechanism. Some mutations somehow causes constitutive expression of IME4 leads to insufficient repression of *RME2* gene product whether it was expressed normally. On the other hand, another interesting case is that, the upregulation of *HMLa* and *HMRα* genes. *HMRα1, HMRα2, HMRa1* and *HMRa2* were upregulated 5.86, 4.12, 4.17 and 4.03 fold of wild-type, respectively. *MFA1* encoding mating-type a factor pheromone gene was upregulated 1.38 fold of wild-type. It is clear that mating type switching did not occur in mutant individual F1, because of the diploidization experiments were successful same as the wild-type. How this case happened and why the normally silenced genes were expressed? The answer is that the mechanism of silencing in mating-type loci was disrupted. In *S.*

cerevisiae the silencing of mating-type loci is maintained via repressive heterochromatin. The heterochromatin repression of *HMLa* and *HMRα* genes is determined by *E* and *I* silencers. The Orc1 replication origin of recognition complex binds to the sinencers and then the Rap1 and/or Abf1 proteins composes the baseline for Sir proteins; Sir1, Sir2, Sir3 and Sir4. Sir proteins interact with histone proteins to construct, spread and maintain the heterochromatin complex (Hickman et al., 2011; Rusche et al., 2002). In Figure 4.3, the up and downregulated genes are indicated. The *ORC1, SIR2, SIR3, SIR4* and *RAP1* genes were down regulated 2.15, 3.07, 1.68, 1.78 and 1.35 fold of wild-type respectively, in mutant individual *F1*. Thus, the mutant individual did not compose the well-ordered heterochromatin structure for silencing the *HMLa* and *HMRα* genes. It was also shown that some mutations on Sir proteins resulted in the expression of *HMLa* and *HMRα* (Kassir and Simchen, 1985; Montelone, 2003). In addition, *HMLa* and *HMRα* genes were located on chromosome III, near the centromere (Montelone, 2003) and upregulation of those silenced genes maybe the result of EMS induced or especially, freeze-thaw induced frame-shift or reverse mutations on centromeres (Todorova et al., 2012).

The up and down regulated genes of *F1* are indicated in Figure 4.2 with arrows.
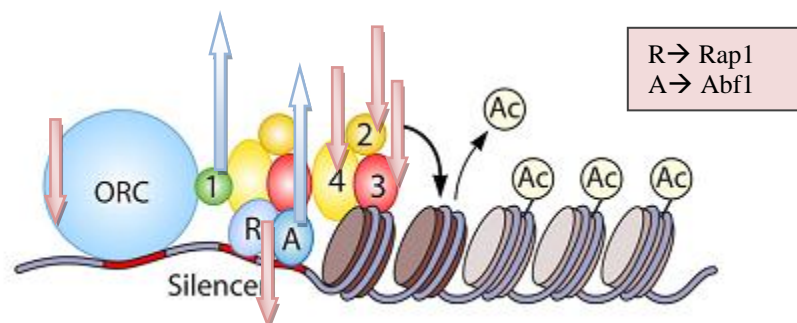
Figure 4.2: Silincing of mating-type loci (HMLa and HMRα) via repressive heterochromatin. Pink arrows indicate the downregulation of genes and the blue arrow indicates upregulation (Hickman et al., 2011).

The percentage of downregulated genes with their corresponding functional categories were analyzed with Funcat database (Figure 3.27). The genes under protein synthesis, transcription, protein with binding function or cofactor requirement (structural or catalytic),cell cycle and DNA processing and cellular transport functional categories were downregulated. Those results were also similarly correlated with the results of Murata and colleagues (2006). They were found out that cold exposure (+4 °C) leads to down regulation of genes responsible from

protein synthesis, proteins with binding functions or cofactor requirements, protein activity regulation and protein fate (Murata et al., 2006). It was also shown that ribosomal genes, protein modification and protein synthesis genes were repressed under cold stress conditions similar with our freeze-thaw stress responses (Schade et al., 2004).

The subcellular localization of the upregulated genes were analyzed with Funspec database. According to the Funspec database subcellular localization results;Nucleus, nucleolus, cytoplasm, plasma membrane, nuclear matrix, bud tip and nuclear pore genes were determined downregulated in *F1*.

The Princeton growth rate/gene expression relationship database was used to analyse our microarray data. When the growth rate decreased due to stress elements, some of the ESR (environmental stress response) genes were upregulated and some of them were downregulated.

In yeast, cellular gene expression programme quickly change according to the environmental conditions to survive. The quick response of the cellular transcription programme is achieved via two cellular response strategies; internal feedback strategy and feedforward strategy (evolutionary-tuned signaling pathways) (Levy et al., 2007). Most of the growth rate-dependent cellular responsive genes are in the group of general transcription program of ESR.

In the suggested feedback strategy, the cellular growth rate controls and coordinates the gene expressions via operating the histone modifications, sensing translation rates and sensing the biomass production, internal nutrient or energy pools. Here, cells generate a predominant response without detailed knowledge about the growth rate limiting condition (Levy and Barkai, 2009).

In the feed-forward strategy, environmental data processed via signalling pathways and the actual growth rate determined. Here cells generate quick responses against the specific problem and they are not wait to change the cellular growth rate. This strategy is supported by most of the experiments. Cells take precaution via signalling pathways instead of waiting for the growth rate reduction (Levy and Barkai, 2009).

The relationship between gene expression and growth rate via feedback and feed-forward strategies are indicated in Figure 4.2.
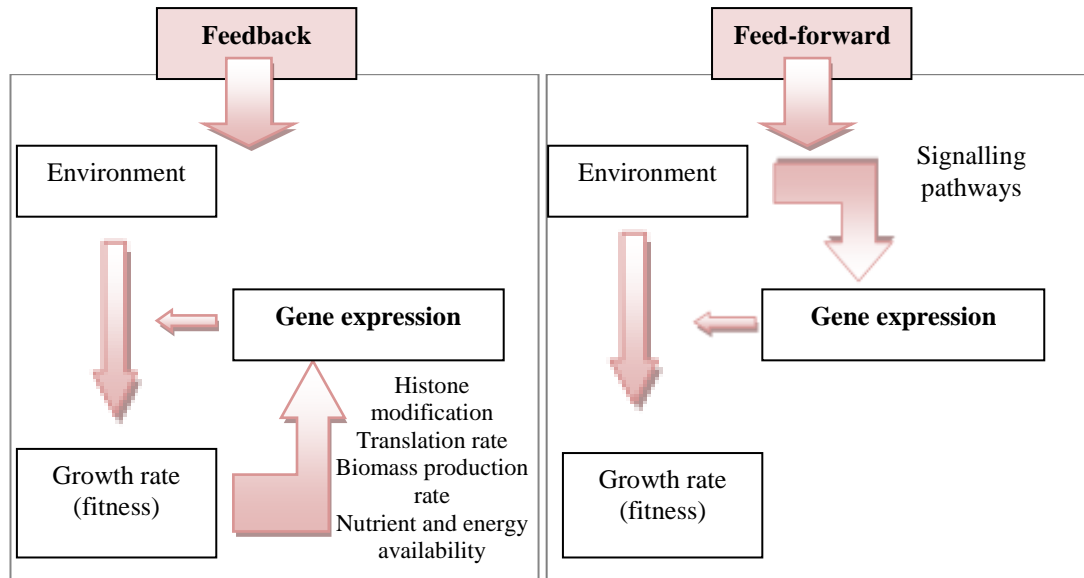
Figure 4.3: Relationship of gene expression and growth rate via feedback and feed-forward strategies (Levy and Barkai, 2009).

Here, there is two large clusters of genes in ESR that are induced or repressed under the stress conditions (Gasch et al., 2000). The related ESR gene expressions were induced and repressed in F1 to adjust growth rate, however there is no stress, evidently. Brauer, (2008), stated that " ESR genes as defined previously may in fact not be responding directly to stress, but instead are responding to a reduction in growth rate secondary to the stress". The general yeast stress response genes were somehow adjusted as if the F1 was exposed to any environmental stress condition.

4.2 Studies with the Industrial Baker's Yeast *Saccharomyces cerevisiae R625*

In industrial applications, beginning from upstream to downstream processes *S. cerevisiae* cells are exposed to different environmental stress conditions. Therefore it is crucial for cells to overcome these stresses and continue to survive to produce high-quality products. Specifically in baking industry the stress elements are freeze thaw and osmotic stresses (Hernández-López et al., 2007). Since, yeast viability in frozen dough has a great economical interest, the freeze-thaw stress influenced by many chemical, temporal and physiological factors, including nutritional status, freezing-thawing rate, freezing-thawing temperature, duration of frozen storage, growth phase and growth rate is important in industrial processes. Here, the main

target is to obtain desired phenotypes for production technology and quality improvement (Branduardi et al., 2008; Codon et al., 2003 Lewis et al., 1993).

A large number of successful studies are exist about haploid *S. cerevisiae* strains. On the other hand, several studies were performed via evolutionary engineering on polyploid industrial *S. cerevisiae* strains. One of the example of industrial yeast strain is Sanchez and colleagues research, (2008). They were improved metabolic engineered recombinant xylose and arabinose utilizing industrial *S. cerevisiae* strains via evolutionary engineering (Sanchez et al., 2010). Another example is that, the improved survival and ethanol production of industrial polyploid yeast strain under the killer toxins in lignocellulosic hydrolysates (Heer and Sauer, 2008).

Paquin and Adams (1983) stated that the fixation of adaptive mutations have 1.6 fold higher frequency in diploid population with respect to haploid ones of *S. cerevisiae* (Sauer, 2001; Paquin and Adams, 1983). Conversely, it is difficult to obtain improved phenotypes in polyploid strains, because of the genetic robustness and gene redundancy results in buffering effect on mutations with respect to haploid ones (Sonderegger et al., 2004; Sanchez et al., 2010; Comai, 2005).

In this thesis project, evolutionary engineering was used to obtain freeze-thaw resistant industrial baker's yeast mutant strains. For this reason, wild-type polyploid *S. cerevisiae R625* baker's yeast strain was chemically mutagenized by 900 µl EMS for 30 min. Then, the genetically variant mutant population was named as *R625_M*.

Screening of the *R625* (polyploid_wild type) and genetically variant mutant population *R625_M* were obtained by applying 1-4 cycle freeze-thaw stress via 5-tube MPN method. The MPN results indicated that the survival ratio of *R625_M* under increasing freeze-thaw stress cycle was too low when compared to wild type (Figure 3.43). To obtain freeze-thaw stress resistant generations, pulse increasing stress selection strategy was adopted. Ten mutant generations were obtained, after 10 repetative cycles of freeze-thaw stress application. There was a fluctuation in percent survival ratios between generations rather than a smooth decline and the final freeze-thaw stress resistant mutant generation (*R625_FG10*) had 0.14 % survival ratio (Figure 3.44). Thereafter, selection of mutant individuals were performed from the final mutant generation *R625_FG10*. Ten mutant individuals (*P1*, *P2*, *P3*, *P4*, *P5*, *P6*, *P7*, *P8*, *P9*, P10) were selected randomly. Then, the phenotypic analysis were

performed to characterize the mutant individuals. Screening of the freeze-thaw response of mutant individuals was performed via spotting assay and 5-tube MPN method. According to the spotting assay results, two cycles of freeze-thaw stress application was effective on polyploid wild-type, *P1*, *P2*, *P3* and *P6*. On the other hand, mutant individuals *P4*, *P5*, *P7*, *P8*, *P9*, *P10* and final generation *R625_10FG* seems to have 10 fold higher survival than the polyploid wild-type (Figure 3.47).So, before starting to MPN, we decreased the number of individuals via spotting assay.

In order to determine the freeze-thaw stress responses of the mutant individuals, survival ratios of two, three and four cycles freeze-thaw stress application was applied to the mutant individual, polyploid wild type and final generation *R625_10FG*. Mutant individual *R625_P8* was the most freeze-thaw resistant yeast among other mutant individuals with 15 % survival ratio.

In order to analyse different stress responses of the freeze-thaw resistant mutant individuals, cross-resistance analysis were performed by using continuous stress screening strategy via spotting assay. Polyploid wild type and freeze-thaw resistant mutant individuals; *P3*, *P4*, *P7*, *P8*, *P9* and *P10* were exposed to toxic levels of boron, chromium, nickel, copper, magnesium, cobalt and zinc metal stresses. 40 mM magnesium stress level did not effect on growth and cells were easily form colonies on magnesium solid agar plate. Mutant individuals; *P3*, *P4*, *P7*, *P8*, *P9* and *P10* have cross-resistance to zinc and cobalt. Polyploid wild type and freeze-thaw resistant mutant individuals were sensitive to nickel and copper stresses.

Thereafter, cross-resistance analysis were performed by using continuous stress screening strategy via 5-tube MPN. Polyploid wild-type and freeze-thaw resistant mutant individuals; *P3*, *P4*, *P7*, *P8*, *P9*, *P10* were exposed to toxic levels of boron, chromium, cobalt, zinc metal stresses, osmotic, oxidative and ethanol stresses. Mutant individuals; *P4*, *P8* and *P9* have tolerance to boron. Mutant individuals; *P8*, *P9* and *P10* have tolerance to iron. Mutant individuals; *P8* and *P9* have tolerance to cobalt and all of the mutant individuals have cross-resistance to zinc. All of the mutant individuals have cross-resistance to oxidative stress (H_2O_2), except *P9* (Figure 3.57, Figure 3.58). Mutant individuals; *P5* and *P7* have tolerance to 7 % ethanol, however, all the mutant individuals were sensitive to ethanol at 10 % stress condition (Figure 3.59). Among other mutant individuals the most freeze-thaw

resistant mutant individual *P8* had cross-resistance to boron, chromium, cobalt, zinc and oxidative stresses except, ethanol stress.

The cross-resistance results of polyploid wild-type and mutant individual *P8* were analyzed via a computational programme, principle component analysis (PCA). By adapting the multiple cross-resistance data on two dimensional plane, we can observe the variance between variables and this data gives us a qualitative conclusion. The response is completely related with the distance between the component scores. Here, similar behaviour between individuals, according to the first principal component at the x-axis, Polyploid mutant individuals *P9* and especially, *P8* are indicated high variance in response when compared to wild-type and the other mutant individuals. It is obvious that *P8* had the highest resistance and the variability (Figure 3.60). Similar behaviour between variables (observations), according to the first principal component at the x-axis, zinc stress is indicated difference in response among other stresses. However, it is obvious that there is a high variance between wild-type and mutant individuals in response to different cross-stresses. The cross-resistance phenotypes are too different from each other at different cross-stresses (Figure 3.61).

Physiological analysis of polyploid wild-type and freeze-thaw resistant mutant individual *P8* were performed at normal growth conditions in a batch culture without stress treatment. Growth curve and metabolite analysis were examined.

The specific growth rate (μ) of polyploid wild-type was 0.222 h^{-1} and the generation time was calculated as 3.12 h. The growth rate (μ) of mutant strain was 0.210 h^{-1} and the generation time was calculated as 3.30 h (Figure 3.63). The specific growth rate of *P8* was 0.946 fold of wild-type. During the growth curve analysis, samples were taken for metabolite analysis via HPLC and glucose oxidase/peroxidase assay. Extracellular glucose, acetate, glycerol and ethanol concentrations (mg/ml) were determined by using high performance liquid chromatography (HPLC).

The glucose concentrations were decreased normally due to the cellular consumptions during the growth. *P8* used glucose slower than *R625* (Figure 3.65). The glycerol amounts (mg/ml) in the culture supernatant of *P8* was higher than *R625* (Figure 3.66).

The acetate amount in the exogenous medium of *R625* was higher at the stationary phase. However, it is still too low for *P8*, near to zero levels.

Ethanol was produced during the growth of *R625* and *P8*. The ethanol production rate of *P8* was lower than the polyploid wild-type until the stationary phase, by then ethanol production was increased in *P8* (Figure 3.67).

Determination of these metabolites was important in order to determine the relationship between growth and exhaustion/production of metabolites.

The reserve carbohydrates glycogen and trehalose were analyzed by using glucose oxidase/peroxidase assay. The samples were collected during the growth at spesific time intervals.

It is obvious that, intracellular reserve carbohydrates trehalose and glycogen were higher in *P8* with respect to wild-type at normal growth conditions without freeze-thaw stress treatment.

4.3 Comparisons of the Laboratory and Industrial Baker's Yeast

In industrial applications, it is crucial for cells to overcome stress factors and continue to survive to produce high-quality products. Specifically in baking industry freeze-thaw stress is important for the yeast viability in frozen dough (Hernández-López et al., 2007).

Here, we successfully obtained freeze-thaw resistant mutant individuals from both laboratory and industrial strains. Although the industrial baker's yeast was polyploid, the selection of the desired phenotype was performed via evolutionary engineering without any problem.

Mutant individual *F1* was selected from the genetically variant haploid mutant population and the mutant individual *P8* was selected from the genetically variant polyploid mutant population. In order to determine the freeze-thaw stress responses of the haploid and polyploid mutant individuals, survival ratios of two cycles freeze-thaw stress application were compared (Figure 4.4).
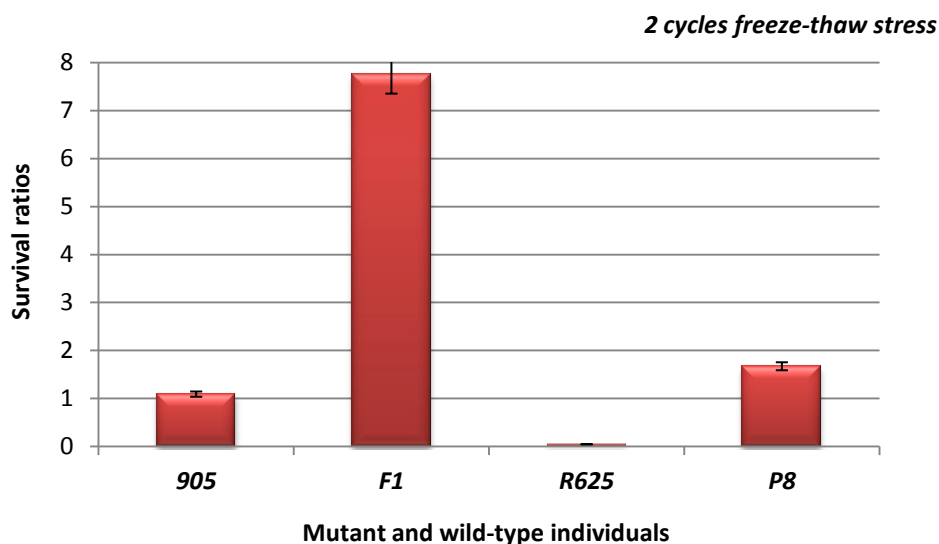
Figure 4.4: Survival ratios of F1 and P8 after 2 cycles of freeze-thaw stress application.

The haploid mutant individual *F1* had the highest resistance to freeze-thaw stress. The reason might be that the haploids ones have the genetic robustness and gene redundancy resulted ftom the buffering effect on possible mutations (Sonderegger et al., 2004; Sanchez et al., 2010; Comai, 2005).

According to the cross-resistance analysis, mutant individual *F1* and *P8* had a common cross-resistance to boron, cobalt, zinc and oxidative stress (H_2O_2).

Physiological analysis of haploid and polyploid freeze-thaw resistant mutant individuals were performed at normal growth conditions in batch cultivation without stress treatment. Growth curve and metabolite analysis were examined.

The growth of polyploid yeasts dominantly higher than the haploid ones (Gerstain and Otto, 2011). However, in this case, the generation time of polyploid wild-type and mutant individual P8 was lower than that of the haploid *905*. On the other hand, the haploid *905* reached higher OD_{600} values than the polyploid *R625*. Importantly, in both haploid and polyploid mutant individuals, the growth rate characteristics was not dramatically reduced. In bioreactor cultivation the generation times of the strains were reduced and the cells grew faster. Interestingly, *F1* grew faster in the bioreactor cultivation different from the shake flask cultivation (Table 4.2).

Table 4.2: Comparison of haploid and diploid growth data in shake flask and bioreactor cultivation.

	Shake flask			Bioreactor		
	specific growth rate (h^{-1})	generation time	specific growth rate fold of wild-type	specific growth rate (h^{-1})	generation time	specific growth rate fold of wild-type
905	0.208	3.33		0.44	1.58	
F1	0.186	3.73	0.894	0.47	1.48	1.068
R625	0.222	3.12		0.48	1.44	
P8	0.210	3.30	0.946	0.40	1.73	0.833

When the metabolite production were analiysed for both shake flask and bioreactor cultivation results and it was observed that they were consistant for wild-types and mutant individuals. However, the metabolite concentrations were different due to the cultivation conditions. In both mutant individuals, the glucose concentrations were decreased slower than their corresponding wild-types. The glycerol concentrations (mg/mL) in the culture supernatant of *P8* was higher than *F1*. The acetate concentrations (mg/mL) in the culture supernatant of *P8* was lower than *F1*, near to zero levels. The ethanol production rate of *P8* and *F1* were similar. The intracellular reserve carbohydrate trehalose and glycogen concentrations (mg/mL) were higher in *F1* with respect to *P8*.

The results indicated that both laboratory and industrial mutant individuals gained high freeze-thaw stress resistance. The genetic robustness and gene redundancy might be the results of buffering effect on mutations in polyploidy industrial strain with respect to haploid laboratory strain. This might be the answer of why mutant individual *F1* was better in freeze-thaw stress defence than the mutant individual *P8*.

In conclusion, it is more safe and acceptable to use improved baker's yeast with high freeze-thaw resistance without including any foreign genes that do not belong to the yeast natural genome. Thus, this is the safer way to use baker's yeast in industry with the highly re-regulated genome resulted with freeze-thaw resistance (Sasano et al., 2012c). Here, it is important that we succeed to obtain highly freeze-thaw resistant mutant individual from an industrial strain.

REFERENCES

Abrahart, R. J., & See, L. (2000). Comparing neural network and autoregressive moving average techniques for the provision of continuous river flow forecasts in two contrasting catchments, *Hydrolog.Process.,14*, 2157–2172.

Aguilera, J., Randez-Gil, F., & Prieto, J.A. (2007). Cold response in Saccharomyces cerevisiae: new functions for old mechanisms. *FEMS Microbiol. Rev., 31(3),* 327-341.

Alves-Araujo, C., Almeidaa, M.J., Sousaa, M. J., & Leao, C. (2004). Freeze tolerance of the yeast Torulaspora delbrueckii: cellular and biochemical basis, *FEMS Microbiol. Lett., 240,* 7-14.

Ando, A., Nakamura, T., Murata, Y., Takagi, H., & Shima, J. (2007). Identification and classification of genes required for tolerance to freeze-thaw stress revealed by genome-wide screening of *Saccharomyces cerevisiae* deletion strains, *FEMS Yeast Res., 7(2),* 244-53.

Bailey, J.E., Sburlati, A., Hatzimanikatis, V., Lee, K., Renner, W.A., & Tsai, P.S. (1996). Inverse metabolic engineering: a strategy for directed genetic engineering of useful phenotypes, *Biotechnology and Bioengineering, 52,* 109-121.

Bauer, E.F., & Pretorius, L.S. (2000). Yeast Stress Response and Fermentation Efficiency: How to Survive the Making of Wine, *S. Afr. J. Enol. Vitic., 21,* 27-51.

Beese-Sims, S.E., Lee, J., & Levin, D.E. (2011). Yeast Fps1 glycerol facilitator functions as a homotetramer, *Yeast, 28(12),* 815-819.

Belinchon, M.M., & Gancedo, J.M. (2007). Glucose controlsmultiple processes in *Saccharomyces cerevisiae* through diverse combinations of signaling pathways, *FEMS Yeast Res., 7,* 808–818.

Berthels, N.J., Cordero-Otero, R.R., Bauer, F.F., Pretorius, I.S., & Thevelein, J.M. (2008). Correlation between glucose/fructose discrepancy and hexokinase kinetic properties in different *Saccharomyces cerevisiae* wine yeast strains, *Appl. Microbiol. Biotechnol., 77(5),* 1083-91.

Branduardi, P., Smeraldi, C., & Porro, D. (2008). Metabolically Engineered Yeasts: 'Potential' Industrial Applications, *J. Mol. Microbiol.Biotechnol.,15,* 31-40.

Brauer, M.J., Huttenhower, C., Airoldi, E.M., Rosenstein, R., Matese, J.C., Gresham, D., Boer, V.M., Troyanskaya, O.G., & Botstein, D. (2008). Coordination of Growth Rate, Cell Cycle, Stress Response, and Metabolic Activity in Yeast, *Mol. Biol. Cell, 19(1),* 352–367.

Breslow, D.K., Cameron, D.M., Collins, S.R.,Schuldiner, M., Ornstein, J.S., Newman, H.W., Braun, S., Madhani, H.D., Krogan, N.J., Jonathan, S., & Weissman, J.S. (2008). A comprehensive strategy enabling high-resolution functional analysis of the yeast genome, *Nat. Methods*, *5(8),* 711–718.

Çakar, Z.P., Alkım C., Turanlı B., Tokman N., Akman S., Sarıkaya M., Tamerler C., Benbadis L., & François J.M. (2009) Isolation of cobalt hyper-resistant mutants of *Saccharomyces cerevisiae* by in vivo evolutionary engineering approach, *J. Biotechnol.*, *143,* 130–138

Çakar, Z.P., Alkım C., Turanlı B., *&* Yılmaz Ü. (2012). Evolutionary engineering of *Saccharomyces cerevisiae* for improved industrially important properties, *FEMS Yeast Research*, *12(2),* 171–182.

Cakar, Z.P., Şeker, U.Ö.Ş., Tamerler, C., Sonderegger, M., & Sauer, U. (2005). Evolutionary engineering of multiple-stress resistant *Saccharomyces cerevisiae*, *FEMS Yeast Res.*, *5,* 569-578.

Carlquist, M., Fernandes, R.L., Helmark, S., Heins, A.L., Lundin, L., Sørensen, S.J., Gernaey, K.V., & Lantz, A.E. (2012). Physiological heterogeneities in microbial populations and implications for physical stress tolerance, *Microb. Cell Fact.*, *11(94),* 1-13.

Codon, A.C., Rincon, A.M., Moreno-Mateos, M.A., Delgado-Jarana, J., Rey M., Limon, C., Rosado, I.V., Cubero, E., Penate, X., Castrejon, F., & Benitez, T. (2003). New Saccharomyces cerevisiae Baker's Yeast Displaying Enhanced Resistance to Freezing, *J. Agric. Food.Chem.*, *51,* 483−491.

Comai, L. (2005). The advantages and disadvantages of being polyploid, *Nature Reviews Genetics*, *6,* 836-846.

Dang, NX, & Hincha, DK. (2011). Identification of two hydrophilins that contribute to the desiccation and freezing tolerance of yeast (*Saccharomyces cerevisiae*) cells,*Cryobiology*, *62(3),* 188-93.

Driessen, M., Osinga, K.A., & Herweijer, M.A. (1991). New yeast strainswith enhanced trehalose content. Process to obtain such yeasts and the useof these yeasts. European patent application 91200686.3.

Dumont, F., Marechal, P.A., & Gervais, P. (2006).Involvement of Two Specific Causes of Cell Mortality in Freeze-Thaw Cycles with Freezing to -196°C, *App. and Env. Mic.*, *72,* 1330–1335.

Eason, R.G., Pourmand, N., Tongprasit, W., Zelek, S. Herman, Z.S., Anthony, K., & Jejelowo, O. (2004). Characterization of synthetic DNA bar codes in *Saccharomyces cerevisiae* gene-deletion strains, *Genetics*,*101(30),* 11046–11051.

Eglinton, J.M., Heinrich, A.J., Pollnitz, A.P., Langridge, P., Henschke, P.A., & de Barros-Lopes, M. (2002). Decreasing acetic acid accumulation by a glycerol overproducing strain of Saccharomyces cerevisiae by deleting the ALD6 aldehyde dehydrogenase gene, *Yeast*, *19(4),* 295-301.

Ferreira, C., & Lucas, C. (2007). Glucose repression over *Saccharomyces cerevisiae* glycerol/H+ symporter gene STL1 is overcome by high temperature, *FEBS Lett.*, 2007 *581(9),* 1923-1927.

Forsberg, H., & Ljungdahl, P.O. (2001a). Genetic and Biochemical Analysis of the Yeast Plasma Membrane Ssy1p-Ptr3p-Ssy5p Sensor of Extracellular Amino Acids, *Mol. Cell. Biol.*, *21(3),* 814–826.

Forsberg, H., & Ljungdahl, P.O. (2001b). Sensors of extracellular nutrients in Saccharomyces cerevisiae, *Curr. Genet.*, *40(2),* 91-109.

Gasch, A.P. (2007). Comparative genomics of the environmental stress response in ascomycete fungi, *Yeast*, *24(11),* 961-76.

Gasch, A.P., Spellman, P.T., Kao, C.M., Carmel-Harel, O., Eisen, M.B., Storz, G., Botstein, D., & Brown, P.O. (2000). Genomic expression programs in the response of yeast cells to environmental changes, *Mol. Biol. Cell.*, *11(12),* 4241-57.

Gelfand, B., Mead, J., Bruning, A, Apostolopoulos, N., Tadigotla, V., Nagaraj, V., Sengupta, A.M., & Vershon, A.K. (2011). Regulated antisense transcription controls expression of cell-type-specific genes in yeast, *Mol. Cell. Biol.*, *31(8),* 1701-9.

Gerstein, A.C., & Otto, S.P. (2011). Cryptic Fitness Advantage: Diploids Invade Haploid Populations Despite Lacking Any Apparent Advantage as Measured by Standard Fitness Assays, *PLoS One*, *6(12),* 1-13.

Heer, D., & Sauer, U. (2008). Identification of furfural as a key toxin in lignocellulosic hydrolysates and evolution of a tolerant yeast strain, *Microb. Biotechnol.*, *1(6),* 497-506.

Heinisch, U.J., Dupres, V., Wilk, S., Jendretzki, A., & Dufrene, Y.F. (2010). Single-Molecule Atomic Force Microscopy Reveals Clustering of the Yeast Plasma-Membrane Sensor Wsc1, *Plosone*, *5(6),* 1-9.

Hernández-López, M. J., Pallotti, C., Andreu, P., Aguilera, J., Prieto, J.A., & Randez-Gil, F. (2007).Characterization of a *Torulaspora delbrueckii* diploid strain with optimized performance in sweet and frozen sweet dough.International, *Journal of Food Microbiology*, *116,* 103-110.

Herrero, E., Ros, J., Bellí, G., & Cabiscol, E. (2008). Redox control and oxidative stress in yeast cells, *Biochim. Biophys. Acta.*, *1780(11),* 1217-35.

Herskowitz, I. (1988). Life Cycle of the Budding Yeast *Saccharomyces cerevisiae*, *Microbiol. Rev.*, *52(4),* 536–553.

Hickman, M.A., Froyd C.A., & Rusche L.N. (2011). Reinventing Heterochromatin in Budding Yeasts: Sir2 and the Origin Recognition Complex Take Center Stage, *Eukaryot. Cell* , *10(9),* 1183–1192

Hubálek, Z. (2003). Protectants used in the cryopreservation of microorganisms, *Cryobiology.*, *46(3),* 205-29.

Izawa, S., Sato, M., Yokoigawa, K., & Inoue, Y. (2004a). Intracellular glycerol influences resistance to freeze stress in *Saccharomyces cerevisiae*: analysis of a quadruple mutant in glycerol dehydrogenase genes and glycerol-enriched cells, *Appl. Microbiol. Biotechnol., 66,* 108-114.

Izawa, S., Ikeda, K., Maeta, K., & Inoue, Y. (2004b). Deficiency in the glycerol channel Fps1p confers increased freeze tolerance to yeast cells: application of the fps1delta mutant to frozen dough technology, *Appl. Microbiol. Biotechnol., 66(3),* 303-5.

Jamieson, D.J. (1998). Oxidative stress responses of the yeast *Saccharomyces cerevisiae*, *Yeast, 14(16),* 1511-27.

Jendretzki, A., Wittland, J., Wilk, S., Straede, A., & Heinisch, J.J. (2011). How do I begin? Sensing extracellular stress to maintain yeast cell wall integrity, *Eur. J. Cell. Biol*., *90(9),* 740-744.

John, N. & Stephens, M. (2008). Interpreting principal component analyses of spatial population genetic variation, *Nature Genetics*, *40,* 646-649.

Kanwal, S., Saharan, R.K., Mahmood, A., & Sharma, S.C. (2011). Effect of Reserve Carbohydrates on Oxidative Stress in Yeast *Saccharomyces cerev*isiae Y6210, *Curr. Res. J. .Biol. Sci., 3(6),* 633-636.

Karotki, L., Huiskonen, J.T., Stefan, C.J., Ziółkowska, N.E., Roth, R., Surma, M.A., Krogan, N.J., Emr, S.D., Heuser, J., Grünewald, K., & Walther, T.C. (2011). Eisosome proteins assemble into a membrane scaffold, *J. Cell. Biol*., *195(5),* 889-902.

Kassir, Y., & Simchen, G. (1985). Mutations leading to expression of the cryptic HMRa locus in the yeast *Saccharomyces cerevisiae*, *Genetics*, *109(3),*481-92.

Klar, A.J. (2010). The yeast mating-type switching mechanism: a memoir, *Genetics*, *186(2),* 443-9.

Kronberg, M.F., Nikel, P.I., Cerrutti, P., & Galvagno, M.A. (2008). Modelling the freezing response of baker's yeast prestressed cells: a statistical approach, *Journal of Applied Microbiology*, *104,* 716–727.

Lagorce, A., Hauser, N.C., Labourdette, D., Rodriguez, C., Martin-Yken, H., Arroyo, J., Hoheisel, J.D., & François, J. (2003). Genome-wide analysis of the response to cell wall mutations in the yeast *Saccharomyces cerevisiae*, *J. Biol. Chem., 278(22),* 20345-20357.

Lagorce, A., Le Berre-Anton, V., Aguilar-Uscanga, B., Martin-Yken, H., Dagkessamanskaia, A., & François, J. (2002). Involvement of GFA1, which encodes glutamine-fructose-6-phosphate amidotransferase, in the activation of the chitin synthesis pathway in response to cell-wall defects in *Saccharomyces cerevisiae*, *Eur. J. Biochem., 269(6),* 1697-707.

Landolfo, S., Zara, G., Zara, S., Budroni, M., Ciani, M., & Mannazzu, I. (2010). Oleic acid and ergosterol supplementation mitigates oxidative stress in wine strains of *Saccharomyces cerevisiae*, *Int. J. Food Microbiol.*, *141(3),* 229-35.

Lawrence, C.W. (1991). Classical mutagenesis techniques, *Methods Enzymol*., *194,* 456-464.

Lee, J.C., Straffon, M.J., Jang, T.Y., Higgins, V.J., Grant, C.M., & Dawes, IW. (2001).The essential and ancillary role of glutathione in

Saccharomyces cerevisiae analysed using a grande gsh1 disruptant strain, *FEMS Yeast Res., 1(1),* 57-65.

Levin, D.E. (2005). Cell Wall Integrity Signaling in *Saccharomyces cerevisiae*. *Microbiol. Mol. Biol. Rev.*, *69(2),* 262–291.

Levy, S., & Barkai, N. (2009). Coordination of gene expression with growth rate: A feedback or a feed-forward strategy?, *FEBS Lett.*, *583,* 3974–3978.

Levy, S., Ihmels, J., Carmi, M., Weinberge, A., & Friedlander, G. (2007). Strategy of Transcription Regulation in the Budding Yeast, *PLoS ONE, 2(2),* 1-10.

Lewis J. G., Learmonth R. P., & Watson K. (1993). Role of Growth Phase and Ethanol in Freeze-Thaw Stress Resistance of *Saccharomyces cerevisiae*, *App. and Env. Mic.*, *59,* 1065-1071.

Li, J., Coïc, E., Lee, K., Lee, C.S., Kim, J.A., Wu, Q., & Haber, J.E. (2012). Regulation of budding yeast mating-type switching donor preference by the FHA domain of Fkh1, *PLoS Genet.*, *8(4),* 1-14.

Lin, S.J., & Culotta, V.C. (1995). The ATX1 gene of *Saccharomyces cerevisiae* encodes a small metal homeostasis factor that protects cells against reactive oxygen toxicity, *Proc. Natl. Acad. Sci.*, *92(9),* 3784–3788.

Lindquist, J. (2012) A Five-Tube MPN Table (on-line) Available from: http://wwwjlindquistnet/generalmicro/102dil3ahtml (December 2012, last date accessed)

Londesborough, J., & Vuorio, O. (1993). Increasing the trehalose content oforganisms by transforming them with combinations of the structural genesfor trehalose synthase. International patent application PCT/FI93/00049.

López-Martínez, G., Rodríguez-Porrata B., Margalef-Català M., & Cordero-Otero R. (2012). The *STF2p* Hydrophilin from *Saccharomyces cerevisiae* Is Required for Dehydration Stress Tolerance, *PLoS ONE*, *7(3),* 1-10.

Luikenhuis, S., Perrone, G., Dawes, I.W., & Grant, C.M. (1998). The yeast *Saccharomyces cerevisiae* contains two glutaredoxin genes that are required for protection against reactive oxygen species, *Mol. Biol. Cell*, *9(5),* 1081-91.

Mamvura, T.A., Iyuke, S.E., Sibanda, V., & Yah C.S. (2012). Immobilisation of yeast cells on carbon nanotubes, *S. Afr. J. Sci.*, *108,* 1-8.

Masson, J.Y., & Ramotar, D. (**1998).** The transcriptional activator Imp2p maintains ion homeostasis in *Saccharomyces cerevisiae*, *Genetics, 149(2),* 893-901.

Merico, A., Ragni, E., Galafassi, S., Popolo, L., & Compagno, C. (2011). Generation of an evolved *Saccharomyces cerevisiae* strain with a high freeze tolerance and an improved ability to grow on glycerol, *J. Ind. Microbiol. Biotechnol.*, *38(8),* 1037-1044.

Momose, Y., Matsumoto, R., Maruyama, A., & Yamaoka, M. (2010).Comparative analysis of transcriptional responses to the

cryoprotectants, dimethyl sulfoxide and trehalose, which confer tolerance to freeze–thaw stress in Saccharomyces cerevisiae, *Cryobiology*, *60,* 245–261.

Montelone, B.A. (2003). *"Yeast Mating Type"*, In: Nature *Encyclopedia of Life Sciences*, London: Nature Publishing Group

Moriya, H., & Johnston, M. (2004). Glucose sensing and signaling in *Saccharomyces cerevisiae* through the Rgt2 glucose sensor and casein kinase I, *Proc. Natl. Acad. Sci. U. S. A.*, *101(6),* 1572-7.

Muller, EG. (1991). Thioredoxin deficiency in yeast prolongs S phase and shortens the G1 interval of the cell cycle, *J. Biol. Chem.*, *266(14),* 9194-202.

Murata, Y., Homma, T., Kitagawa, E., Momose, Y., Sato, M.S., Odani, M., Shimizu, H., Hasegawa-Mizusawa, M., Matsumoto, R., Mizukami, S., Fujita K., Parveen, M., Komatsu, Y., & Iwahashi, H. (2006). Genome-wide expression analysis of yeast response during exposure to 4 °C, *Extremophiles*, *10(2),* 117-28.

Myers, D.K., Joseph, V.M., Pehm, S., Galvagno, M., & Attfield, P.V. (1998). Loading of *Saccharomyces cerevisiae* with glycerol leads to enhanced fermentation in sweet bread doughs, *Food Microbiology*, *15(1)***,** 51–58

Nevoigt, E. (2008). Progress in Metabolic Engineering of *Saccharomyces cerevisiae*, *Microbiol. Mol. Biol. Rev.*, *72(3),* 379–412.

Novembre, J., & Stephens, M. (2008). Interpreting principal component analyses of spatial population genetic variation, *Nature Genetics*, *40,* 646 – 649.

Odani, M., Komatsu, Y., Oka, S., & Iwahashi, H. (2003). Screening of genes that respond to cryopreservation stress using yeast DNA microarray, *Cryobiology*, *47,* 155–164.

Olsson, L., & Nielsen, J. (2000). The role of metabolic engineering in the improvement of Saccharomyces cerevisiae: utilization of industrial media, *Enzyme Microb. Technol.*, *26(9-10),* 785-792.

Oud, B., van Maris, A.J., Daran, J.M., & Pronk, J.T. (2012). Genome-wide analytical approaches for reverse metabolic engineering of industrially relevant phenotypes in yeast, *FEMS Yeast Res.*, *12(2),* 183-96.

Özcan, S, Dover J., & Johnston, M. (1998). Glucose sensing and signaling by two glucose receptors in the yeast *Saccharomyces cerevisiae*. *EMBO J.*, *17,* 2566–2573.

Paquin C, & Adams J (1983). Frequency of fixation of adaptive mutations is higher in evolving diploid than haploid yeast populations, *Nature*, *302,* 495-500.

Park, J., Grant C., Attfield, P. V., & Dawes I.W. (1997). The Freeze-Thaw Stress Response of the Yeast Saccharomyces cerevisiae Is Growth Phase Specific and Is Controlled by Nutritional State via the RAS-Cyclic AMP Signal Transduction Pathway, *App. and Env.Mic.*, *63,* 3818-3824.

Park, J.I., Grant, C.M., Davies, M.J., & Dawes, I.W. (1998). The cytoplasmic Cu,Zn superoxide dismutase of *Saccharomyces cerevisiae* is required for resistance to freeze-thaw stress. Generation of free radicals during freezing and thawing, *J. Biol. Chem.*, *273(36),* 22921-8.

Parks, H.D., Beeser, A.E., Clancyi, M.J. & Cooper, T.G. **(1996).** The *S. cerevisiae* Nitrogen Starvation-Induced Yvh lp and Ptp2p Phosphatases Play a Role in Control of Sporulation, *YEAST, 12,* 1135-1151.

Parrou, J.L., & François, J. (1997). A simplified procedure for a rapid and reliable assay of both glycogen and trehalose in whole yeast cells, *Anal. Biochem.*, *248(1),* 186-8.

Pérez-Torrado, R., Panadero, J., Hernández-López, M.J., Prieto, J.A., & Randez-Gil, F. (2010). Global expression studies in baker's yeast reveal target genes for the improvement of industrially-relevant traits: the cases of CAF16 and ORC2, *Microb. Cell Fact.*, *9,* 56.

Ren, H., Wang, X., Liu, D., & Wang, B. (2012). A glimpse of the yeast Saccharomyces cerevisiae responses to NaCl stress *African Journal of Microbiology Research*, *6(4),* 713-718.

Roberts. S. & Jackson, J.A.(1991). Active normal faulting in central Greece: An overview, in *The Geometry of Normal Faults,* Spec. Publ. Geol. Soc. Lond., *56,* p. 125-142, Eds. Roberts, A.M., Yielding, G. and Freeman, B., Blackwell Scientific Publications,Oxford.

Rodrıguez-Vargas, S., Sanchez-Garcıa, A., Martınez-Rivas, J.M., Prieto, J.A., & Randez-Gil, F. (2007). Fluidization of Membrane Lipids Enhances the Tolerance of *Saccharomyces cerevisiae* to Freezing and Salt Stress, *Appl. Environ. Microbiol.*, *73(1),* 110–116.

Rubio-Texeira, M., Van-Zeebroeck, G., Voordeckers, K., &Thevelein, J.M. (2010). *Saccharomyces cerevisiae* plasma membrane nutrient sensors and their role in PKA signaling, *FEMS Yeast Res.*, *10,* 134–149.

Ruepp, A., Zollner, A., Maier, D., Albermann, K., Hani, J., Mokrejs, M., Tetko, I., Güldener, U., Mannhaupt, G., Münsterkötter, M., & **Mewes, H.W.** (2004). The FunCat, a functional annotation scheme for systematic classification of proteins from whole genomes, *Nucleic Acids Res.*, *32(18),* 5539-45.

Ruotolo, R., Marchini, G., & Ottonello S. (2008). Membrane transporters and protein traffic networks differentially affecting metal tolerance: a genomic phenotyping study in yeast, *Genome Biol. 9(4),* R67.

Rusche, L.N., Kirchmaier, A.L., & Rine, J. (2002). Ordered Nucleation and Spreading of Silenced Chromatin in *Saccharomyces cerevisiae*, *Mol. Biol. Cell*, *13,* 2207–2222

Sahara, T., Goda, T., & Ohgiya, S. (2002). Comprehensive Expression Analysis of Time-dependent Genetic Responses in Yeast Cells to Low Temperature, *The Journal of Biological Chemistry*, *277(51),* 50015–50021.

Salas-Mellado, M. M. & Chang, Y. K. (2003).Effect of formulation on the quality

of frozen dough bread dough, *Brazilian Archives of Biology and Technology*, *46,* 461-468.

Sanchez, R.G., Karhumaa, K., Fonseca, C., Nogué, V.S., Almeida, J.R.M., Larsson, C.U., Bengtsson, O., Bettiga, M., Hahn-Hägerdal, B., & Gorwa-Grauslund, M.F. (2010). Improved xylose and arabinose utilization by an industrial recombinant strain using evolutionary engineering, *Biotechnol Biofuels*., *3,* 1-13.

Santagapita, P.R., Kronberg, F., Wu A., Cerrutti ,P., Buera, M.P., & Galvagno, M.A. (2007). Exploring differential scanning calorimetry as a tool for evaluating freezing stress sensitivity in Baker's yeasts, *Thermochimica Acta*, *465, 67-72.*

Santt, O., Pfirrmann, T., Braun, B., Juretschke, J., Kimmig, P., Scheel, H., Hofmann, K., Thumm, M, & **Wolf, D.H.** (2008). The yeast GID complex, a novel ubiquitin ligase (E3) involved in the regulation of carbohydrate metabolism. *Mol. Biol. Cell*., *19(8),* 3323-3333.

Sasano' Y., Haitani, Y., Hashida, K., Ohtsu, I., Shima, J., & Takagi, H. (2012b). Simultaneous accumulation of proline and trehalose in industrial baker's yeast enhances fermentation ability in frozen dough, *Journal of Bioscience and Bioengineering*, *113(5),* 592–595.

Sasano, Y., Haitani ,Y., Hashida, K., Ohtsu, I., Shima, J., & Takagi H. (2012a). Overexpression of the transcription activator Msn2 enhances the fermentation ability of industrial baker's yeast in frozen dough.*Biosci. Biotechnol. Biochem.*, *76(3),* 624-7.

Sasano, Y., Haitani, Y., Hashida, K., Ohtsu, I., Shima, J., & Takagi, H. (2012c). Enhancement of the proline and nitric oxide synthetic pathway improves fermentation ability under multiple baking-associated stress conditions in industrial baker's yeast, *Microb. Cell Fact.*, *11,* 1-8.

Sauer, U. (2001). Evolutionary engineering of industrially important microbial phenotypes. *Adv. Biochem. Eng. Biotechnol.*, *73,* 129-69.

Schade, B., Jansen, G., Whiteway, M., Entian, K.D., & Thomas, D.Y. (2004). Cold Adaptation in Budding Yeast**,** *Mol Biol Cell*, *15(12),* 5492–5502.

Shah, J.C., & Clancy, M.J. (1992). IME4, a Gene That Mediates Al4T and Nutritional Control of Meiosis in *Saccharomyces cerevisiae*, *Mol. Cell. Biol*., *12(3),* 1078-1086.

Shima , J. & Takagi, H. (2009). Stress-tolerance of baker's-yeast (*Saccharomyces cerevisiae*) cells: stress-protective molecules and genes involved in stress tolerance, *Biotechnol. Appl. Biochem*., *53,* 155–164.

Shima, J., Y. Sakata-Tsuda, Y. Suzuki, R. Nakajima, H. Watanabe, S. Kawamoto, & H. Takano. (2003). Disruption of the CAR1 gene encoding arginase enhances freeze tolerance of the commercial baker's yeast *Saccharomyces cerevisiae*, *Appl. Environ. Microbiol*., *69,* 715–718.

Snowdon, C., Schierholtz, R., Poliszczuk, P., Hughes, S., & van der Merwe, G. (2009). ETP1/YHL010c is a novel gene needed for the adaptation of Saccharomyces cerevisiae to ethanol, *FEMS Yeast Res.*, *9(3),* 372-80.

Sonderegger, M., Jeppsson, M., Larsson, C., Gorwa-Grauslund, M.F., Boles, E., Olsson, L., Spencer-Martins, I., Hahn-Hägerdal, B., & Sauer, U. (2004). Fermentation performance of engineered and evolved xylose-fermenting *Saccharomyces cerevisiae* strains, *Biotechnol. Bioeng.*, *87(1),* 90-8.

Takahashi, S., Ando, A., Takagi, H., & Shima, J. (2009). Insufficiency of Copper Ion Homeostasis Causes Freeze-Thaw Injury of Yeast Cells as Revealed by Indirect Gene Expression Analysis, *Appl. Environ. Microbiol.*, *75 (21),* 6706–6711.

Tanghe, A, Dijck, V.P., Dumortier, F., Teunissen, A., Hohmann, S., & Thevelein, J.M. (2002).Aquaporin Expression Correlates with Freeze Tolerance in Baker's Yeast, and Overexpression Improves Freeze Tolerance in Industrial Strains, *App.and Env. Mic.,68,* 5981-5989.

Tanghe, A., Carbrey, J. M., Agre, P., Thevelein, J. M., & Dijck, P. V. (2005). Aquaporin Expression and Freeze Tolerance in *Candida albicans*, *App. and Env. Mic.*, *71,* 6434-6437.

Tanghe, A., Dijck, P.V., Colavizza, D. & Thevelein, J. M. (2004). Aquaporin-Mediated Improvement of Freeze Tolerance of *Saccharomyces cerevisiae* is Restricted to Rapid Freezing Conditions, *Appl.Environ. Microbiol.*, *70(6),* 3377-3382.

Tanghe, A., Teunissen, A., Van Dijck, P., & Thevelein, J.M. (2000). Identification of genes responsible for improved cryoresistance in fermenting yeast cells, *Int. J. Food Microbiol.*, *55(1-3),* 259-62.

Todorova, T., Pesheva, M., Stamenova, R., Dimitrov, M., & Venkov P. (2012). Mutagenic effect of freezing on nuclear DNA of *Saccharomyces cerevisiae*, *Yeast*, *29(5),* 191–199.

Trueblood, C. E., Wright, R. M., & Poyton, R. 0.(1988). Differential regulation of the cytochrome c oxidase subunit V multigene family by heme and the HAP2 and REOI genes, *Mol. Cell. Biol.,* *8,* 4537-4540.

Tulha, J., Lima, A., Lucas, C., & Ferreira, C. (2010). *Saccharomyces cerevisiae* glycerol/H+ symporter Stl1p is essential for cold/near-freeze and freeze stress adaptation. A simple recipe with high biotechnological potential is given, *Microb. Cell Fact.*, *9,* 82.

Van-Dijck, P., Gorwa, M.F., Lemaire, K., Teunissen, A., Versele, M., Colombo, S., Dumortier, F., Ma P., Tanghe, A., Loiez, A., & Thevelein, J.M. (2000). Characterization of a new set of mutants deficient in fermentation-induced loss of stress resistance for use in frozen dough applications, *Int. J. Food Microbiol.*, *55(1-3),* 187-92.

Van-Dijck, P., Colavizza, D., Smet, P., & Thevelein J.M. (1995). Differential importance of trehalose in stress resistance in fermenting and nonfermenting *Saccharomyces cerevisiae* cells, *Appl. Environ. Microbiol.*, *61(1),* 109–115.

Vargas, S.R., Estruch, F., & Randez-Gil, F. (2002).Gene Expression Analysis of Cold and Freeze Stress in Baker's Yeast, *App. and Env. Mic.,* *68,* 3024-3030.

Verstrepen, K.J., Iserentant, D., Malcorps, P., Derdelinckx, G., Dijck, P.V., Winderickx, J., Pretorius, I. S., Thevelein, J.M., & Delvaux, F.R. (2004). Glucose and sucrose: hazardous fast-food for industrial yeast, *Trends in Biotech.*, *22,* 531-537.

Verstrepen, K.J., Iserentant, D., Malcorps, P., Derdelinckx, G., Van Dijck, P., Winderickx, J., Pretorius, I.S., Thevelein, J.M., & Delvaux, F.R. (2004). Glucose and sucrose: hazardous fast-food for industrial yeast?, *Trends Biotechnol.*, *22(10),* 531-7.

Wei, P., Li, Z., Lin, Y., He, P., & Jiang, N. 2007. Improvement of the multiple-stress tolerance of an ethanologenic *Saccharomyces cerevisiae* strain by freeze-thaw treatment, *Biotechnol. Lett., 29,* 1501-1508.

Wong Sak Hoi, J, Beau, R, & Latgé, JP. (2012). A novel dehydrin-like protein from Aspergillus fumigatus regulates freezing tolerance, *Fungal Genet. Biol.*, *49(3),* 210-216.

Wong Sak Hoi, J., Beau, R., & Latgé, J.P. (2012). A novel dehydrin-like protein from *Aspergillus fumigatus* regulates freezing tolerance, *Fungal Genet. Biol.*, *49(3),* 210-216.

Woods R.A., & Gietz R.D. (2001). High-efficiency transformation of plasmid DNA into yeast, *Methods Mol. Biol.*, *177,* 85-97.

Wysocki, R., & Tamás, M.J. (2010). How *Saccharomyces cerevisiae* copes with toxic metals and metalloids, *FEMS Microbiol. Rev.*, *34(6),* 925-51.

Yeast molecular biology. (n.d.). Horst Feldmann Adolf-Butenandt-Institute University of Munich.Date retrieved: 22.09.2012, adress: http://biochemie.web.med.uni-muenchen.de/Yeast_Biol/

Yu, K.O., Jung, J., Ramzi, A.B., Choe, S.H., Kim, S.W., Park, C., & Han, S.O. (2012). Increased ethanol production from glycerol by *Saccharomyces cerevisiae* strains with enhanced stress tolerance from the overexpression of SAGA complex components, *Enzyme. Microb. Technol.*, *51(4),* 237-43.

Zeyl, C. (2009). The role of sex in fungal evolution, *Curr. Opin. Microbiol.*, *12(6),* 592-8.

CURRICULUM VITAE

Name Surname: Ülkü YILMAZ

Place and Date of Birth: Ankara, 1979

E-Mail: lkyilmaz@yahoo.com

B.Sc.: Erciyes University

M.Sc.: İstanbul Technical University

List of Publications:

Articles:

Küçükgöze G., Alkım C., **Yılmaz Ü**., Kısakesen H.İ., Balta B., Gündüz S., Akman S., Çakar Z.P. 2013. Evolutionary engineering and molecular characterization of nickel-resistant *Saccharomyces cerevisiae*. (in progress).

Cakar, Z., Turanli-Yildiz, B., Alkim, C., **Yilmaz, Ü**. 2012. Evolutionary engineering of *Saccharomyces cerevisiae* for improved industrially important properties, *FEMS Yeast Research*, *12,* 172-182.

Cakar, Şen, M., **Yılmaz, Ü**., Baysal, A., Akman, S., Çakar, Z.P. 2011. ''In vivo evolutionary engineering of a boron-resistant bacterium: *Bacillus boroniphilus*.'', *Antonie van Leeuwenhoek*, *99(4),* 825-35

Posters:

Küçükgöze G., Alkım C., **Yılmaz Ü**., Kısakesen H.İ., Balta B., Gündüz S., Akman S., Çakar Z.P. Evolutionary engineering and molecular characterization of nickel-resistant *Saccharomyces cerevisiae*, 15th International Biotechnology Symposium and Exibition, 16-21 September 2012, Daegu, Korea.

Yılmaz Ü., Özgül M., Üstün M., Şahin D., Z.P. Çakar, " Evolutionary engineering and molecular characterization of freeze-thaw resistant *Saccharomyces cerevisiae*", 2012, Abstract book, Page no: 106, 82. 1st International Congress of the Molecular Biology Assn. of Turkey, İstanbul, Turkey.

Tartık M., **Yılmaz Ü**., Üstün M., Özmeral Ö., Z.P. Çakar, " Molecular characterization of a boron resistant yeast mutant obtained by evolutionary engineering", 2012, Abstract book, Page no: 93, 63. 1st International Congress of the Molecular Biology Assn. of Turkey, İstanbul, Turkey.

Balaban, B.G., **Yilmaz, Ü**., Gündüz, S., Akman, S., Çakar, Z.P. 'Physiological and molecular characterization of iron stress-resistant *Saccharomyces cerevisiae* mutant obtained by evolutionary engineering', New Biotechnol., Abstract book, Page no: 29, S144, 15th European Congress on Biotechnology, İstanbul, 23-26 Eylül 2012

Ü. Yılmaz, M. Şen, A. Baysal, S. Akman and Z.P. Çakar, "Boron-Resistant Yeast: *Saccharomyces cerevisiae*, Improved by in vivo Evolutionary Engineering" 2011, 17th International Symposium on Boron, Borides and Related Materials (ISBB Congress), Abstract book, Page no: 329.

M. Şen, **Ü. Yılmaz**, A. Baysal, S. Akman and Z.P. Çakar, " Boron-Resistant Bacterium: *Bacillus boroniphilus*, Improved by in vivo Evolutionary Engineering" 2011, 17th International Symposium on Boron, Borides and Related Materials (ISBB Congress), Abstract book, Page no: 331

Balaban, B.G., **Yılmaz, Ü**., Gündüz, S., Akman, S., Çakar, Z.P. 'Characterization of an iron-resistant yeast mutant obtained by evolutionary engineering'. ICEST 2011, Abstract book, Page no: 48

Küçükgöze, G., **Yılmaz, Ü**., Alkım, C., Gündüz, S., Akman, S., Çakar, Z.P.'Evolutionary engineering of nickel-resistant *Saccharomyces cerevisiae*.' ICEST 2011, Abstract book, Page no: 89.

Tekarslan, Ş.H., **Yılmaz, Ü**., Akşit, A., Alkım, C., di Paolo, F., Trotta, M., Çakar, Z.P. 'Evolutionary engineering of cobalt- resistant *Rhodobacter sphaeroides*' ICEST 2011, Abstract book, Page no: 109.

Alikişioğlu, N.S., Küçük, F.S., **Yılmaz, Ü.**, Alkim, C., Cakar, Z.P. Molecular characterization of freeze-tolerant *Saccharomyces cerevisiae* obtained by evolutionary engineering. Poster presentation. 4th Conference on Physiology of Yeast and Filamentous Fungi (PYFF4), 1-4 June 2010, Rotterdam, The Netherlands

Yılmaz, Ü., Şen, M., Çakar, Z.P. 2009. In vivo evolutionary engineering of a boron-resistant mutants of *Saccharomyces cerevisiae*. International Conference on Nanomaterials and Nanosystems (NanoMats 2009), Poster presentation, Abstract book, Page no: 171 (P79), ITU, 2009, Istanbul, Turkey.

Yılmaz, Ü., Alkım, C., Turanlı Yıldız, B., Tokman, N., Akman, S., Tamerler, C., Sarıkaya, M., Çakar, Z.P. 2008. Evolutionary engineering of chromium-resistant yeast. XII. International Congress on Bacteriology and Applied Microbiology, IUMS 2008, Page no: 184 (BP-319), 2008, Istanbul, Turkey.